

A Parametric study of creep on EPS embankments

A thesis submitted by Tebarek Ahmed for Norwegian University of Science and Technology

In partial fulfillment of the degree of master

June 2012

Project Title :	Date: 11-06-2012		
A Parametric Study of Creep on EPS Geofoam Embankments	Number of pages (with appendices): 125		
	Master thesis	x	Semester project
Name : Tebarek Ahmed Awol			
Supervisor: Arnfinn Emdal			
External supervisor : Jan Vaslestad and Murad Sani (Norwegian Public Road Administration)			

Abstract:

Expanded polystyrene (EPS) has been grown as one of the leading polymers which is used in small strain geotechnical applications such as light weight fill embankments. In design of such embankments, EPS should be able to fulfill major design criterias of which assessment of creep is the most important aspect. Therefore, the main aim of this study was to have a parametric study of creep on EPS embankments.

Literature reviews on EPS material has showed scatter of results mainly on mechanical parameters. Inconsistent laboratory testing procedures, specimen variation and interpretation of results are mentioned as a reason for the cause of parameter variation.

To evaluate the parameters of EPS, two basic tests have been used in this study- short term loading tests as well as long term loading tests. Short term loading tests are carried out to evaluate the compressive strength and the stiffness parameters of EPS under different specimens and testing procedures while long term loading of EPS is analyzed based total deformation results obtained under 30Kpa constant loading of the specimens for 5 consecutive days.

In this study, three different sized (50mm, 100mm and 150mm) cubic samples, three different shaped (cubic, cylinder and disc) samples, three different loading rates (5mm/min, 3mm/min and 1mm/min) and four specimen temperatures (-20, -10, -5 and 20 °C) are used to investigate parameters of EPS. Results suggest that stiffness of the polymer increases as sample size increases and the same response in increase of stiffness and compressive strength is showed when disc shaped samples, small loading rates and low specimen temperatures are used in general.

The long term deformation behavior of EPS for the same set of specimen variation is repeated. Results confirmed the decrease in creep and total deformation when sample sizes increases. Creep test results on small samples tend to overestimate as compared to full scale projects. Disc shaped samples rather give less immediate deformation, however, deformation rate is high enough to give an overestimate along the time scale. In addition, temperature decrease on specimens brought an expected increase in creep.

Finite element simulation of EPS geofoam are evaluated using hardening and soft soil models in PLAXIS 2D. EPS parameters calibrated using HS-model gives a practical fit compared with laboratory results and similar trends in long term deformation of EPS embankments are achieved using SSC model in PLAXIS 2D. A slight tendency of overestimation in stiffness is shown when soil models are used.

Study regarding creep modeling of EPS embankments is discussed. Empirical equations (Findley equation), equations using isochronous stress-strain curves, sherby-dorn plots and mechanical creep models are studied. Equations developed using creep test results obtained by full scale laboratory test on EPS embankment is used for further discussion. Practical estimation of total deformation was possible up on results found.

Keywords:

1. creep
2. EPS
3. parameter study

(Sign.)



Master Thesis description for

Tebarek Ahmed Awol

Title:

A Parametric Study of Creep on EPS Geofoam Embankments

Background

Application of Expanded Polystyrene, EPS, for infrastructure mainly in road construction is increasing from time to time. It's low density, high compressive strength behaviour and faster construction time among other behaviours makes it to be popular as a light weight fill material. The performance of the fill is the cumulative effect of the subsoil under and the EPS fill. Parameter study of EPS during it's loading time is then important to establish a good prediction of the performance of the fill.

Task description

The main aim of this study is to make parametric study of EPS in the EPS geofoam embankment. The task should address suggestions of input material parameters, Modulus of elasticity and poisson's ratio, from back calculation through FEM codes (Plaxis 2D) of the measured data obtained from monitoring programme on the field. A number of iterations is used until a reasonably close fit is found. Discussion on the type of model to be used shall be briefly discussed related with EPS geofoam embankment.

Laboratory test on small scale EPS specimen from the same quality shall be tested to verify the values obtained from above. Specimens of different size and shape (cylindrical, cube) can be used. Up on results, discussions is required on the recommended sampling technichs from NPRA in Hb274 and the samples used here.

In more detail the work will/may be focusing on:

1. A short literature study on E and ν of EPS up on different loads and loading rate.
2. Short term and long term laboratory tests shall be carried out on different sized and shaped specimens of EPS. Document E, compressive strength and total deformation. Discussion up on the result found in here. Suggest typical values of E and ν to be used.
3. Analyze the effect of temperature on short and long term behavior of EPS. Perform laboratory creep and compressive strength test on EPS specimens at different temperature and discuss up on results.
4. Discuss finite element simulation for EPS using hardening soil and soft soil creep models in PLAXIS 2D. To analyze a full scale laboratory creep test performed on EPS blocks in 1993 by Roald Aabøe using PLAXIS 2D. Compare and discuss to

the outcomes found in literature and laboratory test. (The full laboratory test to be analyzed here is constructed by Norwegian road research laboratory, NRRL (now called Road technology department)).

5. Run the full scale test for different loads on PLAXIS 2D for the same test. Try to establish a relation between load, time and total strain. Discuss different creep models.

This project work is proposed by the National Public Road Administration in Norway which will provide background material and advice through Dr. Jan Vaslestad, MSc. Murad Sani.

Trondheim, January 2012

Supervisor at NTNU

Dr. Arnfinn Emdal

Preface and Acknowledgement

This master's thesis was undertaken at the Geotechnical Division of the Norwegian University of Science and Technology (NTNU). The study emphasizes on the study of parameters of EPS on EPS embankments. Laboratory tests have been conducted on EPS material using equipment sets provided by the geotechnical department and road and pavement technology department.

I would like to express my sincere gratitude to my advisor, Dr. Arnfinn Emdal from NTNU for his insightful guidance and continuous support throughout this study. I am equally grateful to my external advisor from Statens vegvesen, Dr. Jan Vaslestad for his support in the initiation and supervising this study. Moreover, I would like to express my gratitude for Statens Vegvesen, east region for their financial support to perform laboratory test. I also would like to thank Murad sani for his continuous support as an external advisor.

I am very thankful to workshop and laboratory technicians for their support on the execution of laboratory test, despite their busy schedules. Special thanks go to all my friends and staff members in geotechnic and geohazard department for making my two years study special.

Finally, I would like to forward my deepest gratitude to all my families and friends for their support and encouragement throughout this period.

Thanks to you all

Tebarek Ahmed

Contents

1 Introduction	1
1.1 Purpose of report	1
1.2 Problem description.....	1
1.3 Scope and limitation of report	2
1.4 Structure of the report	3
2 Background and Literature review	4
2.1 Expanded Polystyrene - composition, production processes and types	4
2.2 Compressive strength	6
2.3 Tension	9
2.4 Flexural strength.....	9
2.5 Deformation	10
3 Short term compressive strength of EPS	13
3.1 Introduction	13
3.2 Unconfined Compression Strength Test	15
3.3 Discussion	19
3.4 Conclusion.....	25
4 Long term deformation, creep of EPS geof foam	27
4.1 Introduction	27
4.2 Creep Test	30
4.3 Discussion	33
4.3.1 Total deformation	33
4.3.2 Effect of sample size and shape on total deformation.....	33
4.3.3 Effect of temperature on total deformation	35
4.4 Accelerated creep tests	36
4.5 Conclusion.....	38
5 FEM simulation of EPS geof foam	39
5.1 Design criteria of EPS geof foam embankment	39
5.2 Soil models for EPS geof foam	39
5.3 Calibration of EPS parameters using soil models in PLAXIS 2D	47
5.4 FE simulation of a full scale creep test using PLAXIS 2D	50
5.5 Conclusion.....	54

6 Creep Modeling	55
6.1 Introduction	55
6.2 Empirical models.....	56
6.2.1 Findley equation	56
6.2.2 General power-law equation	62
6.2.3 Other empirical equations	64
6.3 Model using isochronous stress-strain curves	64
6.4 Models using creep strain rate, Sherby dorn plot.....	66
6.5 Other creep models.....	70
6.6 A real case history – Løkkeberg bridge	72
6.7 Conclusion.....	75
7 Summary and Conclusions	76
7.1 Summary	76
7.2 Conclusion.....	77
8 Recommendations	78
9 References	79
10 Appendix	81
Appendix A European standard	81
A.1 European Standard classification of EPS products (EN 13163:2001)	81
A.2 Factory Production control (EN 13163:2001).....	83
Appendix B Laboratory test on EPS geofom block	91
B.1 Laboratory test description	91
B.2 Test – A Uniaxial compressive strength test on samples of EPS blocks.....	91
B.3 Test – B Long term deformation test on samples of EPS blocks	98
Appendix C Accelerated creep test results	101
Appendix D Geometry, mesh and stress points selected for full scale laboratory creep modeling	104
Appendix E Data and output results for creep modeling	105
E.1 Long term creep test results on 50mm cubic EPS samples by BASF, Germany	105
E.2 Curve fitting for E(t) versus time.....	108

List of Figures

Figure 2.1: EPS polymerization	Error! Bookmark not defined.
Figure 2.2: EPS foam composition (Alltkl.no, 2012).....	5
Figure 2.3: EPS production process [2]	5
Figure 2.4: EPS - Jackopor block.....	6
Figure 2.5: EPS Uniaxial Compression Stress Strain Curves (after Negusse and Elragi, 2000b).....	7
Figure 2.6: Compressive strength vs strain diagram of EPS 100 [2]	7
Figure 2.7: Initial Young's modulus of EPS geofoam[3].....	8
Figure 2.8: EPS geofoam tensile strength (after BASF, Corp., 1997)	10
Figure 2.9: EPS Creep Behavior for Different Stress Levels (after Sheeley, 2000)	12
Figure 3.1: A scheme of EPS under short term loading.....	14
Figure 3.2: Compressive strength versus density relationship of EPS blocks tested in Lithuania [11].....	16
Figure 3.3: Compressive strength versus strain for EPS blocks testes at BASF.....	16
Figure 3.4: Illustration of cellular structure of the EPS specimen [9].....	17
Figure 3.5: Pictorial presentation of sample preparation	18
Figure 3.6: Pictorial presentation of UCS apparatus and test specimen	18
Figure 3.7: stress-strain relationship of EPS specimen	20
Figure 3.8: PICO PT-104 temperature data recording logger	21
Figure 3.9: Effect of loading rate, specimen size, shape and temperature on Eti	22
Figure 3.10: Mechanism of closed cell under the load [12].....	23
Figure 3.11: Effect of loading rate, specimen size, shape and temperature on UCS	24
Figure 3.12: Compressive strength at different temperatures	25
Figure 4.1: Typical compressive strain behavior [9].....	28
Figure 4.2: Creep behavior of 100mm cube of 18 kg/m ³ density at different stress levels[13]	29
Figure 4.3: Volume change of polymer as a function of temperature; V_0 = volume of polymer chains, V_f = free volume in polymer, and V_g = total volume at T_g , T_m = melting temperature [9]	30
Figure 4.4: Pictorial presentation for tested specimens with different size and shape.....	31
Figure 4.5: Typical EPS cell structure under 321-times magnification. [credit: unknown]	32
Figure 4.6: Pictorial presentation of test apparatus	32
Figure 4.7: Effect of sample size on total deformation of EPS	34
Figure 4.8: Effect of sample shape on total deformation of EPS	35
Figure 4.9: Effect of temperature on total deformation of EPS	36
Figure 5.1: σ - ϵ curve of EPS 100 (ref.2).....	40
Figure 5.2: Hyperbolic stress-strain relation for primary loading for a standard drained triaxial test	41
Figure 5.3: Successive values of yield loci for various values of hardening parameter γ_p and failure surface.	43
Figure 5.4: Cap yielding surface of hardening soil model	44
Figure 5.5: SSC model 1D derivation [23&24]	45
Figure 5.6: Yield surface for SSC model [23]	46

Figure 5.7: Calibration of EPS parameters using HS-model in PLAXIS 2D	49
Figure 5.8: Calibration of EPS parameters using SSC-model in PLAXIS 2D.....	49
Figure 5.9: Full scale creep test at NRRL (Aabøe, 1993), [5]	51
Figure 5.10: Total strain registered for full scale creep test at NRRL (Aabøe, 1993) [5].....	51
Figure 5.11: Input geometry	53
Figure 5.12: Generated mesh	53
Figure 5.13: Comparison of full scale test result and SSC model PLAXIS 2D output	54
Figure 6.1: Creep test result output from PLAXIS	59
Figure 6.2: Log10 total strain vs Log10time result output from PLAXIS	59
Figure 6.3: Log10 creep vs Log10 time result output from PLAXIS.....	60
Figure 6.4: Stress-strain output from PLAXIS.....	61
Figure 6.5: Comparison between measured and calculated total deformation results	63
Figure 6.6: ISSC curve [19]	64
Figure 6.7: Normalized isochronous curves [20]	65
Figure 6.8: Normalized isochronous curves for full scale laboratory creep test,1993.....	68
Figure 6.9: E(t) versus time for full scale laboratory creep test,1993	67
Figure A.1: Relationship between compressive stress at 10 % deformation and apparent density for indirect testing; $1 - \alpha=0,9$; $n=495$	87
Figure A.2: Relationship between thermal conductivity (at 50 mm reference thickness and 10 °C mean temperature) apparent density for indirect testing; $1 - \alpha =0,9$; $n= 3873$	88
Figure B.1: Technic of sample preparation.....	93
Figure B.2: E-modulus of EPS-rate effect	94
Figure B.3: E-modulus of EPS-shape effect	94
Figure B.4: E-modulus of EPS-size effect	95
Figure B.5: E-modulus of EPS-temperature effect	95
Figure B.6: Unconfined compressive strength of EPS-rate effect	96
Figure B.7: Unconfined compressive strength of EPS-shape effect	96
Figure B.8: Unconfined compressive strength of EPS-size effect	97
Figure B.9: Unconfined compressive strength of EPS-temperature effect	97
Figure B.10: Test machine used to measure long term deformation of EPS specimens.....	98
Figure C.1: TTS-accelerated creep test [12]	101
Figure C.2: SIM-accelerated creep test [12]	102
Figure C.3: TTSS-accelerated creep test [12]	103
Figure D.1 Geometry, mesh and stress points selected for full scale laboratory creep modeling in PLAXIS 2D.....	104
Figure E.1 Creep test results from BASF: Total strain vs time.....	105
Figure E.2 Creep test results from BASF: Total strain vs log10time.....	106
Figure E.3 Creep test results from BASF: Log10Total strain vs Log10time.....	107
Figure E.4 Curve fitting for E(t) vs time.....	108

List of tables

Table 2.1: EPS block typical dimension	6
Table 2.2: EPS Types in United Kingdom (after Sanders, 1996)	7
Table 2.3: Production engineering parameters of EPS produced at Jackon (www.jackon.no)..	8
Table 2.4: Typical physical properties of EPS and minimum allowable values [1]	8
Table 2.5: Values of Poisson's ratio.....	9
Table 2.6: ASTM C 578-95 EPS Flexural Strength.....	9
Table 2.7: EU design parameters for EPS [6]	12
Table 3.1: Mechanical characteristics of EPS under short term loading	15
Table 5.1: Summary of input parameters for calibration in PLAXIS 2D	48
Table 5.2: Calibrated test results using HS and SSC model in PLAXIS 2D	48
Table 5.3: Input parameters for long term deformation in PLAXIS 2D	52
Table 5.4: Parameters from back calculation for SSC model	52
Table 6.1: Input parameters for PLAXIS	58
Table 6.2: Initial strain and initial tangent calculated using Findley and Chambers approach	61
Table 6.3: Findley equation parameters calculated from PLAXIS output	61
Table 6.4: Comparison of general power law equation parameters from PLAXIS output and LCPC method.....	63
Table 6.5: Summary of formulas for prediction of total deformation.....	75
Table A.1: Classification of EPS products.....	81
Table A.2: Classification of load bearing EPS products with acoustical properties.....	81
Table A.3: Levels of dynamic stiffness.....	82
Table A.4: Levels of compressibility	82
Table A.5: Minimum product testing frequencies	83
Table A.6: Minimum product testing frequencies for the reaction to fire characteristics.....	85
Table B.1: Number and type of specimens used for UCS test.....	92
Table B.2: Data of specimens used for UCS test	93
Table B.3: Number and type of specimens used for long term deformation test.....	98
Table B.4: Data of specimens used for long term deformation test	99
Table B.5: Total material used for the tests	100

Summary

This investigation aimed at the parametric study of EPS as a light weight fill embankment in road construction. Both short and long term deformation characteristics as well as mechanical parameters of EPS are discussed based on laboratory test outcomes and literature reviews.

Literature reviews on EPS material has showed scatter of results mainly on mechanical parameters. Inconsistent laboratory testing procedures, specimen variation and interpretation of results are mentioned as a reason for the cause of parameter variation.

To evaluate the parameters of EPS, two basic tests have been used in this study- short term loading tests as well as long term loading tests. Short term loading tests are carried out to evaluate the compressive strength and the stiffness parameters of EPS under different specimens and testing procedures while long term loading of EPS is analyzed based total deformation results obtained under 30Kpa constant loading of the specimens for 5 consecutive days.

In this study, three different sized (50mm, 100mm and 150mm) cubic samples, three different shaped (cubic, cylinder and disc) samples, three different loading rates (5mm/min, 3mm/min and 1mm/min) and four specimen temperatures (-20, -10, -5 and 20 oC) are used to investigate parameters of EPS. Results suggest that stiffness of the polymer increases as sample size increases and the same response in increase of stiffness and compressive strength is showed when disc shaped samples, small loading rates and low specimen temperatures are used in general.

The long term deformation behavior of EPS for the same set of specimen variation is repeated. Results confirmed the decrease in creep and total deformation when sample sizes increases. Creep test results on small samples tend to overestimate as compared to full scale projects. Disc shaped samples rather give less immediate deformation, however, deformation rate is high enough to give an overestimate along the time scale. In addition, temperature decrease on specimens brought an expected increase in creep.

Finite element simulation of EPS geofoam are evaluated using hardening and soft soil models in PLAXIS 2D. EPS parameters calibrated using HS-model gives a practical fit compared with laboratory results and similar trends in long term deformation of EPS embankments are achieved using SSC model in PLAXIS 2D. A slight tendency of overestimation in stiffness is shown when soil models are used.

Study regarding creep modeling of EPS embankments is discussed. Empirical equations (Findley equation), equations using isochronous stress-strain curves, sherby-dorn plots and mechanical creep models are studied. Equations developed using creep test results obtained by full scale laboratory test on EPS embankment is used for further discussion. Practical estimation of total deformation was possible up on results found.

Several conclusions are made up on this study: EPS is non-niform when it comes to mechanical parameter due to its production process, a value of $E=5\text{MPa}$ and $\nu=0.1$ is advised to be used for embankment design, EPS parameter calibration using HS model gives practical

result and total deformation in EPS under a constant compressive load of 50%*compressive strength is less than 2% for its entire design time except for special circumstances.

Chapter 1

Introduction

1.1 Purpose of report

Since the beginning usage of polymer materials for geotechnical engineering purposes, characterization of material behavior under different loading conditions has been the prime interest for several years. One of the polymer families which have been used consistently for geotechnical application is expanded polystyrene (EPS) blocks. Among its several uses, EPS has been used consistently in road construction as light weight fill material during which it is subjected to short and long term loading. Even if several field monitoring and laboratory tests have been carried out to investigate the behavior of EPS, its multipurpose uses demand to know more each time. Hence, engineering parametric studies of EPS under short term and long term loading is important to establish and predict the performance of the material during practice.

The main engineering characteristics of polymer materials including EPS are derived from the molecular structure of the material itself. Therefore, any sort of external influence (e.g temperature) which affect the chemical structure of the cellular bonds and the air trapped between them, changes the behavior EPS. Important engineering parameters of EPS under short term loading, compressive strength, Poisson's ratio and modulus of elasticity, tend to vary based on the density, size and shape of specimen used besides temperature.

As one of the main design criteria for EPS structures is the long term compressive deformation, investigation on the time dependent behavior of EPS geofoam blocks are prime important. Several models have been proposed to capture the long term behavior of polymers since 1940s. The two major approaches used to estimate the long term deformation of EPS are: time dependent and time independent models. The most widely used time dependent model and the prime focus for this study is proposed by Findley as in Findley equation which gives practically accurate value. Other derivatives of Findley equation, for example the general power rule law and simplified Findley equation, models based on isochronous stress-strain curves and mechanical models using spring and dashpot have been used throughout the years.

1.2 Problem description

During this master study, an engineering parametric study of the most widely used EPS type, EPS geofoam block, will be presented on the coming successive chapters. The problems that are elaborated during this study are the following:

1. Engineering material properties of EPS under short term loading will be investigated. Compressive strength, E-modulus and poisson's ratio will be studied from results obtained by performing UCS test on EPS block test specimens. The effect of sample size and shape as well as strain rate and temperature on the short term behavior of EPS

will be studied. Comparison with literature values and empirical relationships developed between parameters will be shown.

2. Long term deformation, creep, behavior of EPS block will be studied. Laboratory creep test results on different sample size and shape will be presented. Comparison with standard and literature will be studied.
3. Finite element simulation of EPS geofoam using PLAXIS 2D will be studied. EPS parameters will be calibrated using soil models, hardening soil (HS) and soft soil creep (SSC) model. Long term deformation of EPS geofoam will be modeled using SSC model and results will be discussed.
4. Time dependent creep models for EPS will be studied.

1.3 Scope and limitation of report

The primary aim of this study is to investigate the parameters of EPS during short term loading and the time stress-strain behavior of EPS based on my laboratory results and results obtained from full scale laboratory creep test performed by Roald Aabøe in 1993 at the Norwegian road research laboratory (NRRL). The EPS used for the laboratory test and sequentially for this study are EPS geofoam blocks which are most commonly used in road embankment construction. EPS blocks produced at Jackson AS, Norway is used for laboratory test.

In this study, some of the important engineering parameters of EPS and elaboration on scatter of results from different results reported are discussed.

Mathematical creep models have been used to model the behavior of polymers since 1950s including Findley equation. Findley parameters have been calculated from test results of EPS blocks nevertheless not from finite element calculations. This report gives the impression to how much the characteristics of EPS can be modeled using soil models in PLAXIS. In addition, finite element output results are used to calculate coefficients for power function models developed using isochronous stress-strain curves.

However, this study has limitations both from laboratory test as well as output results from finite element calculation using PLAXIS 2D.

- Limitation on results obtained from laboratory tests caused by inaccuracy on measuring the dimension of the blocks and weight measurements.
- Inaccuracy in measuring the immediate deformation of EPS under loading.
- Inaccuracy in measuring the long term deformation OF the specimen due to friction between metal rods, vibration etc.
- Limitations related with using finite element models including idealization of the full scale laboratory creep test in to a simple 2D model in PLAXIS.
- Inaccuracy and limitation resulting from discretization in PLAXIS. Element mesh size, number of mesh and type of nodes used for finite element manipulation adds its own value for the overall limitation of the outcome.

- Limitation generally arises from mathematical models, iterations as well as computer and software bugs.

1.4 Structure of the report

This report consist a total of 10 chapters of which 5 are main chapters. Chapter two will consist of background and literature review on engineering parameters of EPS from different well known authors on the same topic. Summary of parameters on short term and long term loading as well as design parameters for EPS stated in European standard will be presented. Chemistry, manufacturing and production process of EPS will be also presented.

In chapter three, short term compressive strength of EPS geofam block will be presented. Results from UCS test on different sample size, shape and temperature of EPS specimens will be presented. Comparison of initial modulus and compressive strength results obtained with literature values will be commented.

In chapter four, long term deformation behavior of EPS geofam block will be discussed based on results from laboratory test. Effect of sample size and shape will be discussed. Correlation between small scale laboratory tests and full scale field tests will be presented.

Chapter five will deal with finite element simulation of EPS geofam embankment using PLAXIS 2D. Constitutive models comparison for soil and polymers in general will be presented and discussed. EPS parameter calibration using HS and SSC model in soil test will be followed. Finally, long term deformation of EPS using SSC model and further discussion will be provided.

In chapter six, creep modeling for EPS geofam blocks will be presented. Time dependent models like that of Findley equation and its derivatives the general power law equation, the simplified Findley equation and LCPC equation will be discussed in detail. Coefficients for the material model will be calculated using output from finite element, PLAXIS 2D. Subsequent comparison models and summary of formulas will be presented. In addition, creep model using ISSC curves and mechanical models using spring and dashpot will be presented.

Finally, recommendations on the overall outcome of this study and further research areas, conclusion, reference and appendices will follow consecutively from chapter seven to chapter ten.

Chapter 2

Background and Literature review

2.1 Expanded Polystyrene - composition, production processes and types

2.1.1 Composition of EPS

Since the 1800's scientists have tried to produce plastic material. In the early nineteenth century, completely synthetic plastics were developed from hydrocarbons, whose structure is conducive to easy polymerization. Polystyrene, the polymer from which EPS is made, was invented in 1938.

EPS's main component is styrene (C_8H_8), which is derived from petroleum or natural gas and formed by a reaction between ethylene (C_2H_4) and benzene (C_6H_6); benzene is produced from coal or synthesized from petroleum. Styrene is polymerized either by heat or by an initiator such as benzoyl peroxide to form the low-density, loosely attached cells in which EPS is noted for. A group of styrene called polystyrene must first then be suspended in water to form droplets. A suspension agent, such as specially precipitated barium sulfate or copolymers of acrylic and methacrylic acid and their esters is then added to the water. All are similarly viscous and serve to hold up the droplets, preventing them from sticking together. The beads of polystyrene produced by suspension polymerization are tiny and hard. To make them expand, special blowing agents are used, including propane, pentane (used for EPS), methylene chloride, and the chlorofluorocarbons.

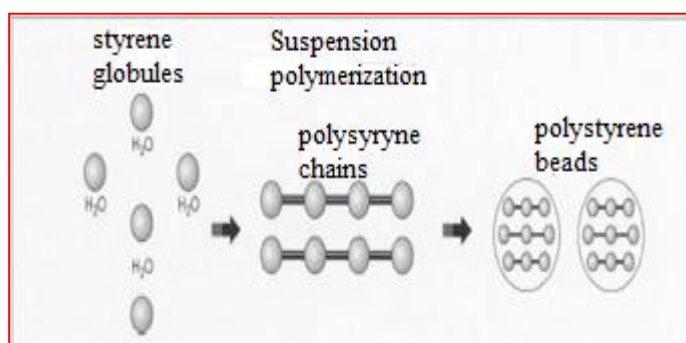


Figure 2.1 EPS polymerization

2.1.2 Production process

There are many kinds of plastics in the world, any plastics when react with the Blowing Agent will become "Foam" which generally called "Foam Plastics". Here, it is only mentioned about foam that produced from Polystyrene / PS (C_8H_8) plastic so-called "Expanded Polystyrene". Expandable Polystyrene / EPS are foam that use Pentane gas (C_5H_{12}) as the blowing agent. During the material production process called "Polymerization" the polystyrene resin granules impregnated with the blowing agent. The overall production and molding process is presented in figures 2.2 and 2.3 below.

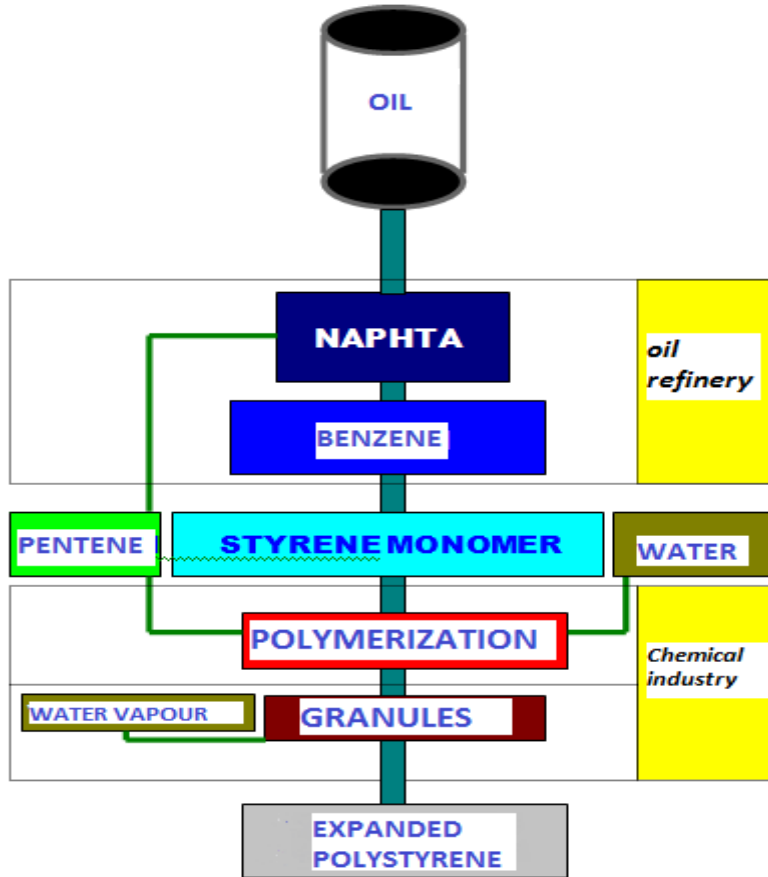


Figure 2.2: EPS foam composition (Alltkl.no, 2012)

1st stage - Pre-expansion

The raw material is heated in special machines called pre-expanders with steam at temperatures of between 80-100°C. The density of the material falls from some 630kg/m³ to values of between 10 and 35kg/m³. During this process of pre-expansion the raw materials compact each other and turn into cellular plastic beads with small closed cells that hold air in their interior.

2nd stage - Intermediate Maturing and Stabilization

On cooling, the recently expanded particles which contain vacuum in their interior must be compensated for by air diffusion. This process is carried out during the material's intermediate maturing in aerated silos. The beads are dried at the same time. This is how the beads achieve greater mechanical elasticity and improve expansion capacity — very important in the following transformation stage.

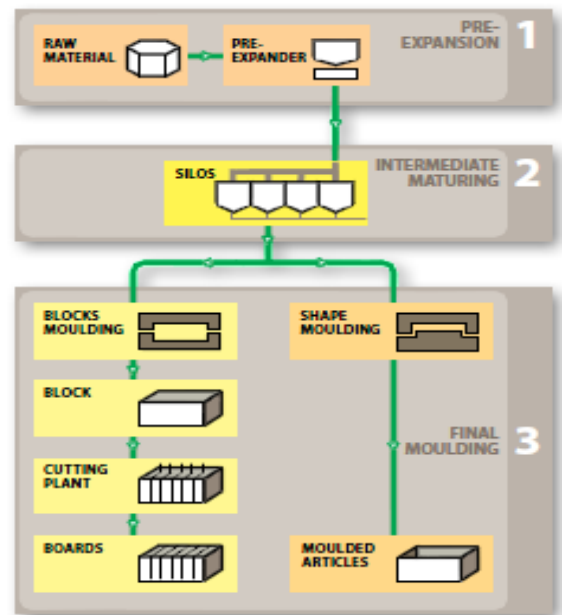


Figure 2.3: EPS production process [2]

3rd stage - Expansion and Final Molding

During this stage, the stabilized pre-expanded beads are transported to moulds where they are again subjected to steam so that the beads bind together. In this way molded shapes or large blocks are obtained (that are later sectioned to the required shape like boards, panels, cylinders etc).

2.1.3 Typical EPS dimension used for light weight fill

The overall dimensioning of EPS blocks varies according to their usage. But, typical dimensions used for geofoam embankment construction in Norway are as follows:

Table 2.1: EPS block typical dimension

Width (mm)	Length (mm)	Thickness (mm)
600	1200	300-500

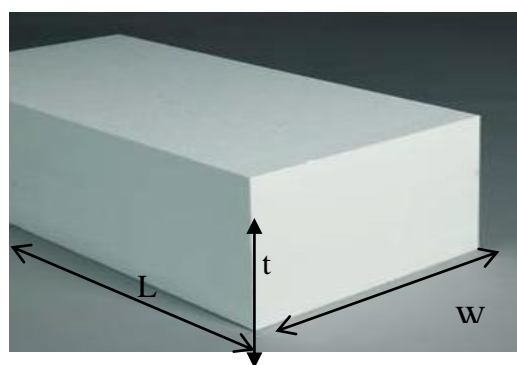


Figure 2.4: EPS - Jackopor block
(www.jackon.no)

2.2 Compressive strength

After briefly describing the production and composition of EPS, in this section engineering parameters and characteristics of EPS will be dealt.

2.2.1 Stress strain curves

Figure 2.5 shows the uniaxial compression stress strain curve of EPS geofoam for two different densities. The two densities shown are considered the extreme values for most engineering applications done so far. Specimens are 0.05m cubes tested at a displacement rate of 0.005m/min. From the figure, the stress strain curve can be simply divided into two main straight lines connected with a curved portion. The slope of the straight-line portion increases with density. The stress at any strain level increases with the density as well.

There is no defined shear rupture for EPS geofoam under compression. Up to 70 % strains can be reached without any break point and the tests were stopped because of the maximum travel of the machine head was reached. The 1%, the 5%, and the 10% strains are common reference strain level, at which the stress is considered as the strength of the material [3].

Compressive strength measurements taken on test specimens from EPS100 blocks in Norway showed the same characteristic. A steep increase in stress – strain curve for the first portion of a straight line followed by a mild slope will develop as illustrated in figure 2.6.

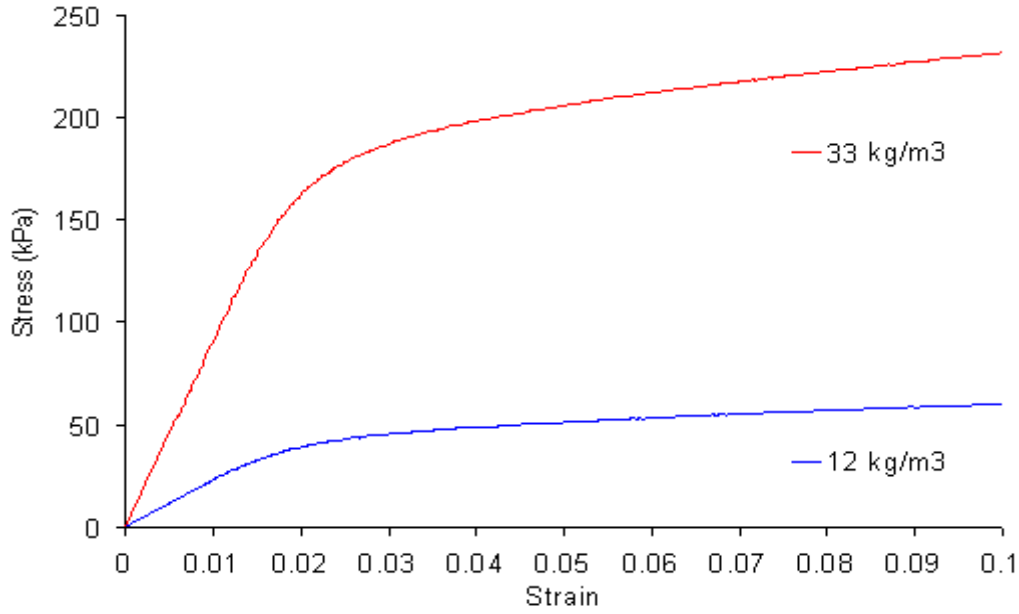


Figure 2.5: EPS Uniaxial Compression Stress Strain Curves (after Negussey and Elragi, 2000b)

Table 2.2: EPS Types in United Kingdom (after Sanders, 1996)

Density (kg/m ³)	12	15	18	22	29
Compressive Strength at 10% Strain (kPa)	35	69	90	104	173

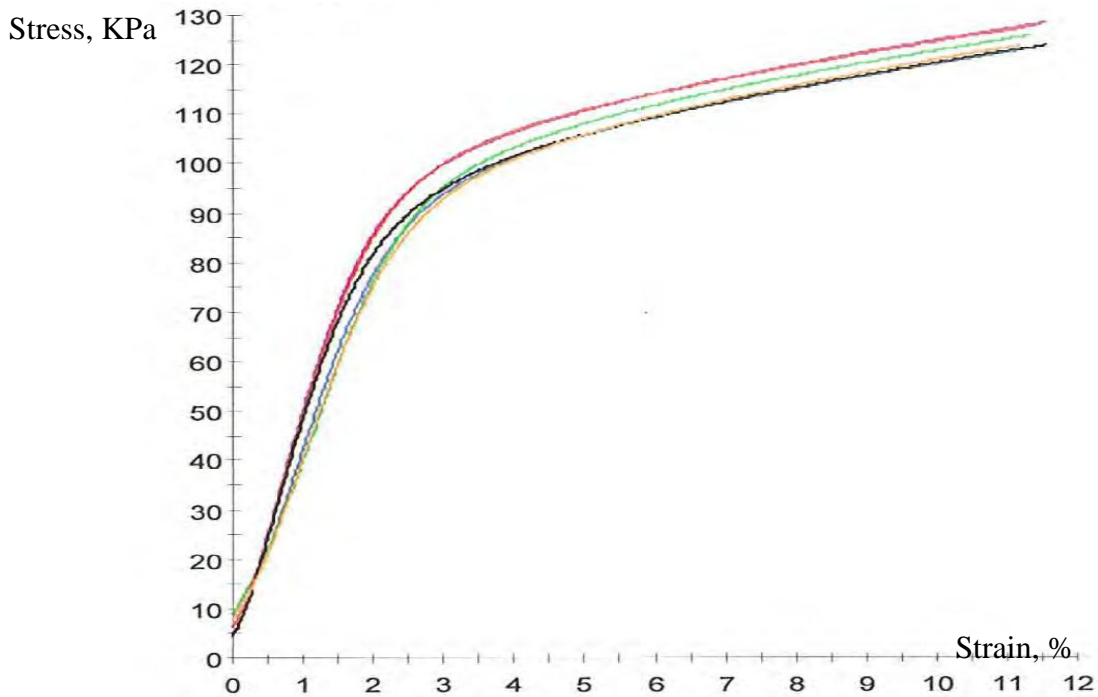


Figure 2.6: Compressive strength vs strain diagram of EPS 100 [2]

Table 2.3: Production engineering parameters of EPS produced at Jackon (www.jackon.no)

Material Designation	Compressive strength, Kpa		E – modulus, short term, MPa
	Short term	strength@2% strain	
Jackopor 60	60	18	2,0
Jackopor 80	80	24	2,6
Jackopor 100	100	30	3,9
Jackopor 150	150	45	3,9
Jackopor 200	200	60	5,0
Jackopor 300	300	60	5,0

2.2.2 Initial Elastic Modulus

The initial tangent modulus or Young’s modulus of EPS varies, some say it is linearly varying and some suggest non-linearity. Generally, the elastic modulus tends to increase as density increases. Table 2.4 shows material parameters for EPS established by AASHTO in USA.

Table 2.4: Typical physical properties of EPS and minimum allowable values [1]

Material Designation		Dry density/ unit weight, Kg/m ³		Compressive strength @10%, KPa	Elastic limit stress, KPa	Initial tangent Young’s modulus, MPa	Modulus of Elasticity, MPa
ASTM C 578	AASHTO	Min	Range				
I	EPS40	15	15 - 19	69 – 96,6	40	4	1,24 – 1,52
VIII	EPS50	18	18 - 21	90 - 124	50	5	1,72 - 2,14
II	EPS70	22	22 - 29,2	104 - 145	70	7	2,21 – 2,48
IX	EPS100	29	29 - 35,4	173 – 227,5	100	10	3,17 – 3,45

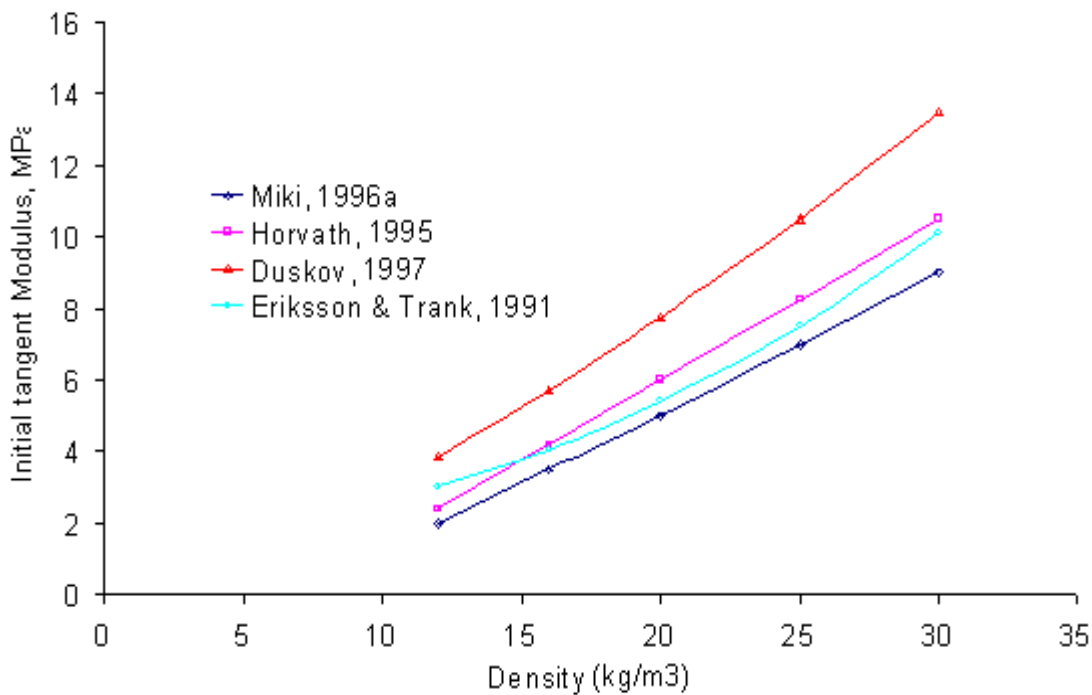


Figure 2.7: Initial Young’s modulus of EPS geofoam[3]

2.2.3 Poisson's ratio

A value ranging from 0.05 to 0.5 registered from different tests and recent test have been showing a negative poisson's value as well. The issue with Poisson's ratio of EPS is its erratic value from loading to loading. However, there is a common consensus among practitioners and designers to use 0.1 as its appropriate value.

Table 2.5: Values of Poisson's ratio

Reference	Yamanaka, et al. (1991)	Negusse and Sun (1996)	GeoTech (1999a)	Duskov et al. (1998)	Ooe, et al. (1996)	Sanders (1996)	Momoi and Kokusyo (1996)
Poissons's Ratio	0.075	0.09 and 0.33	0.05	0.1	0.08	0.05 up to 0.2	0.5

2.2.4 Cyclic Loading

EPS geofam may experience cyclic loading in a number of situations. This can include traffic loading and dynamic loading. The majority of laboratory testing and field observations suggest that the cyclic load behavior of block molded EPS geofam is linear elastic provided that the strains are no greater than approximately 1%.

For three loading cycle tests, the initial tangent modulus in the second and third cycles is much less than those for the first cycle, when the three cycles are loaded to 10% strain (Eriksson and Trank, 1991). Flaate (1987) reported that cyclic load tests show that EPS geofam will stand up to an unlimited number of load cycles provided the repetitive loads are kept below 80% of the compressive strength [3].

2.3 Tension

Tensile strength of EPS material can be an indication of the quality of fusion of the prepuffs and any recycled EPS geofam used in the process (Horvath, 1995b). From *figure 2.8*, it can be seen that the tension strength increases with the density [3].

2.4 Flexural strength

The density of EPS plays an important role in determining the engineering characteristics. As illustrated in table 2.6 below, typical flexural strength of EPS varies from 70 to 350 depending on the density of the material.

Table 2.6: ASTM C 578-95 EPS Flexural Strength

Density (kg/m ³)	12	15	18	22	29
Minimum Flexural Strength (kPa)	70	173	208	276	345

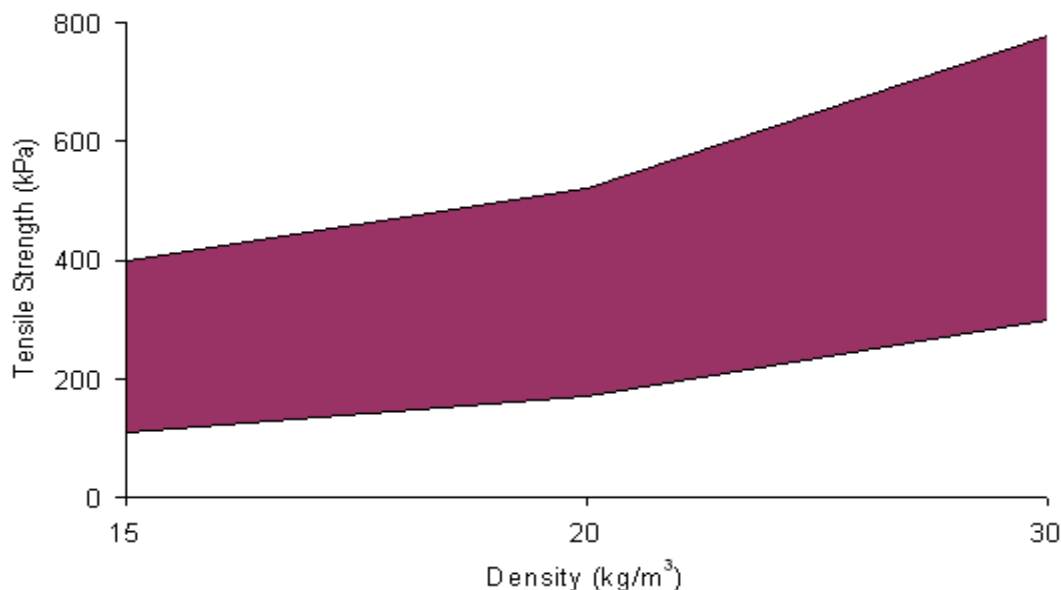


Figure 2.8: EPS geofoam tensile strength (after BASF, Corp., 1997)

2.5 Deformation

2.5.1 Immediate deformation

Different tests carried out to determine the deformation of EPS geofoam suggested that sample size, density and degree of loading has an effect on determination of both immediate and creep deformation.

In general, an immediate strain of $\epsilon < 1\%$ can be expected for a loading stress of less than 25% of the compressive strength of EPS geofoam. More than 1% strain can be achieved for a loading stress of $> 50\%$ [4].

2.5.2 Creep

EPS geofoam is susceptible to time dependent creep deformation when a constant stress level is applied. A number of parameters affect the creep behavior of EPS geofoam, among which is the density, degree of loading and sample size.

Creep deformations decrease with density increase (Sun, 1997). This is rather can be explained by the increase in elasticity of modulus as density increases (*figure 2.7*).

Creep is highly dependent on degree of loading. Almost negligible creep is measured for less than 25% loading and would be considerable as loading increases. *Figure 2.9* represents the results of three 0.05m cube specimens each are subjected to an unconfined axial stress for a period of over 500 days. The stresses are 30%, 50% and 70% of the strength of the material. The three specimens are of type VIII (EPS50) and minimum density of 18kg/m³. It can be seen from the figure that the creep behavior is stress level dependent. For the lower stresses, very little creep deformation occurred after 500 days [3].

In addition to the loading, sample size significantly affects the creep behavior of EPS geofoam as well. Prediction of total strain based on test results from smaller samples would overestimate the actual strain. As an example, both full scale and laboratory performed at Norwegian road research laboratory (Aabøe, 1993 and 2000) is used. A test was done with 2m height of geofoam loaded to 52.5% of its compressive strength. Results observed in a three year period show continuous deformation with time. The strain after three years was about 1% and slightly increasing with time however, for the same loading in smaller samples equivalent strain can be reached within fewer periods [5].

Apart from this there are two time dependent creep empirical formulas developed: the general power-law equation and Findley equation.

The general power rule equation: $\varepsilon = \varepsilon_o + \varepsilon_c$ (2.1)

Where: ε_o – immediate deformation

ε_c – time dependent strain

ε – total strain

$$\varepsilon = (\sigma/E_h) + 0,00209(\sigma/\sigma_p)^{2,47} [t^{\{-0,9\log_{10}[1-(\sigma/\sigma_p)]\}}] \quad (2.2)$$

$$\sigma_p = 6,41\rho - 35,2 \quad (2.3)$$

$$E_{ti} = 479 \rho - 2875 \quad (2.4)$$

$$E_{ti} = 450 \rho - 3000 \quad (2.5)$$

Where:

σ and σ_p are applied and plastic stress in KPa

E_{ti} is the initial modulus at 1%

ρ is EPS density

Findley equation: $\varepsilon = 1,1\sinh(\sigma/54,2) + 0,0305\sinh(\sigma/33,0)(t)^{0,2}$ (2.6)

Where: σ is applied stress and t is time in hrs.

2.6 Stress distribution

A general value for horizontal stress reduction could be of in the range of 10 – 30% (10% is usually used) while vertically it falls within the range of 1:2 [5].

2.7 Durability

No deficiency effects are to be expected from EPS fills placed in the ground for a normal life cycle of 100 years. Aabøe (2000) explained that this should hold true provided possible buoyancy forces resulting from fluctuating water levels are properly accounted for, the blocks are properly protected from accidental spills of dissolving agents and the applied stress level from dead loads is kept below 30-50% of the material strength [3].

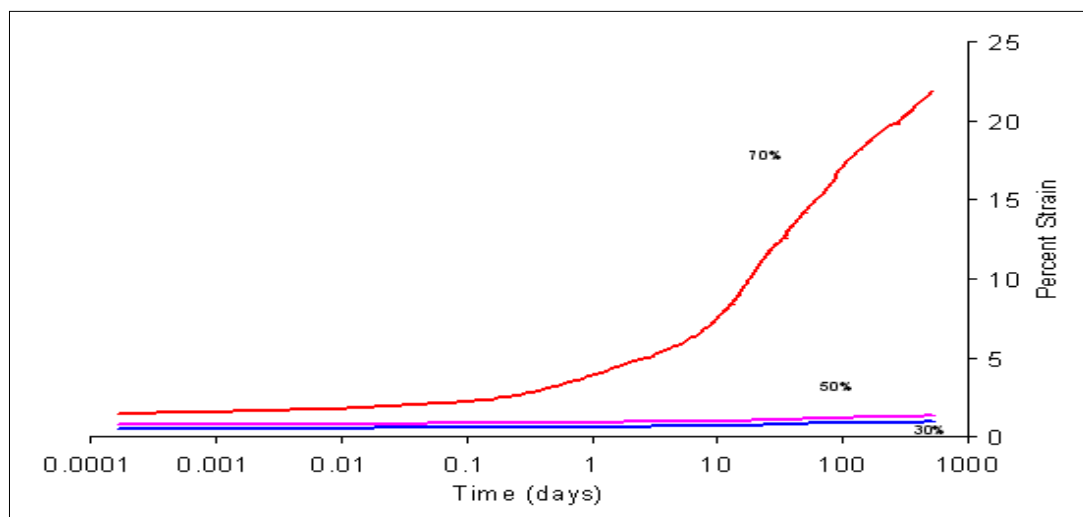


Figure 2.9: EPS Creep Behavior for Different Stress Levels (after Sheeley, 2000)

2.8 EU design parameters for EPS

The product standard for EPS in Civil Engineering Applications (EN 14933) came into force in March 2009. After years of application EU came up with naming EPS by their strength or grade. See table 2.7 for summary of design parameters for EPS under EU.

Table 2.7: EU design parameters for EPS [6]

Property			EPS product type				
Description	Symbol	Unit	EPS60	EPS100	EPS150	EPS200	EPS250
Declared value short-term compressive strength	σ_{10}	KPa	60	100	150	200	250
Design value short-term compressive strength	$\sigma_{10,d}$	KPa	48	80	120	160	200
Modulus of elasticity	$E_t; E_{dyn}$	KPa	4000	6000	8000	10000	12000
Declared value permanent compressive strength	$\sigma_{10,Perm}$	KPa	18	30	45	60	75
Design value permanent compressive strength	$\sigma_{10,Perm,d}$	KPa	14,4	24	36	48	60
Declared value compressive strength under cyclic load	$\sigma_{10,cyd}$	KPa	21	35	52,5	70	87,5
Declared value compressive strength under cyclic load	$\sigma_{10,cyd,d}$	KPa	17	28	42	56	70

Chapter 3

Short term compressive strength of EPS

3.1 Introduction

During the life time of EPS as a light weight fill material in road embankments, they are mainly subjected to compression as one of the main stressed states. Loads coming from the pavement structure as well as the cover soil and the traffic can demand a high compressive strength from the EPS. Therefore, both short term and long term compressive strength of EPS under loading are the main aspects of design. Short term strength of EPS is essential in determining the capacity of the EPS structure to carry the immediate loads coming to it and its capacity to distribute it to the subsoil. Compressive strength is also needed to check the long term capacity when the load prevails on the EPS.

Under compressive load, it is difficult to determine EPS strength clearly. But, we can specify the allowable loads for EPS by determining some critical stress at which the macrostructure of the EPS changes. While testing, EPS samples shows different mechanical states when they put under compressive load. The end of a stress segment OA ($\sigma_A = \sigma_{cr}$) in *figure 3.1* is the design compressive strength of any load bearing EPS. When the load exceeds the critical stress state in the EPS, σ_{cr} , permanent long term deformation starts to develop. Compressive strength can be measured at failure or at any random strain however, for plastic foam structures, including EPS, compressive strength at 10% strain is usually used as a standard. Hence to classify EPS products and to check whether the test can be repeated during factory production and controlling purposes, compressive strength at 10% (σ_{10}) is used [11].

The compressive strength of the EPS block helps to define the maximum allowable load that is applied so as to limit the long term deformation, over 50 years, within 2%. Based on several test results, the maximum allowed load on top of EPS is $0,3*\sigma_{10}$. In addition, since compressive strength is one of the most important properties of EPS, it is used to classify the products accordingly as well. Classification based on other parameter such as bending strength also exists [10] [Appendix A.1].

Several factors influence the compressive strength of EPS. Temperature, test material size and density can be mentioned. Compressive strength tests performed on different densities of EPS samples shows a linear relationship between σ and ρ . Formulas relating stress with density has been proposed. The LCPC (French Public Works Research Laboratory) established $\sigma - \rho$ relationship based on numerous data as [12]:

$$\sigma_p = 6,41 \rho - 35,2 \quad (3.1)$$

Where:

σ_p - is plastic stress of EPS in KPa, which is defined as the stress corresponding to the onset of yielding (Hovrath,1995).

ρ – Density of the EPS sample

In the same manner, compressive strength test had been conducted for different density EPS samples produced in Lithuanian enterprises to establish relationship with density. Test sample size of 50 ± 1 mm with a loading rate of 4-6mm/min is used. A Regression scheme with linear curve fitting is used to correlate between σ_{10} and ρ as well as σ_{cr} and ρ based on results of a number of tests. Proposed equations are presented as follows [11]:

$$\sigma_{10} = 8,4 \rho - 54,6 \quad (3.2)$$

$$\sigma_{cr} = 5,8\rho - 43,9 \quad (3.3)$$

Where:

σ_{10} - Compression strength corresponding to 10% deformation

σ_{cr} - Critical stress state

ρ - Density

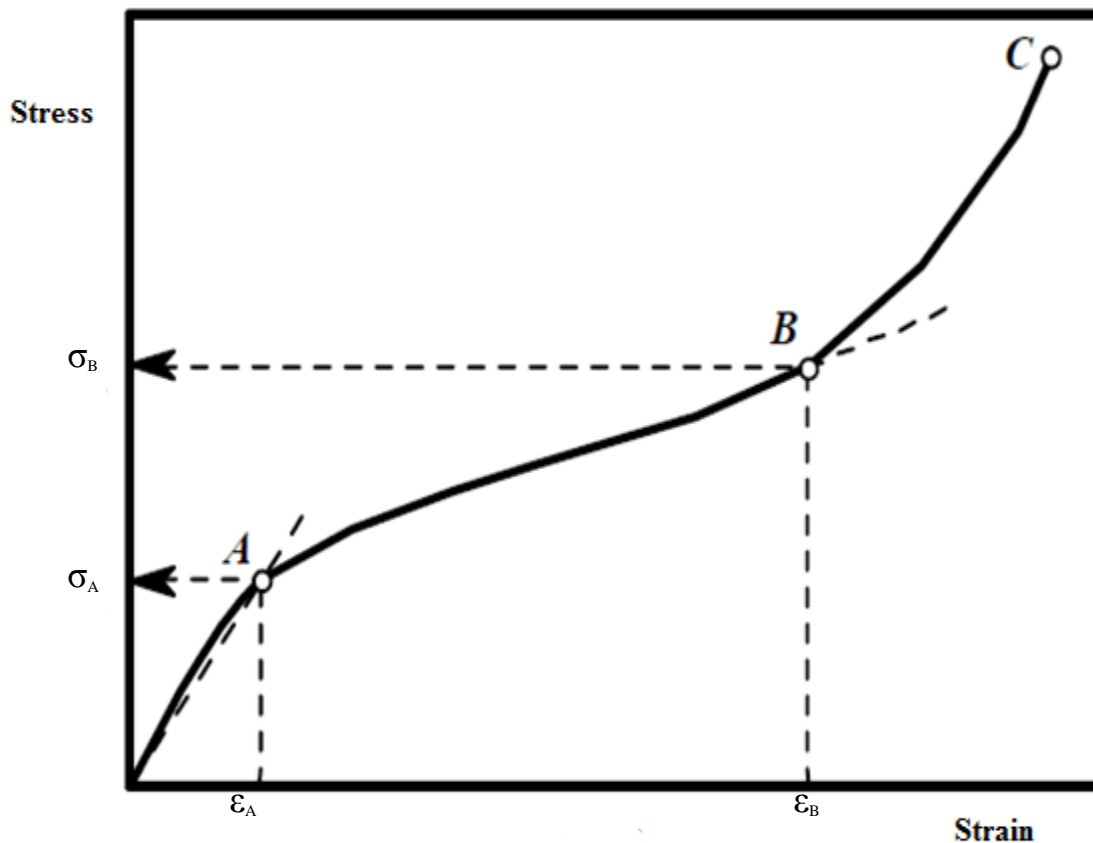


Figure 3.1: A scheme of EPS under short term loading

Test results reported by BASF, German chemical company which produces EPS, suggests a clear pattern for the effect of sample density on stress as seen on figure 3.3.

Table 3.1: Mechanical characteristics of EPS under short term loading

Stress (see <i>Figure 3. 1</i>)	Corresponding stress and its conventional signs
σ_A , corresponding to the end point of the section A	Ultimate (critical) stress σ_{cr}^{*} (when this value is not exceeded, the linear or similar relationship is found between stress and strain)
σ_B , corresponding to the attenuation of flexural deformations of cell walls when their stability is lost	Stress corresponding to maximum possible compaction σ_{comp} of the damaged elements of polystyrene macrostructure
Exceeding the value of σ_B , corresponding to the “flattening” of polystyrene when the elements of macrostructure are damaged	Stress is not a mechanical characteristic of EPS slabs subjected to compression

Not only density has an effect on the compressive strength of geofoams but also the temperature and sample size has an effect on the results too. When temperature rises, the cellular structure of the EPS which tend to provide the resistance to the coming load is affected. Consequently, the compressive strength decreases. On the other hand, test specimens with different size tend to give different results. As the samples to be tested gets smaller, the end effect towards the result is much higher. Test results reported from small scale to full scale tests showed that Young’s modulus is underestimated whenever the sample is smaller. This has a direct effect on the amount of immediate strain and long term deformation of EPS blocks.

In this chapter, short term compressive strength of EPS blocks which are produced in Norway will be tested using unconfined strength test machine (UCS). Relationship of the compressive strength of EPS with temperature fluctuations, sample size and shape will be discussed.

3.2 Unconfined Compression Strength Test

3.2.1 General

The main objective of this test is to study the effect of sample size, shape, load application rate and temperature fluctuation on the compression strength and elastic modulus of the tested specimens using the results obtained from unconfined compressive strength test. Elastic modulus calculated from compressive strength test provides different values on cubical, cylindrical and disc shaped small size samples of EPS. Recorded values of Elastic modulus in literatures have shown that sample size has an effect on determination of parameters.

In this test, UCS will be performed on the three different shapes to see the development of σ - ϵ curves. Compressive strength values obtained from this test will be compared with literature

values. The other objective of this UCS test is to determine the relationship between temperature of test samples and their compressive strength development.

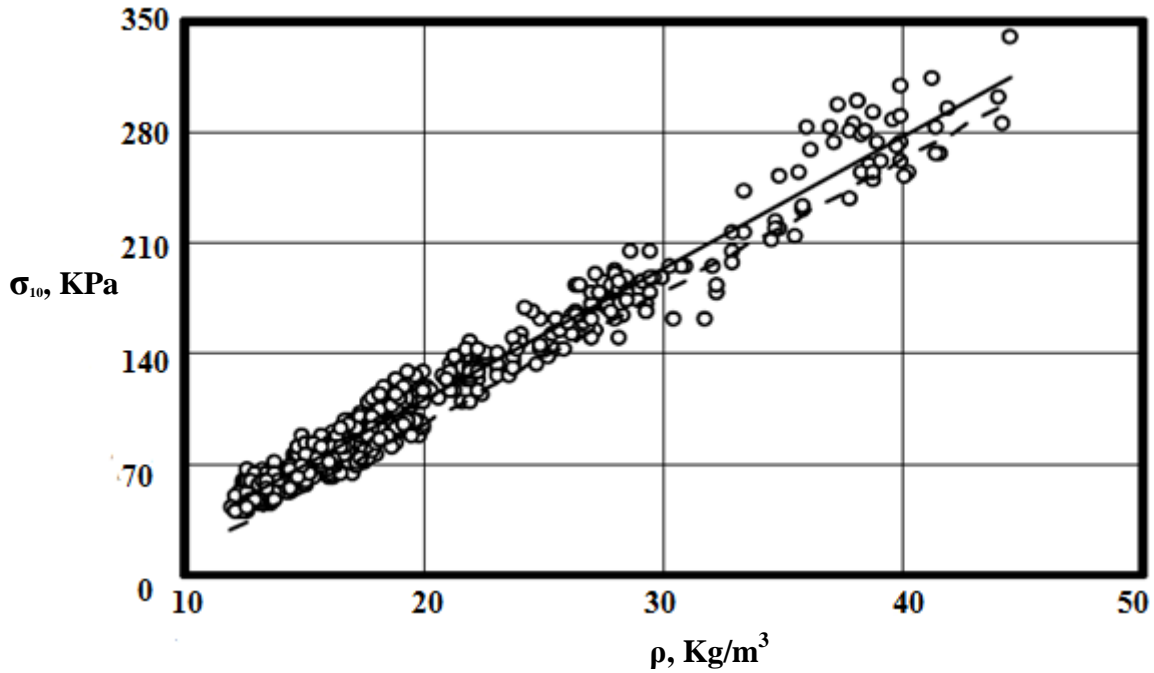


Figure 3.2: Compressive strength versus density relationship of EPS blocks tested in Lithuania [11]

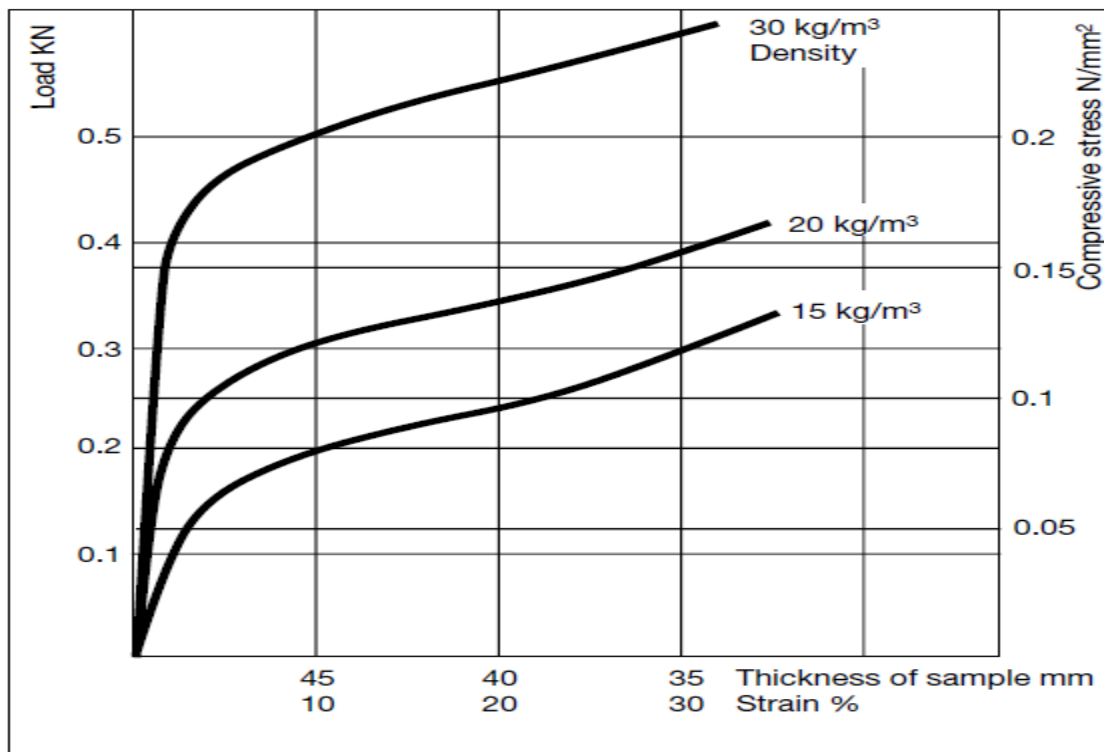


Figure 3.3: Compressive strength versus strain for EPS blocks testes at BASF

EPS during its service life time may be subjected to temperature fluctuations. Due to this, sensitivity of EPS parameters towards temperature is necessary to be checked. Uniaxial

compressive strength tests performed on EPS sample blocks within a temperature range of 20 – 48°C showed a variation in elastic modulus and compressive strength. The intention of this test is to check and establish the temperature dependency of the short term compressive strength and elastic modulus within the temperature range of -20 to 20°C.

3.2.2 Test Material and apparatus

For this study EPS100 with density 30Kg/m³, a commonly used geof foam block in light weight road embankment construction is used. The geof foam is produced at Jackon AS in Oslo, Norway following European production control EN 13163:2001[Appendix A]. Due to the composition and production behavior, the macrostructure of the EPS plays an important role in determining the strength of the material. Hexagonally - shaped cell walls which are produced during the manufacturing process of EPS blocks due to blowing, heating and cooling process of the polystyrene beads, carries the load [9]. Any change on the macrostructure of EPS either on production or by external forces ultimately changes its behavior. Pictorial presentation of the test sample and the macrostructure of the EPS are shown in *figure 3.4* below.

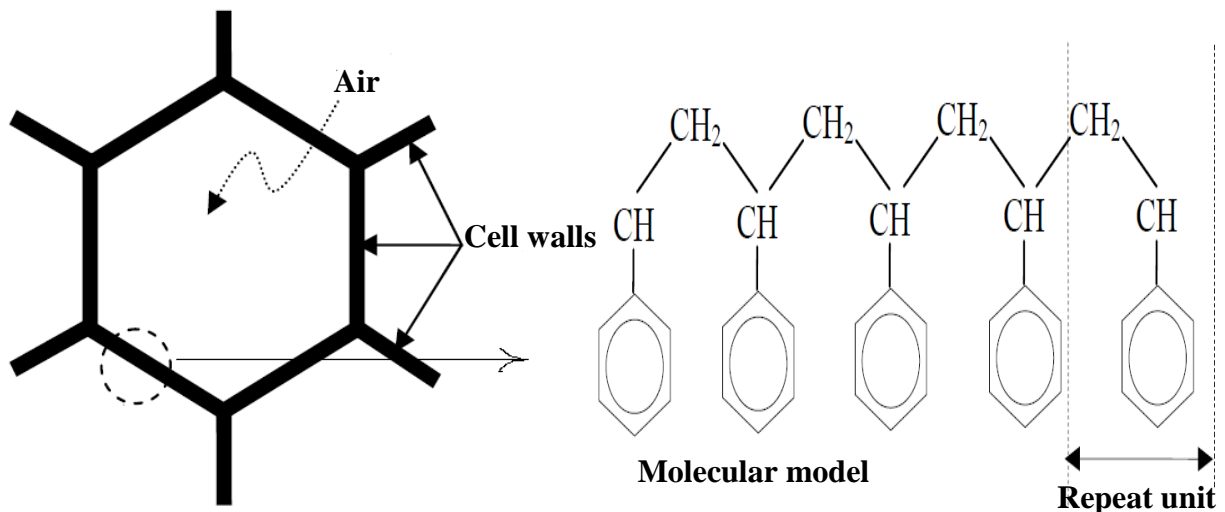


Figure 3.4: Illustration of cellular structure of the EPS specimen [9]

A 2m x 1m x 0.5m dimension standard molded block is used to make the tested samples and standard procedure of sampling technic is used as described in Norwegian handbook manual 274 to obtain the samples [Appendix B.2]. Traditionally used hand saw is used to cut the original block in to a number of chunks to make it easy on handling as well as easy to fit in to a vertical saw machine as illustrated in *figure 3.5*.

Test specimens are prepared in three different shapes, cubical, cylindrical and disc shaped in addition to different sizes which are ranging from 50mm to 150mm cube samples for this test. Cylindrical samples of $\Phi = 50\text{mm}$, $h = 50\text{mm}$ and disc shaped samples with dimensions of $\Phi = 50\text{mm}$, $h = 25\text{mm}$ are prepared using carving knife from 50mm cubic samples.

A standard UCS machine is used to capture the σ - ϵ behavior of the sample as well as their compressive strength. The machine has a hydraulic loading system in which a piston pushes -

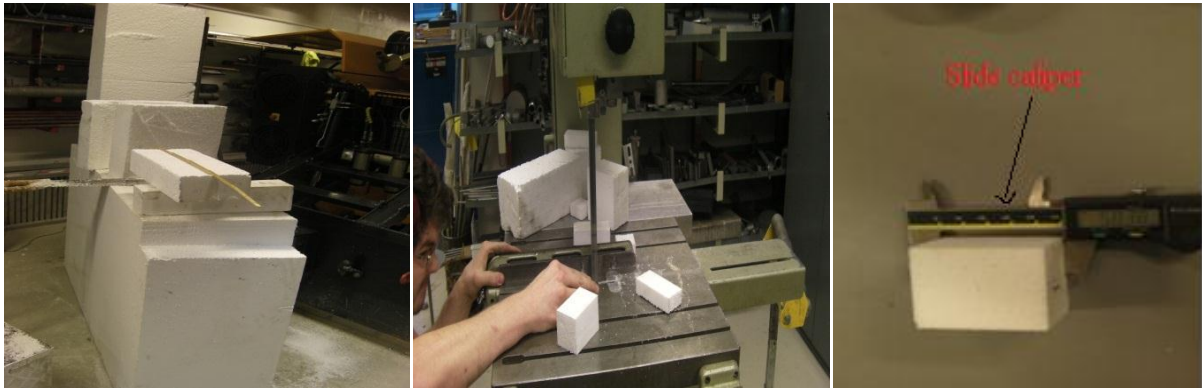


Figure 3.5: Pictorial presentation of sample preparation

from downward to upward direction pushing the sample in the way against a fixed plate and in between deforming the specimen. External or global measurement is taken for both deformation and load. LVDT rod which is installed on top of a horizontal plate, which supports the load cell, is used to capture the deformation of the specimen whereas a 5KN load cell is mounted to read the load applied on to the specimen. All the data were accessible in soft copy through the help of the in-built software in the computer which is in turn connected to the LVDT and load cell through cable.

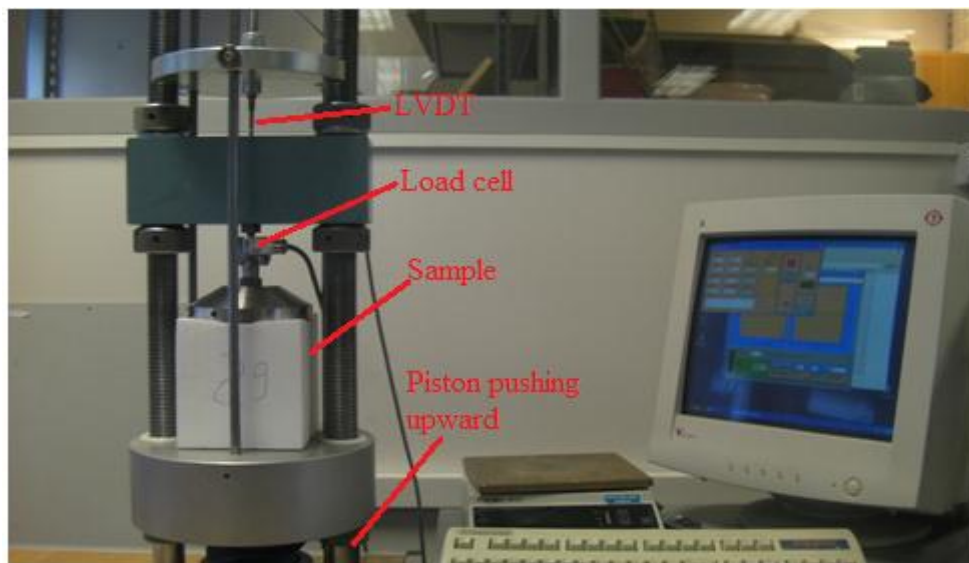


Figure 3.6: Pictorial presentation of UCS apparatus and test specimen

3.2.3 Testing procedure

For all the tests using UCS, a commonly used strain rate of 5mm/min (10%/min) is followed except for tests carried out at 3 and 1mm/min to indicate the relationship between strain rate and compressive strength as well as initial tangent modulus. Since failure doesn't occur easily in EPS under vertical loading, strain can reach up to 70% without the sample fails. Therefore, it was necessary to stop the test after we reached a reasonable strain before exceeding the machines capacity. A maximum strain of 50% is used when the samples were loaded using UCS by maintaining a constant strain rate.

For tests carried out at temperature other than the room temperature, the samples are kept in the frozen lab itself for atleast 24hrs to keep the sample within its intended temperature and simultaneously the temperature is recorded using temperature sensitive rods. Samples are carried to the UCS machine using insulation box and similar UCS tests are carried on these samples as well. Detail sample preparation, test execution, data and data interpretation of the test is presented in [Appendix B.2].

3.3 Discussion

3.3.1 Elastic modulus

Throughout the years EPS has been used in large strain works as in the case of an inclusion in building and small strain application as in light weight fill material in road constructions. For such small strain application, elastic modulus parameters, poisson's ratio as well as compressive strength parameters are very important especially with in a strain range between 0 to 1 %. It has been widely accepted throughout the design and research families on EPS that EPS geofam tend to show linear-elastic behavior for 0-1% strain range and a plastic range follows as another linear line forming a bi-linear curve as illustrated in *figure 3.7*.

Two widely used parameters to describe EPS under small strain application are elastic limit stress and initial tangent (secant) modulus. Elastic limit stress is the stress measured at 1% strain level and indicated the limitation to which we can apply load on EPS embankments within the linear elastic range. In addition, initial tangent (secant) modulus expresses the level of stiffness of the specimen within the elastic range and it is the slope of the "straight" line between 0 to 1% strain levels. Nevertheless, tests carried on EPS samples also show linearity up to 1,5-2% strain and this led into quantifying the allowable load that should be applied on EPS so that the effect will be contained in the elastic region.

Several tests have been reported to determine the stiffness parameter for EPS and a wide variety of results are seen for different size and shape of specimen and other related factors. But, in design practice elastic modulus in the range of 4 to 6MPa is recommended to use. European standard also provides a value of as high as 6MPa for EPS100 (at 10% strain) geofam blocks.

Stiffness parameters calculated during these results are very wide in range and varies accordingly with the type, size, loading rate as well as temperature of the samples used. A variation in density has been also registered which can be attributed to the fact that molding of pre-puffs (beads) is not uniform throughout the block leading to variation in physical and mechanical parameters as will be seen in further discussions. Average density of the samples tested is around 29Kg/m³ with a standard deviation up to 4%.

The elastic and visco-elastic nature of all polymer materials tends to depend their parameters on time. The relative slowness or fastness in loading speed certainly can play a role in the deformation nature of the cellular wall which entraps the air and gives the overall strength and stiffness for the polymer. However, as illustrated in *figure 3.9(a)* there is not such a clear trend between the initial tangent (secant) modulus and loading rate. But, the theoretical

expectation of increasing stiffness as the loading rate decreases can be slightly supported by some results which tend to show the same. Several tests are required to say explicitly a trend between Eti and other factors.

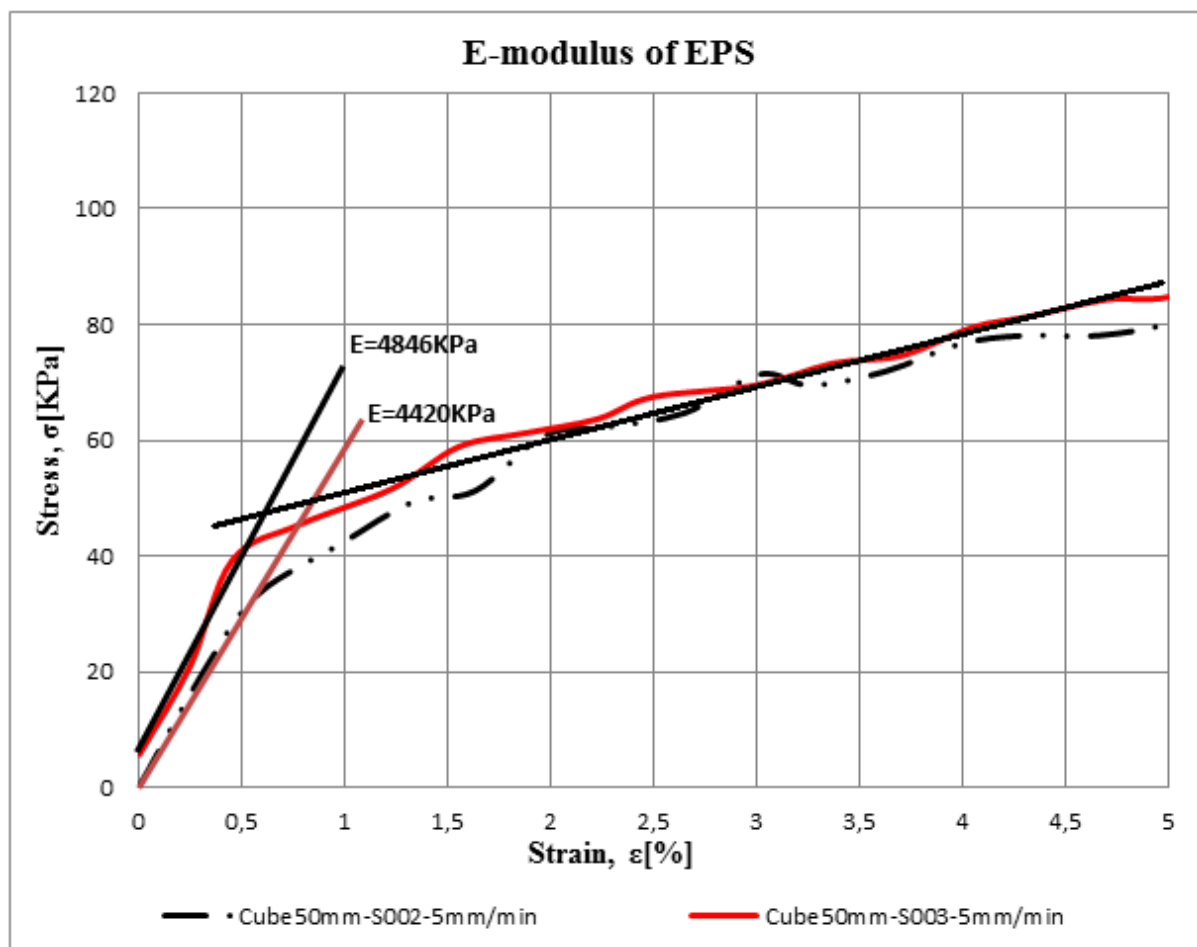


Figure 3.7: stress-strain relationship of EPS specimen

Tracing back to the early use of polymer materials and especially with the start of using EPS for large and small strain projects, 50mm cube has been used as a de-facto standard size for parameter investigation of EPS. However, test results based on cylindrical (Duskov, 1997), cube (Elragi et al., 2000, Eriksson and Trank, 1991) also on disc (Wu, 1986) shaped samples with different dimensions has been reported independently to gain mechanical parameters for EPS. Due to the high scatter of results, the over-cross referencing of results from different specimen size and shape as well as comparison of EPS mechanical parameters, leads to confusions and suspicions where up to what scale the effect of specimens physicality is. To over shade some light, samples of different shape and size are prepared and tested to determine their particular effects on mechanical parameter, Eti. EPS specimens are prepared on 3 different shapes (cube, cylinder and disc) and three sets of different size, only applied on cubically shaped specimens (50mm, 100mm and 150mm), for UCS test under a constant load strain rate of 5mm/min. As illustrated in *figure 3.9 (b) and (c)* both cylindrical and disc shaped samples tend to give a higher value of stiffness compared to cubical shaped samples. A stiffness range between 5,5 to 6,5 MPa can be expected for cubical and disc shaped samples

whereas a slightly lower stiffness values between 4 to 5 MPa is gathered for cubical samples. In addition, as the sample size decreases a slight tendency of underestimating the stiffness parameters are shown.

The macro-structure of polymers is highly dependent on temperature because of the visco-elastic nature of them. In this test, 50mm cube samples were preserved for at least 24 hrs in the ice lab at three distinctive temperatures (-20, -10 and -5 °C) while room temperature ($20\pm 3^{\circ}\text{C}$) is used for the other set of tests. UCS test were performed on the samples at a constant strain rate of 5mm/min to evaluate the effect of lowering temperature on their mechanical parameters. Temperatures of samples were continuously recorded using PC-104 temperature logger using very sensitive temperature rods which are attached to the samples as shown in *figure 3.8*. All the tests were performed at least twice to check the repeatability of the test. As illustrated in *figure 3.9(d)*, inconclusive and inconsistent results were obtained. A lower initial modulus was found for some of the specimens but an increase in stiffness is indicated for samples as their temperature reduces which conciliates with the expectation. An average stiffness of 4,2 MPa at -5 oC to 5,9MPa for temperature at -10 and -20 °C is calculated from test results. Nevertheless, a clear pattern or trends of results were yet again not shown from the results collected.

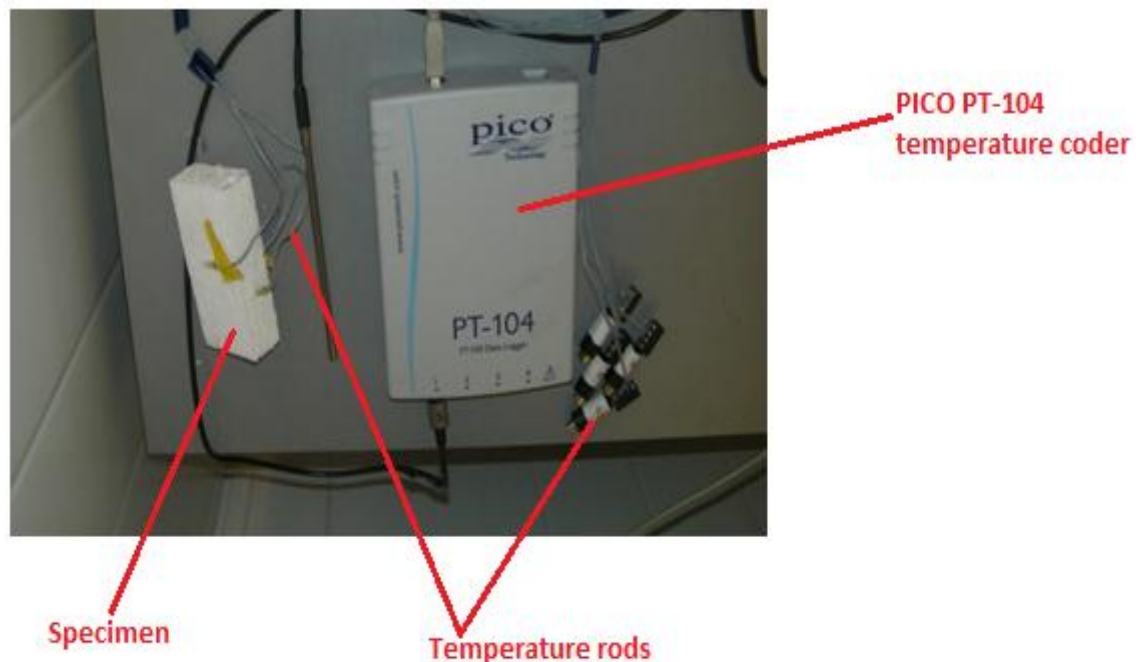


Figure 3.8: PICO PT-104 temperature data recording logger

3.3.2 Poisson's ratio

From several literature reviews and back calculation results obtained from analyzing EPS embankments a common consensus of poisson's ratio in the range of 0,09 to 0,15 can be applicable in practical designs. Nevertheless, for specific application of EPS in small strain practice several samples should be tested with a precise strain gauge measuring device using local measurements.

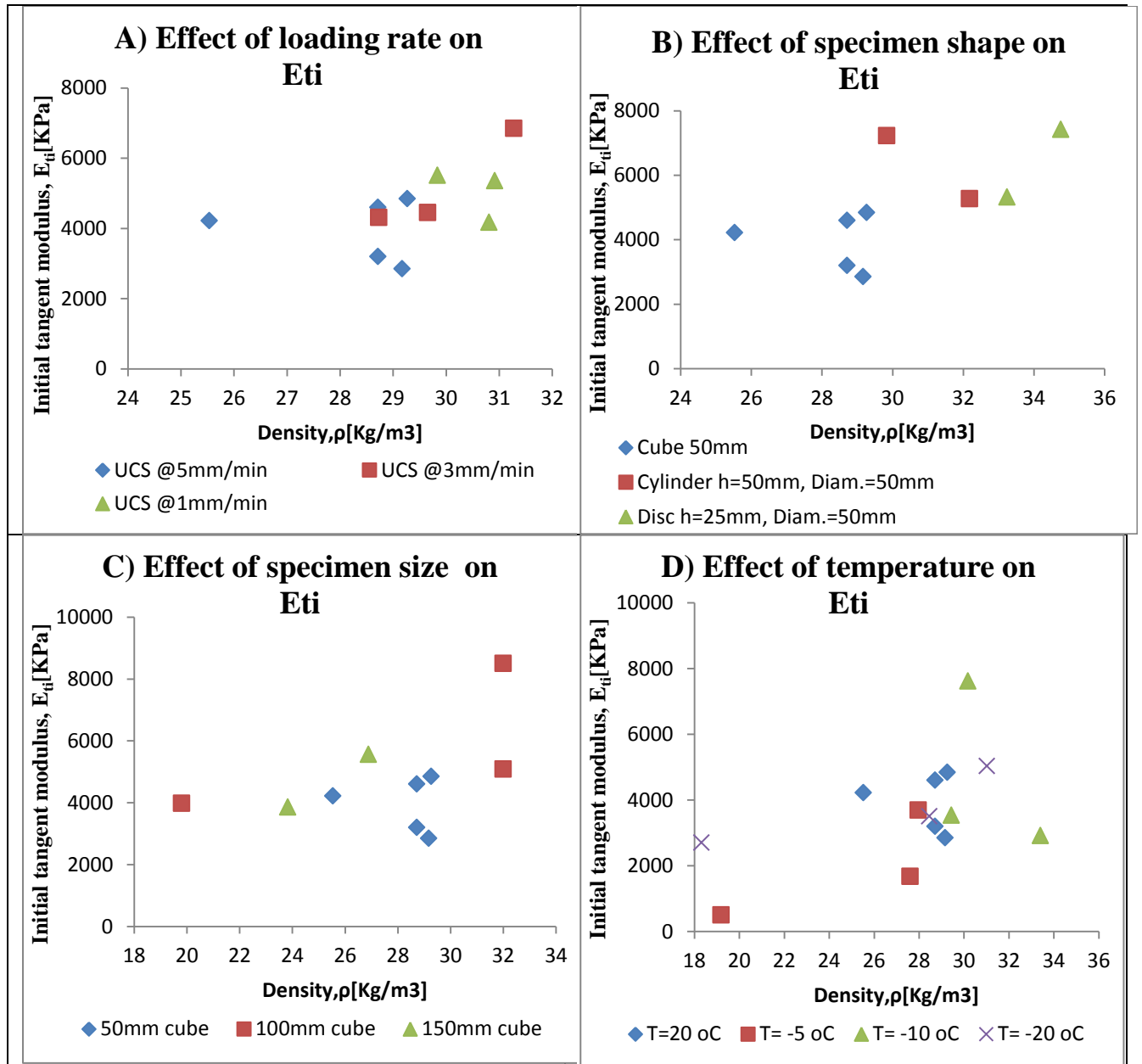


Figure 3.9: Effect of loading rate, specimen size, shape and temperature on Eti

3.3.3 Short term compressive strength of EPS

Even if the property of EPS in the strain range of 0 to 1% is highly important for practical applications, quantifying the parameter in the outer range or non-elastic range is as equally important. One of the peculiar characters of EPS under loading is their ability to undergo large strains before failure, unlike soils. Nevertheless, estimating the load bearing capacity of EPS under which it will never be deformed excessively is of practical importance. For practical design purposes, characterization of the material as well as nomenclature purposes however, compressive strength of EPS is inherently taken to be the compressive stress at 10% strain. Some particular places, e.g Norway, the same terminology is used for the value obtained at 5% strain.

EPS undergoes changes macro-structurally upon loading to it as a mechanism to coup up the changes imposed by external load application. As explained in *figure 3.7*, EPS shows a clear bi-linear stress strain curve at which the elastic and plastic parts are regionalized. However, the reaction mechanism in the macro level of the EPS is different in both regions. In elastic region the load have an impact on the cell edges by bending them and stretching the vertical wall which encloses the air. In the plastic region, the cell walls start to collapse and develop a permanent strain. Some suggestions regarding the development of irrecoverable strain are the onset of permanent hinges, an occurrence of plastic stretching and buckling of cell walls. These can be attributed to the plastic region of the stress/strain curve (Landro et al., 2002; Song et al., 2005) [12]. *Figure 3.10* illustrates the reaction towards external load by the cell walls, which make up EPS structure.

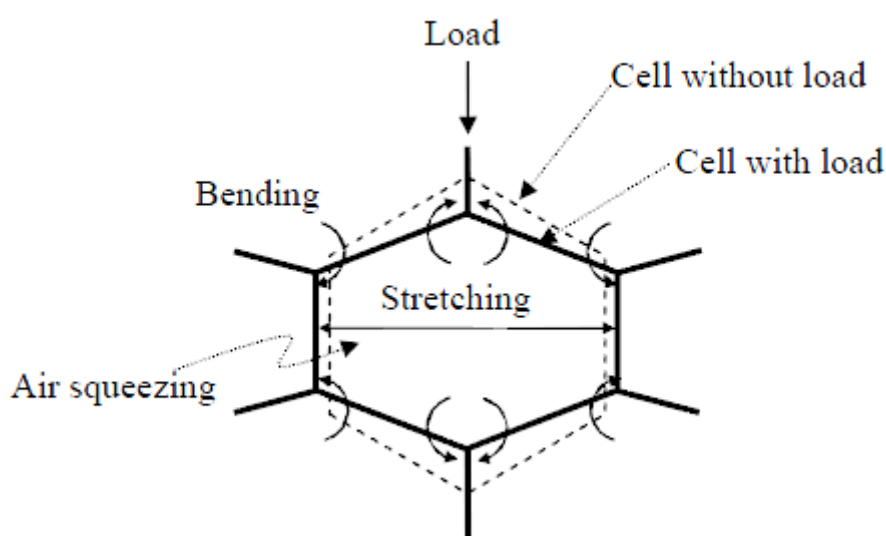


Figure 3.10: Mechanism of closed cell under the load [12].

3.3.4 Effect of loading rate, shape and size of specimen on short term compressive strength of EPS

Three different strain rates have been used as explained earlier (5, 3 and 1mm/min). As illustrated in *figure 3.11(a)*, an increase in compressive strength has been indicated when the loading rate decreases. An average compressive strength of 100, 132 and 111KPa is found for the three loading rates mentioned above respectively. This can be explained to the fact that the cell walls will have a relative ease in duration at lower loading rate to stretch back to some level of their deformed shape and gain extra strength. However, consistent trend wasn't obtained in this case as well.

The test result illustrated in *figure 3.11(b) and (c)* shows the clear pattern of dependency of UCS of EPS on shape and size of specimen. From the three available and most commonly used shapes of specimens (cube, cylinder and disc) an average UCS value of 100, 116 and 132KPa was found during these tests respectively. On the other hand specimen dimension have also shown a big impact on UCS. Nearly 30% increase in compressive strength is shown

between 50 and 100mm cube samples. On the bigger scale, taking result outputs obtained from small samples to design full scale EPS construction can be on a conservative side.

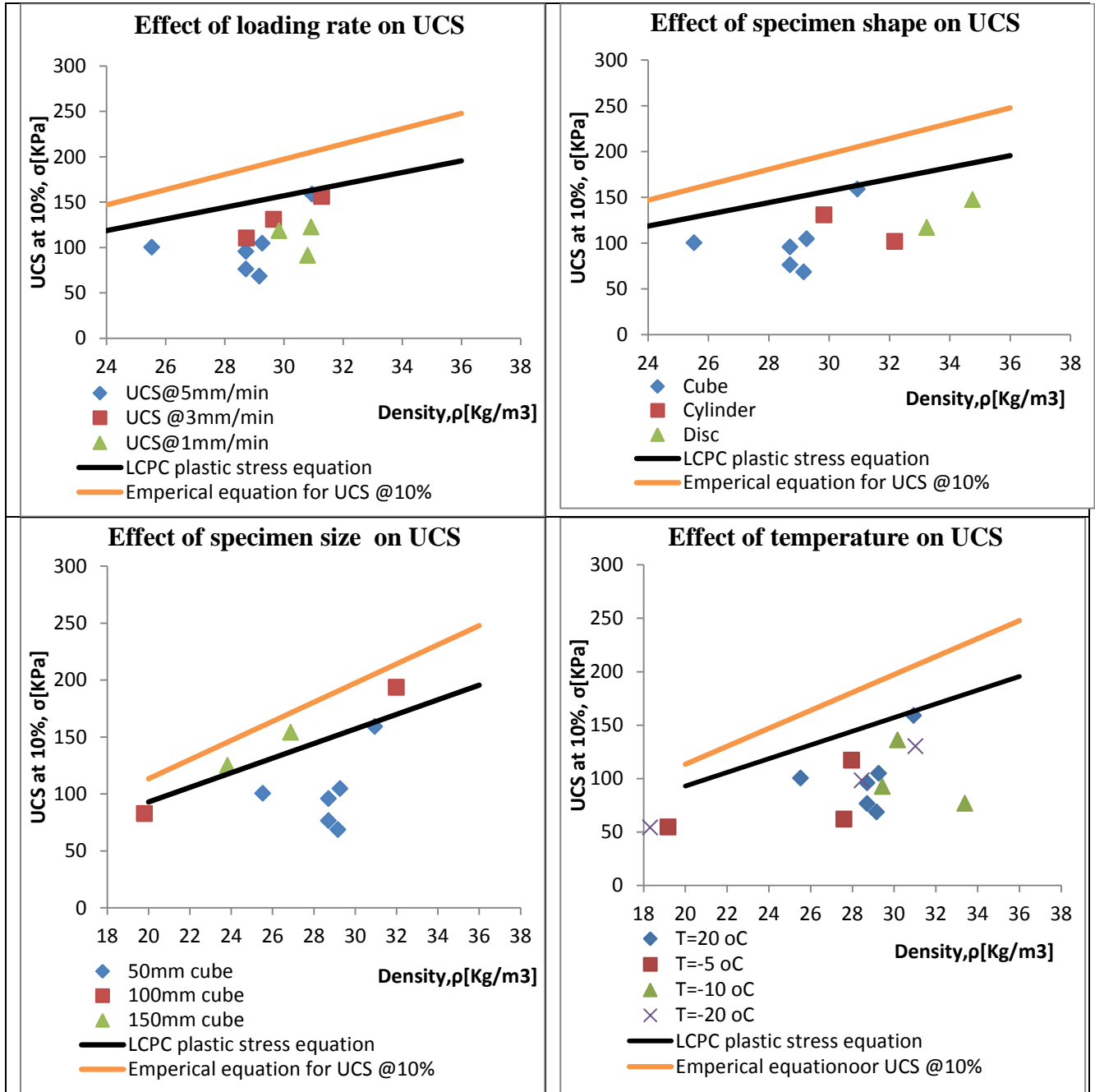


Figure 3.11: Effect of loading rate, specimen size, shape and temperature on UCS

3.3.5 Short term compressive strength of EPS at room and lower temperature ranges

As explained in the previous sections, temperature plays an important role in defining the mechanical parameters of polymers in general and EPS in particular. As shown in appendix B.2, the shape and the development of stress strain diagrams are similar for different temperature ranges. However, compressive strengths differ at a particular strain points. On average, slight increase in strength from 89 to 104 and 114KPa is indicated when the temperature of the specimens decrease from -5 to -10 and -20 °C respectively. This can be

again explained by the effect of temperature on cell walls. Even if EPS is a good insulation material, a decrease in temperature over the specimen may tend to give the cell walls a higher stiffness. On contrary, an increase in temperature may tend to decrease the bonds/fusion between the pre-puffs (beads), which were originally fused together by steam and high pressure during the molding stage of EPS production, and ultimately reduce the strength of the cell walls in general.

In order to show the trend between temperature and compressive strength, test results from Sang-Sik Yeo (2007), is used in addition to the results obtained from this study to create a wider temperature range. As illustrated in *figure 3.12*, a bi-linear relationship can be followed for temperature ranges between 23 to 58 °C when compressive strength decreases as temperature increases [12]. Whereas reverse relationship is shown in the lower temperature ranges where the compressive strength increases as the temperature decreases.

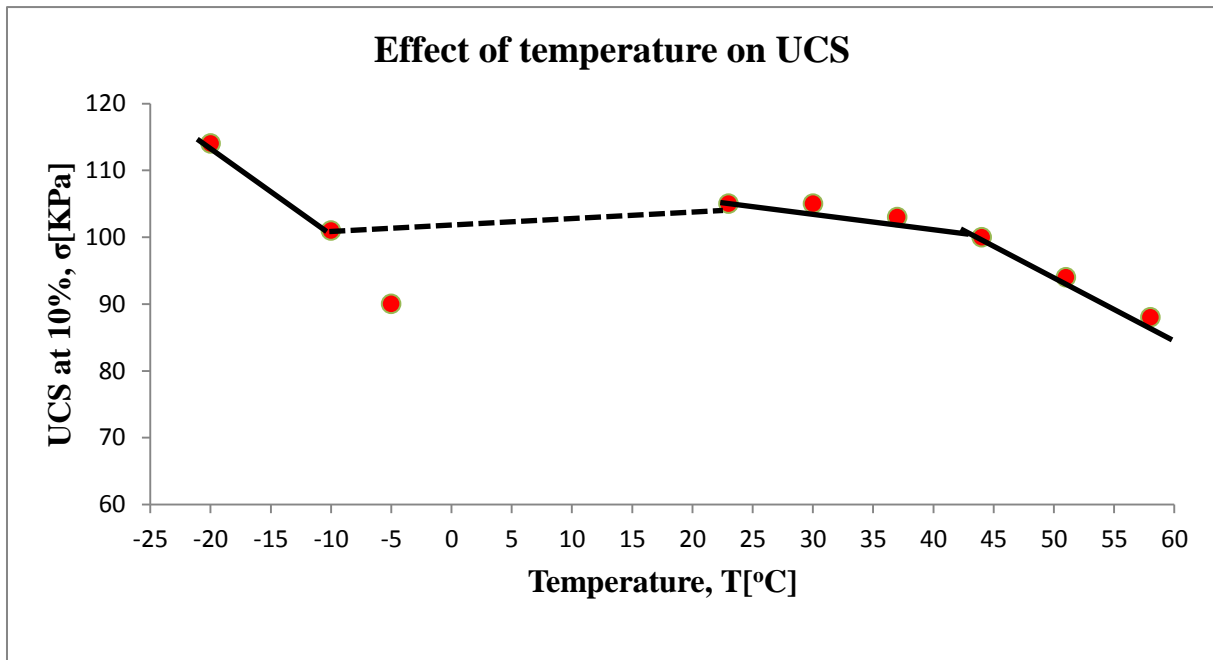


Figure 3.12: Compressive strength at different temperatures

3.4 Conclusion

Mechanical parameters of EPS, initial tangent modulus, poisson's ratio and compressive strength of EPS were evaluated in this chapter. Effects of loading rate, specimen size, shape and temperature have also been discussed.

Decreasing loading rate and increasing specimen size has a tendency of increasing initial tangent modulus. In addition, disc shaped samples in general tend to give a stiffer material parameter, a little over 6MPa, where subsequent lower values were obtained for cylindrical and cubic shaped samples. An overall average stiffness of approximately 5MPa was determined from this study. On the other aspect, a decrease in sample size has a slight tendency of underestimating the stiffness parameters. The effect of temperature in the lower

temperature range also showed an increase in stiffness as the temperature decreases. A 30% increase in stiffness for 5°C temperature difference is shown.

Compressive strength on different specimens under different cases was evaluated and similar attributes were found in the case of compressive strength as indicated for initial modulus. Study of the effect of loading rate shows an increase in compressive strength as loading rate decreases. The same effect has been shown for the increase in sample size and a decrease in sample temperature. A slight decrease in compressive strength is shown when the temperature increases based on a wide temperature (-20 to 58 °C) study of EPS. However, the degree of change is different in different temperature change. A steeper slope from -20 to 0 °C is shown whereas a constant value up to 20 °C is indicated and followed by a mild and steeper slope, having 44 °C as breaking point.

However, results obtained in this lab test showed lack of consistency and trend among data as it has been the problem for many cases.

Chapter 4

Long term deformation, creep of EPS geof foam

4.1 Introduction

Expanded polystyrene (EPS) geof foam blocks are used in many infrastructural works as filling/substitute material. Especially in geotechnics, some of the most important uses of EPS include: as a light weight filling material in road constructions, as apart of approach embankments in bridge as well as filling behind retaining walls to reduce earth pressure load. For such kinds of practices, EPS are subjected to a considerable compressive load which ultimately produces deformation. Long term deformation is therefore one of the major design part of EPS embankments. Codes including European standard dictates the limitation of such deformation for a design periods of 10, 20 and 50years.

Creep behavior refers to a time-dependent deformation process at a stress less than the strength of the material (Nielsen, 1974; Findley, 1960). When EPS is subjected to a permanent load for a long time, they deform by distortion of their lengths and angles of the chemical bonds connecting the atoms and/or by rearrangement of their atoms. These atomistic mechanisms under load lead to changes of the molecular chains in the semi crystalline polymer: uncoiling, straightening, and breaking in an amorphous region (i.e., randomly arranged part) and slipping between the chains in a crystalline region (i.e., orderly patterned part) [9]. The EPS block starts accumulating permanent deformation when the cellular structure started deforming plastically. This mechanism makes the sample to possess a much lower compressive stiffness than before and gradually lead to a rapid increase in the permanent deformation.

The compressive creep behavior can be divided into three stages as shown in *figure 4.1* primary, secondary, and tertiary creep. In the primary (or transient) stage, the strain increases with diminishing strain rate. During the secondary (or steady-state) stage, the strain increases linearly against time, resulting a constant strain rate. The tertiary stage is characterized by a rapid increase of strain. The creep strain rate decreases as creep strain increases [9]. The EPS material under compression acts as strong solid object which undergoes to a large strain without rupture or shear failure.

In order to study the immediate strain and creep of EPS, several researchers have performed tests on samples of EPS with different sizes and shapes. Creep tests have been also performed on both small scale samples and full scale EPS blocks. Long duration creep test results as well as accelerated creep test results are found during literature reviews. But, there is no common standard test procedure and correlation between tests in general. This has been the major problem in the inconsistency and scatter of parameters.

Dimensions of the test specimen, density, temperature, applied stress and duration of the test can affect the outcome of the result of creep test. Most tests reported in literature are performed on 50mm cubic samples, which are standard specimen dimensions for foam

materials. Sun (1997) and Sheeley (2000) have all reported creep results on this type of sample for stress level 30% of the compressive strength at 5% strain. A creep level between 0,8 to 0,95% have been registered.

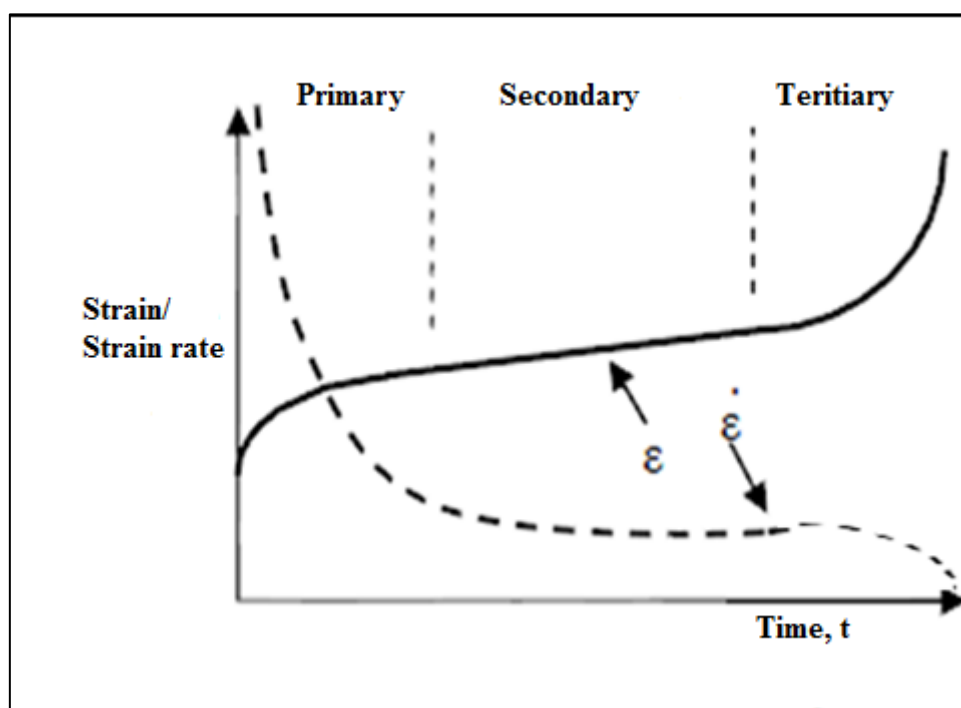


Figure 4.1: Typical compressive strain behavior [9]

Hovrath (1998) also have used test results from 50mm cube samples to furnish variables for Findley equation. However, cylindrical test specimens of dimensions $\phi=200\text{mm}$, 150mm and $h=100\text{mm}$, 300mm have been tested for varies densities and loading stress levels by Duškov M (1997).

Result comparisons from creep test performed on 100mm cubic samples at different load levels between 30% and 80% strength of EPS suggest a remarkable increase in creep development when the load increase. Figure 4.2 shows the difference in creep measurements for different stress levels [13]. For a typical application of EPS in road embankments, its stress level falls within the range of 20 – 50KPa and for this, a creep value of within 2% have been found.

The total deformation of a sample is comprised of an immediate deformation and creep. Immediate deformation of foam materials are considerable compared to long term deformation. Capturing the behavior of deformation at the start is crucial to obtain necessary information on total deformation. Nonetheless, creep is always associated with time. Therefore, the longer the creep test lasts the better to capture the behavior of EPS even if most percentage of the total deformation develops within a couple of days of after the load has been applied. Literature review on these aspects indicates the same. For example: Sheely (2000) has documented 1,35% of creep on 50mm cube samples within 500days of testing period of which 68% was developed in the first day. Duškov M (1997) found out 0,3% and 0,15%

immediate strain out of a 0,5% and 0,25% total deformation measured on cylindrical test samples respectively.

Temperature has also an effect on creep of foam structures. Molecular structure at room temperature has a strong bond attraction because of hydrogen and van der waals bonds. Whenever a temperature change occurred, the molecules in the structure respond by stretching the bond length. When temperature rises the polymers which make up the foam goes in to a transition state from glassy to rubbery. In glassy state the sample can goes to a brittle matter of stretching because of the limitation of space whereas in the rubbery state molecular chains can pass slide one another so that giving it an increase in length.(Ferry, 1980; Li, 2000; Roylance, 2001; Dowling, 2007). For a long term exposure of EPS at different temperature, EPS would go through a relaxation and contraction of polymer molecules which affect the development of creep throughout its service life time.

In this chapter, some of the basic variables which affect creep in the likes of sample size, shape and temperature are discussed. Laboratory creep test results from loading of cubical samples of EPS with different dimension and temperature are analyzed.

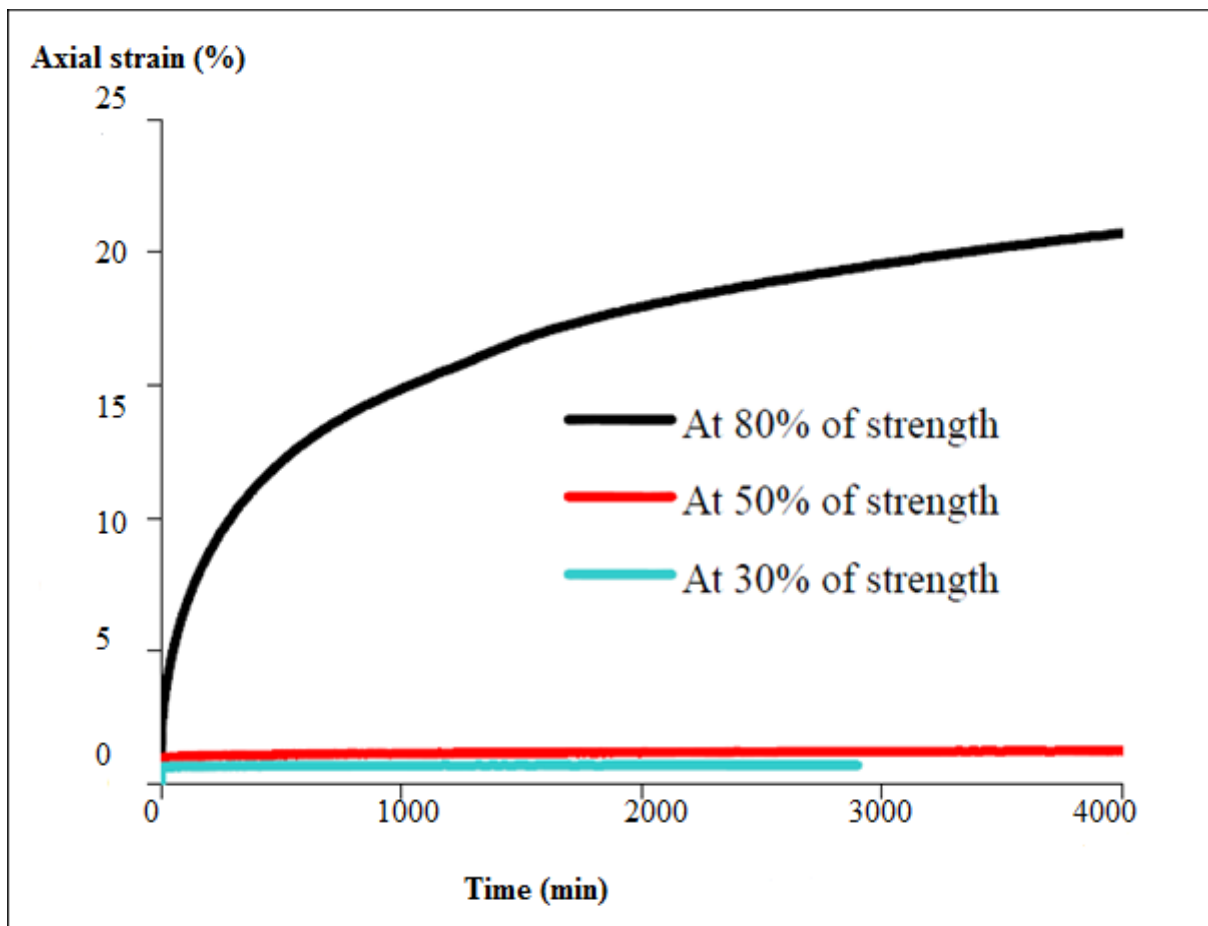


Figure 4.2: Creep behavior of 100mm cube of 18 kg/m³ density at different stress levels[13]

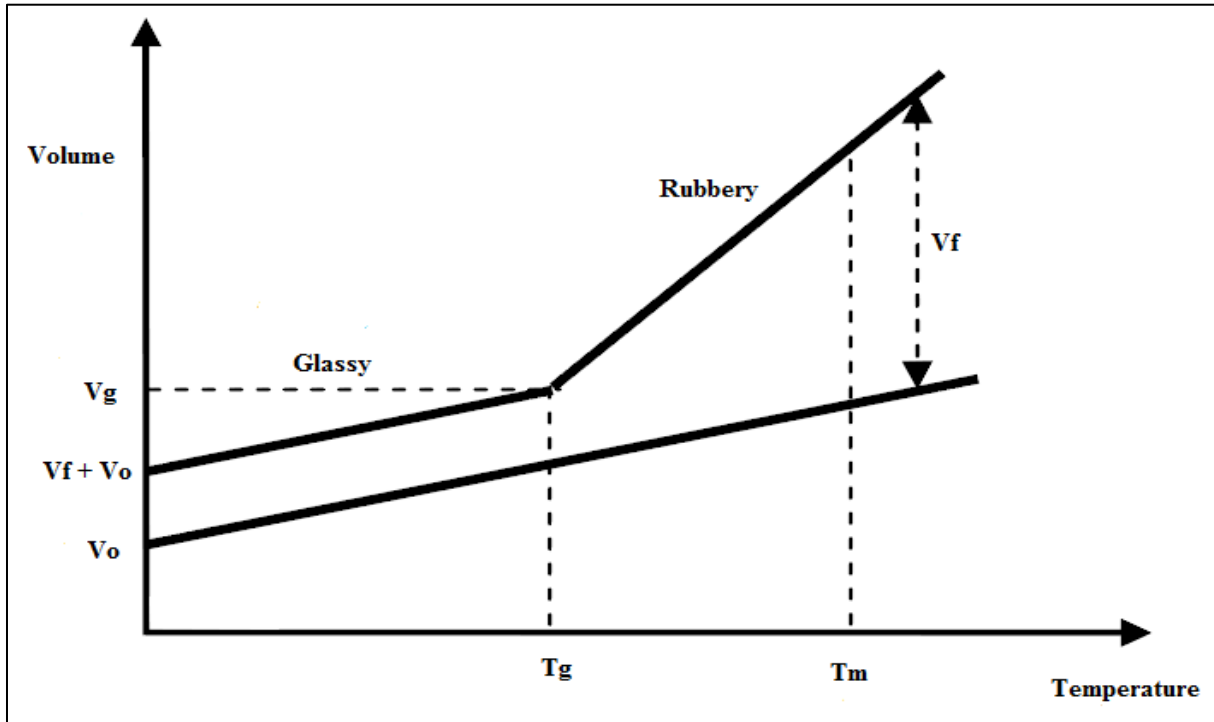


Figure 4.3: Volume change of polymer as a function of temperature; V_o = volume of polymer chains, V_f = free volume in polymer, and V_g = total volume at T_g , T_m = melting temperature [9]

4.2 Creep Test

4.2.1 General

Creep test is one of the essential and repetitive laboratory tests carried out to estimate the likely condition of the test subject within its design life. Characterizing creep behavior of foam structures is important since it is a major part of the design. As described in chapter 3, compressive strength and elastic modulus of EPS gathered from literature and laboratory test result from different sized test samples and at different temperature showed a clear pattern of variation. Therefore, creep development is expected to vary as well. Prediction of their property is even more highly important because of the sensitivity shown to some of the variables, for example, the abrupt increase in deformation when the applied stress level changes (figure 4.2).

Since EPS parameters heavily rely on test results from smaller size test samples, predicting the relation between sample size and recorded values of creep is of greater importance. It has been documented during literature reviews that smaller size samples tend to overestimate the total deformation. Not only the sample size but also the temperature can play an important role in defining the total deformation. The molecular structure of foam is known to be affected by temperature fluctuation. For constant loading of test samples at a controlled temperature, especially at lower temperatures, is of prime importance.

The main aim of this test is therefore, to study the effect of sample size, shape and temperature variation on the development of total deformation. Creep test is performed on 50mm, 100mm and 150mm cubic samples of EPS at -20, -10, -5 and 20°C. A typical dead load of 30KPa is imposed on it for 5 consecutive days. Results from this test are going to be used on the prediction of the likely performance of EPS within the design periods. Result comparison and discussion based on field measured data and published test results on the same topic will be presented in the following subsequent topics.

4.2.2 Test Material and apparatus

The same full EPS block used for UCS test is used here as well with density of 30Kg/m³ and dimensions of 2mx1mx0,5m. Because of the inconsistency or molding induced gradient of non-uniformity, variation on density and ultimately in mechanical parameters are expected. Therefore, samples are taken from the four corner sides and the middle of the block to make sure the entire block is represented.

Three sets of dimension have been used for this creep test; 50mm cube de-facto dimension as well as 100mm and 150mm cube samples. In addition to that, different shaped specimens (cubical, cylindrical and disc) are prepared to carryout creep test and investigate their effect. In order to ensure the repeatability of the test, each test was carried out twice in the same manner. Hand saw at first then vertical machine saw is used to cut the samples out from the original molded block and a smoothly shaped specimen is obtained from that as shown in *figure 4.4* below. A carving knife is used to bring the cylindrical as well as disc shaped samples.

The macrostructure of the sample as shown in pictorial presentation in *figure 4.5* below plays yet again an important role in sustaining a load for long term duration. The cell walls, which are constituted from pre-puffs or beads under high steam and pressure, undergo physical change as a response to loading.

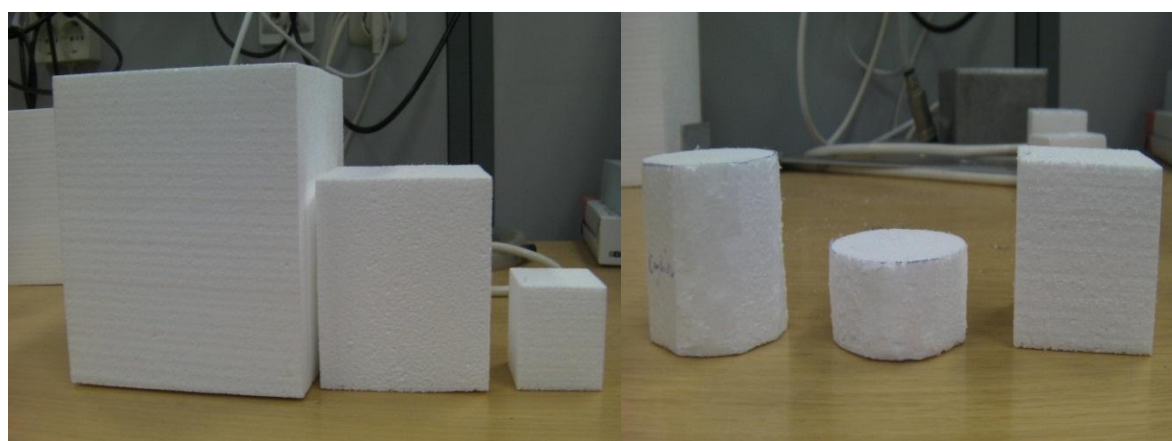


Figure 4.4: Pictorial presentation for tested specimens with different size and shape

A simple machine which used to measure creep for soft soils is rearranged to do the same for the EPS (*see figure 4.5*). The measuring gauge is changed from analogue to a digital altimeter.

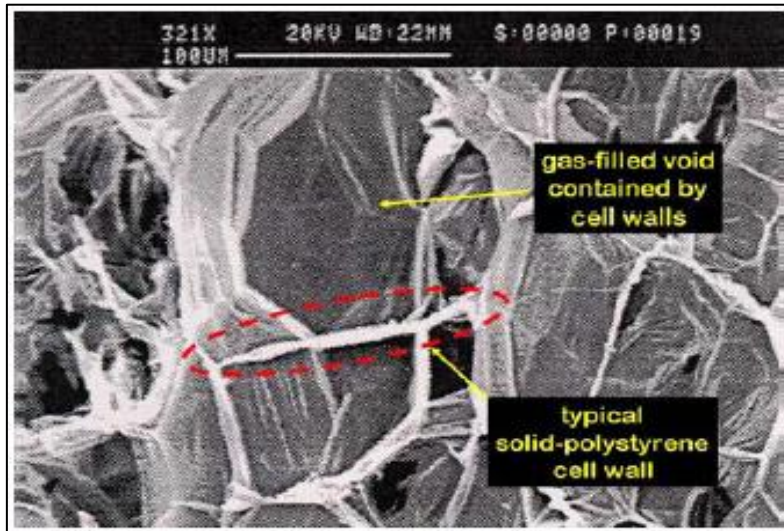


Figure 4.5: Typical EPS cell structure under 321-times magnification. [credit: unknown]

Modifications are made to the testing rod to make it more rigid and vertical by applying a horizontal clamp to the side. A 5cmx5cm plate is attached to the end of the rod to distribute 30KPa dead load imposed on it by a steel plate on top. Tests at lower temperature range is carried out at temperature controlled frozen lab by setting the room temperature at -20, -10 and -5 °C while normal room temperature is used for the other set of tests. Temperature of specimens are measured/controlled using picotech PT-100 data logger, which has four sensitive temperature measuring rods attached to the sample to be tested for the entire duration of the test.

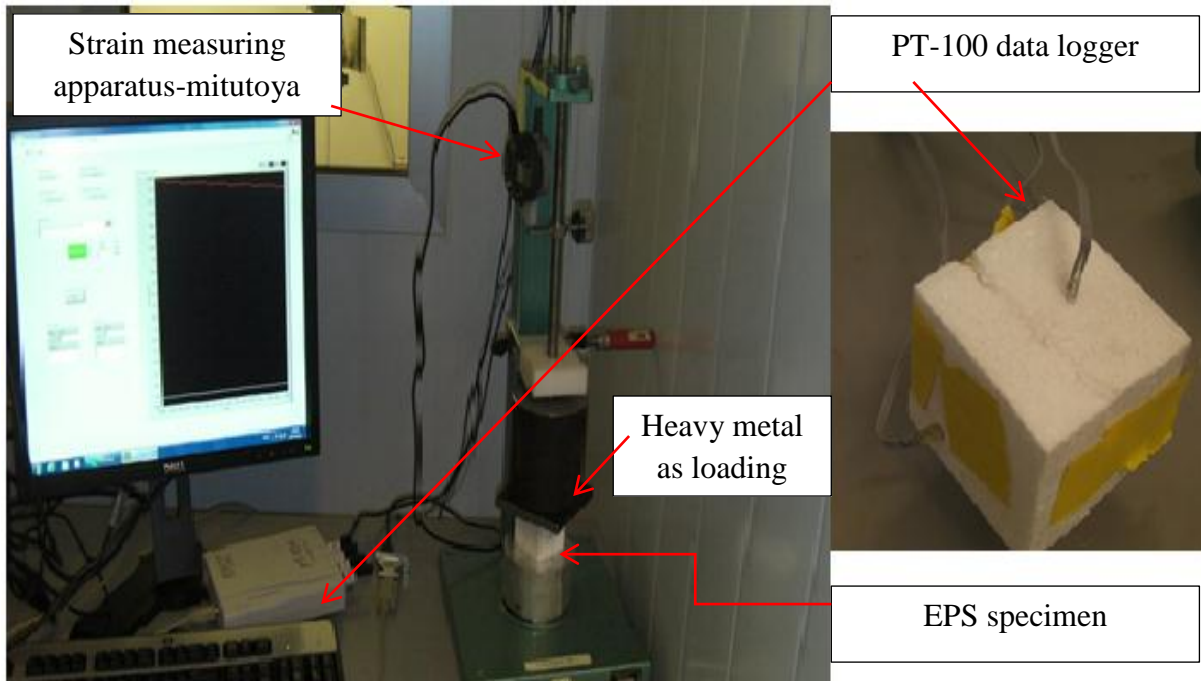


Figure 4.6: Pictorial presentation of test apparatus

4.2.3 Testing procedure

The samples are placed centrally on the base plate of the machine. Load carrying rod is lowered until the plate at the lower end of rod touched the surface of samples. The machine is placed where vibration effect can be minimized. For tests carried out at room temperature the sample is carried out at room temperature whereas the second set of tests is taken inside a temperature controlled lab by setting the temperature of the room to -20, -10 and -5°C. The samples are allowed to stay for at least 24 hrs before the test happened. Deformation measurements are taken by the digital altimeter installed on to the machine. A continuous reading for a consecutive 5 days is taken and analyzed. Detail sampling technics, testing procedure and sample data are presented in appendix B.2 and B.3.

4.3 Discussion

4.3.1 Total deformation

The main cellular structure of EPS, hexagonally shaped wall within which air is entrapped, is the main area that will be affected up on loading. Deformation starts on EPS due to the stretching and bending of cell walls which contributes high to the overall deformation. However, the creep strain of EPS, having a much simpler molecular structure, proceeds with the following steps [12]:

- Uncoiling and
- Straightening of the chains in the amorphous region,
- Slipping between lamellar planes in the crystalline region, and
- Breaking of the chains in the amorphous region (Smeets et al., 2001).

As mentioned in the previous introduction, predicting the total deformation under constant compressive load for EPS is highly of practical importance. In particular, identifying the initial deformation upon an instant loading due to dead weights imposed on the EPS by soil and pavement layer is the key for good performance prediction and the hardest challenge. Further deformation development, primary and secondary creep, for EPS also constitute an amicable amount to the overall deformation.

Field measurements on actual EPS construction sites as well as small and full scale laboratory tests firmly suggest more than half of the total deformation is achieved within the first week up on loading. Field measurement reports from Løkkeberg bridge, where 4,5 and 5m high EPS fill was used as an abutment in both sides for the temporary bridge, indicate that more than 60% of the total 1,35% deformation measured after 10years was immediate deformation. Similarly, Roald Aabøe, 1991 measured nearly 70% immediate deformation out of 1,2% total deformation for a 4mx4mx2m for EPS fill embankment. In addition, similar studies have been reported on small size samples where similar results gathered.

4.3.2 Effect of sample size and shape on total deformation

It is common to see design of EPS fill by using mechanical parameters obtained from small scale laboratory tests performed on 50mm cube samples. However, research results reported

independently on laboratory creep tests indicate that there is a scatter of results in deformation as the size and shape of the sample changes.

Creep test is performed on 50mm, 100mm and 150mm cubic samples of EPS to show the variation of results due to size difference and each test was performed twice accordingly to check repeatability. A compressive load of 30Kpa is applied on the samples continuously for 5 days and deformation is registered simultaneously. Up on results obtained, in general, total deformation registered during this test is higher than the expected values. Nearly 1% total deformation is registered within the first five days for 50mm cube samples, which is slightly higher than the normally anticipated values in the range of 0,7-0,8%. However, a lower values of 0,85% and 0,55% total deformation is gathered as the size of the samples changed from 50mm to 100mm and 150mm cubes respectively. In addition, more than 97% of the total deformation is immediate deformation. *Figure 4.7* shows comparison of total deformation on small scale samples, full block EPS and full scale EPS embankment. A subsequent reduction in total deformation is indicated and this can be attributed to the fact that stiffness increases as the size of the sample increases.

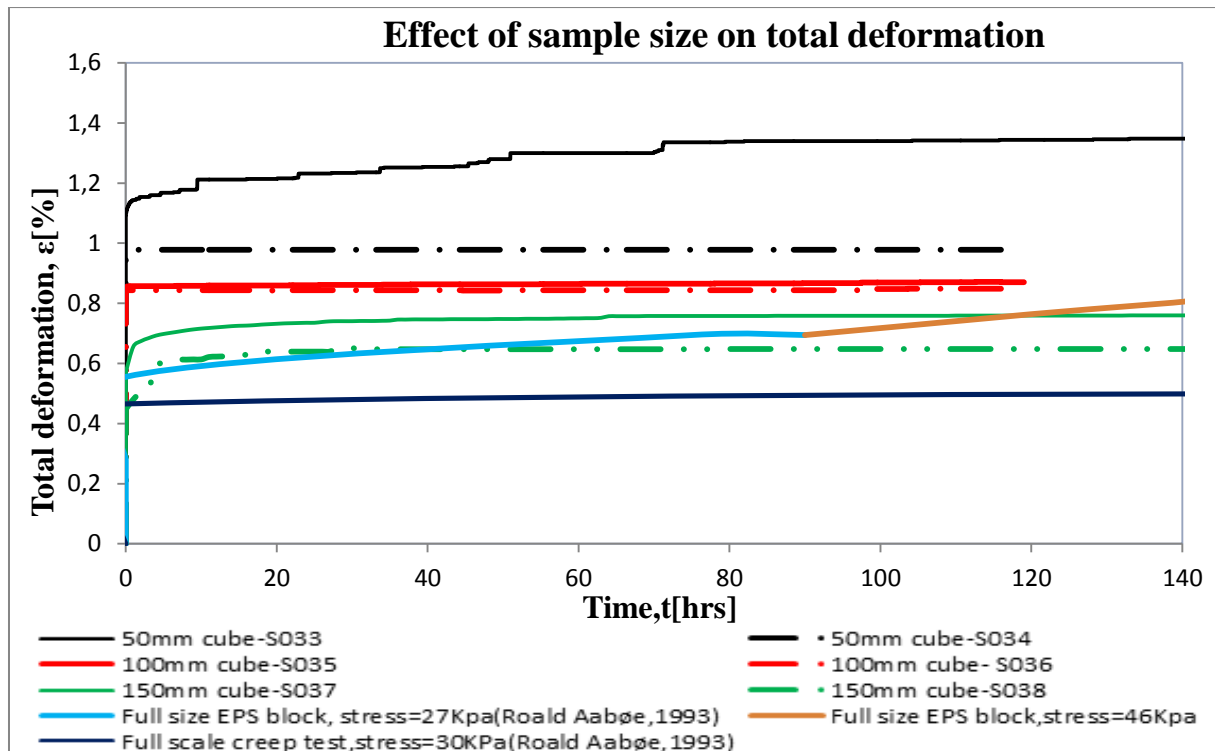


Figure 4.7: Effect of sample size on total deformation of EPS

Effect of sample shape on the outcome of total deformation is investigated by carrying out the same test for cylindrical and disc shaped samples. Almost the same total deformation, 1%, is gathered for cylinder, cube and disc shaped samples. However, the immediate deformation is slightly different as illustrated in *figure 4.8* below. Disc shaped samples mostly give the smallest immediate deformation but the rate of deformation is higher than the rest and for long test periods a highest total deformation can be registered.

4.3.3 Effect of temperature on total deformation

Temperature mainly affects the cellular structure of EPS by increasing or decreasing the molecular activity both in the cell walls and entrapped air. We should see the effect of temperature both in relation with the cell walls and the change in the entrapped air.

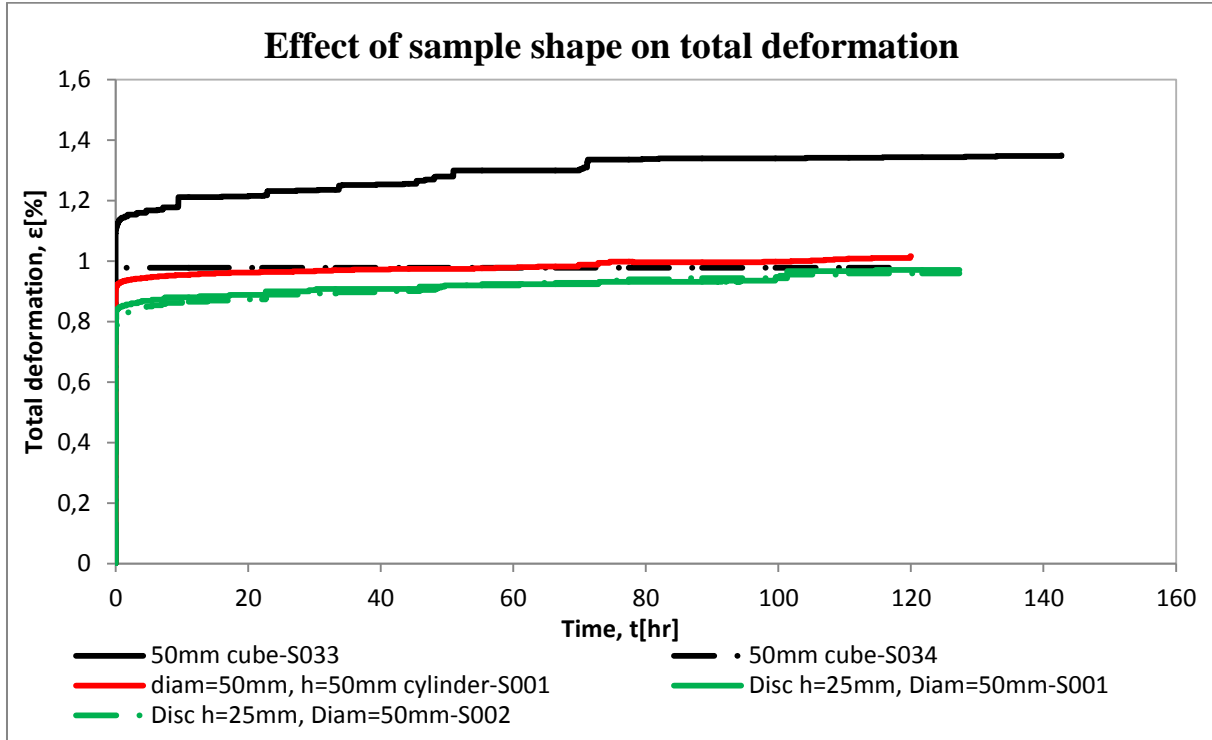


Figure 4.8: Effect of sample shape on total deformation of EPS

Deformation of EPS, in general polymers, happens when the main chain conformation is adjusted on a molecular level by rotation around bonds. These freedoms of rotation are highly controlled by the forces created by intra and inter molecular interactions. However, increasing the thermal energy increases the rate of change which allows larger molecular rearrangements and therefore deformation. Since, there is a direct relationship between temperature and thermal energy both macro and micro level deformation is dependent on temperature.

Diffusion is one of the fundamental processes by which material moves. Diffusion is a consequence of the constant thermal motion of atoms, molecules, and particles, and results in material moving from areas of high to low concentration. Whenever there is an increase in activation energy in the air molecules, the rate of movement will be much faster. Therefore, as temperature of the air increases the likelihood of air moving out of the enclosed cell to the environment is high allowing volume for extra deformation.

Laboratory test carried out to investigate the effect of lowering temperature in the lower level range rather gives a reverse result than the theoretical basis mentioned above. As illustrated in figure 4.9, the immediate deformation of EPS blocks under a constant compressive load of 30KPa shows a reduction as the temperature rises from -20 to -10 and -5 °C. An immediate deformation of 0,89%, 0,76% and 0,67% is found for the three temperatures respectively.

Several tests should be performed on each temperature to check repeatability and to have a good basis for comparison. However, this test slightly demonstrates even to the lower temperature levels where the molecular activities considerably reduce, temperature still affects the deformation of EPS geofoam blocks.

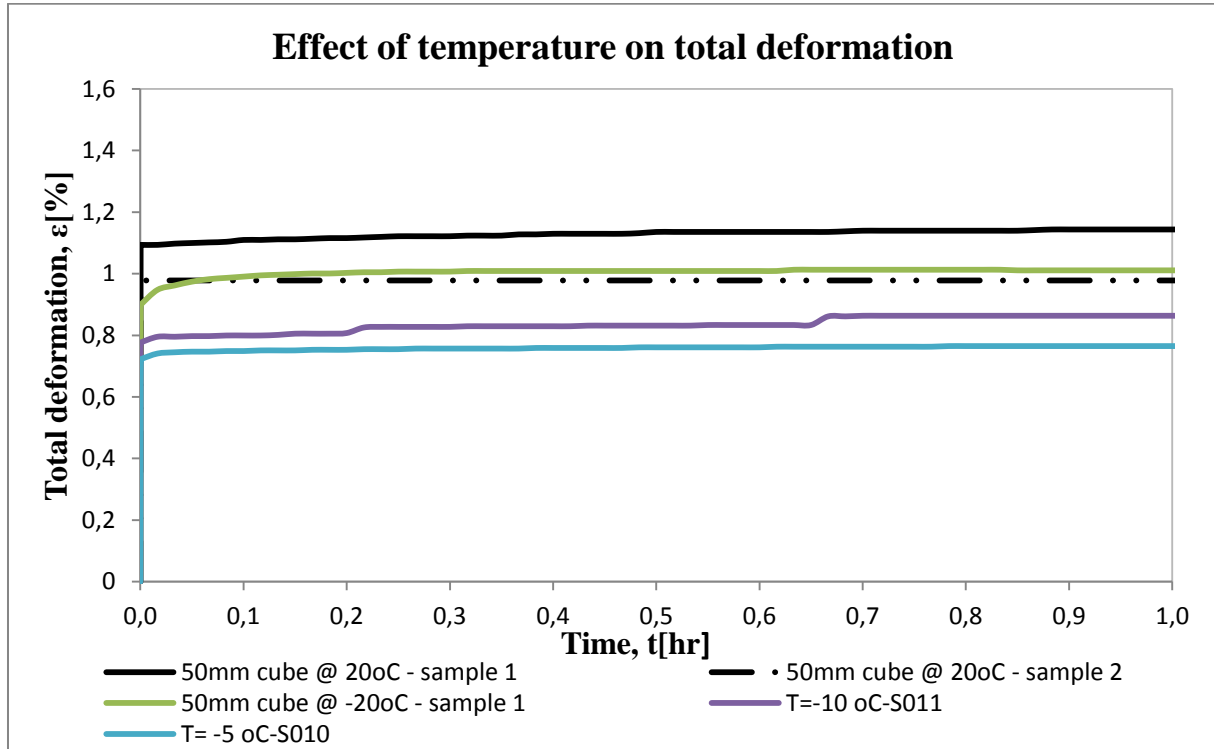


Figure 4.9: Effect of temperature on total deformation of EPS

4.4 Accelerated creep tests

In design practice EPS, polymers in general, have to be designed both for short and long term criteria. Total deformation or creep is one of the design issues that must be addressed properly for longer design periods of 10, 15, 20 or 50 years. However, conventional laboratory creep tests take prolonged time to gain the necessary data for design and usually the test period is not enough. In order to address the issue of time, several accelerated creep tests have been suggested to limit the time taken by the conventional methods. In this section, three of the most commonly used accelerated creep tests: time-temperature superposition method (TTS), stepped isothermal method (SIM) and time temperature stress superposition (TTSS) method will be discussed. Illustration of accelerated creep in graph for all the three types is presented in appendix C.

4.4.1 Time-temperature superposition method

It is known that temperature plays a huge role in the development of creep on polymers. The concept of time-temperature superposition (TTS) comes from the observation that the time-scales of the motions on constituent molecules of a polymer are affected by temperature. More specifically, the motions or relaxations occur at shorter times at high temperatures [27]. Furthermore, by assuming that the whole relaxation spectrum of a polymer can be affected by

increasing temperature, it is possible to look at the long-time properties of materials by simply changing the temperature and moving it to experimental time window in a systematic manner.

The higher temperature creep curves can be shifted along the logarithmic time scale to reconstruct a creep master curve and this can be used to predict long term deformation. After checking kinetic parameters, such as activation energies, from the shift factors then test duration and temperature can be in compliance by simple shift along the logarithmic axis of time. Therefore, master curve, made up of short-time tests, should represent the creep compliance over long times.

Time-temperature superposition is not, however, as simple as frequently implied. This is especially true at temperatures below T_g (glass temperature). Successfully employing time-temperature superposition below T_g is limited by the problem of normalization due to changes in the limiting compliance as a function of temperature. If the limiting compliances change with temperature, then the shape of the compliance curve changes with temperature. Higher temperature curves are then not superposable. In addition, a distribution of activation energies will cause a change in the shape of the relaxation spectrum with temperature. This will also change the shape of the compliance curve with temperature, precluding the use of time-temperature superposition [28].

4.4.2 Stepped isothermal method

The principle of the SIM is that a single element is placed in a testing machine and loaded by a chosen force. The temperature is then rose, typically by a few °C, and kept constant for a fixed period of time, typically a few hours. The sequence is then repeated at a slightly higher temperature, on the same sample. Some manipulation of the data is required in order to compensate for the temperature steps.

In SIM tests, a single specimen is tested at a sequence of temperature levels under a constant load. Three different adjustments are needed for each SIM test to produce a single master creep curve; the creep-rupture prediction comes from the end of the master curve when the specimen fails under a specific load and temperature. The vertical shift allows for the strains caused by the change in temperature, taking account of the creep that occurs while the temperature change is taking place. Rescaling is needed to allow for the previous history of the specimen: when the temperature changes some allowance must be made for the fact that some creep has already taken place under the previous time steps. This adjustment takes the form of a shift in the time direction when plotted against a linear time scale. The horizontal shift takes the form of a shift on a creep strain vs. log (time) plot [29].

4.4.3 Time-temperature-stress superposition

Apart from temperature, stress is also the other external force that changes the internal structure of polymers. TTSS has the same principle and test procedures as what is used in TTS however, loading the samples at different stress is added. The main advantage of using TTSP is it allows you to reduce the maximum temperature that has been used if someone uses TTS. This is to the fact that increasing the stress also facilitates the increase in creep.

4.5 Conclusion

Long term deformation of EPS using laboratory test results and literature studies were evaluated. In addition, the effect of sample size, shape and temperature were also evaluated.

Specimen size has an influence in determination of creep for EPS. As the specimen size increases, the relative stiffness of EPS also increases leading to a decrease in creep. A slightly higher total deformation values are registered during the 5 day test. Deformation value of 1%, 0.85 and 0.55% for 50mm, 100mm and 150mm cube samples respectively. A much lower values are registered for full scale tests. Disc shaped samples produce less immediate deformation than cylinder or cube. However, the rate of deformation increases as time progresses.

Mechanical parameters of polymer materials including EPS are highly dependent on temperature. Laboratory test performed for EPS under lower temperature ranges gives unexpected value. As temperature rises from -20 to -10 and -5 °C, the total deformation decreases. Number of tested sample and uncertainty of measuring methods are raised as a reason. Finally, alternative way of creep test in the lab is discussed.

Chapter 5

FEM simulation of EPS geofilm

5.1 Design criteria of EPS geofilm embankment

EPS geofilm embankment consists of three major components: the top pavement structure, the light weight fill (EPS) and the subsoil foundation. Therefore, failure of EPS geofilm embankment could be the failure of either of its components and for safe design each component should fulfill the required design criteria. The criteria's for each component of the embankment depends on what is failure for the respective side and they are described subsequently.

Design phases of EPS geofilm embankment should address failures which corresponds to serviceability failure (e.g., excessive settlement of the embankment or premature failure of the pavement system) or collapse or ultimate failure (e.g., slope instability of the edges of the embankment).

The objective of pavement system design is to select the most economical arrangement and thickness of pavement materials that will be founded on EPS blocks. The design criterion is to prevent premature failure of the pavement system (as defined by rutting, cracking, or a similar criterion). Proper connection between the thick pavement structure, whether a flexible or rigid, and the fill mass is necessary to avoid the sliding of the pavement structure over the fill mass.

For most cases of EPS fill embankments, the foundation subsoil is soft. Higher settlements can be expected to develop on the subsoil for loads coming from the pavement structure and the light weight fill mass. Settlement is the amount of vertical deformation that occurs from immediate or elastic settlement of the fill mass or foundation soil, consolidation and secondary compression of the foundation soil, and long-term creep of the fill mass at the top of a highway embankment. For the overall embankment to be safe, the total settlement should be within the limit of the allowable settlement. Other design criteria, bearing capacity of the subsoil and global stability of the overall embankment should be well above from the safety standards required. Design failure of soil fill mass on the side of the slope should be also avoided.

The light-weight fill material (EPS) should be able to fulfill the criteria for safe design. Load bearing capacity, immediate and long term creep deformation of EPS are important aspects of design. Since EPS has good compressive strength capacity, the major concern for design of EPS is long term deformation or creep. High deformation on the light weight fill mass causes a ragged and highly deformed pavement structure.

5.2 Soil models for EPS geofilm

Different models exist for soils from sophisticated to simpler ones and selecting appropriate model for EPS is an important step to study its engineering behaviors. Under loading, EPS

shows σ - ϵ curve which has two distinct lines: a linear elastic line and a plastic line. As illustrated in *figure 5.1* below, a typical stress strain diagram of EPS specimen can be approximated well as linear up to 1% strain and displays visco-plastic behavior after the initial linear elastic deformation without apparent rupture, distinguishable slippage, or interaction between particles. Similar stress strain curves has been produced for soils from triaxial and oedometer tests but plastic in nature rather than viscoelastic after elastic deformation. Using similarities in stress strain relationship, therefore, one can calibrate EPS parameters using models usually used for soils. Once calibrated, further parameter studies for EPS can be performed to simulate the different loads and loading rates of EPS subjected during its project life time.

Widely used soil models, hardening soil model and soft soil cree models, will be described in the following topics. Discussions on the outcome of the models will be presented later.

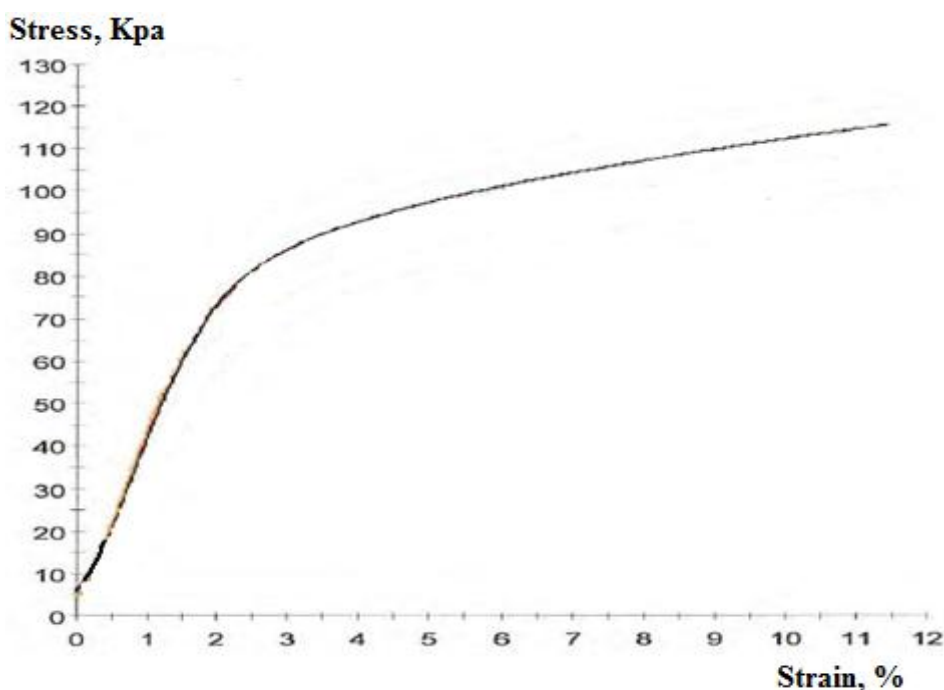


Figure 5.1: σ - ϵ curve of EPS 100 (ref.2)

5.2.1 Hardening Soil model

Limitation of good data to establish σ - ϵ relationship for a soil makes it harder to establish stiffness parameters. Models which are able to capture the soil property during loading and unloading fill the gap of data limitation. Hardening soil model is one of the latest models based on theory of plasticity, which better explains the soil rather closer to the reality.

Hardening soil model is an advanced hyperbolic soil model (often describes the non-linearity of a soil) formulated in the framework of hardening plasticity. The main difference with the Mohr-Coulomb model is the stiffness approach. Here, the soil is described much more accurately by using three different stiffness inputs: triaxial loading stiffness E_{50} , triaxial unloading stiffness E_{ur} and the oedometer loading stiffness E_{oed} . Apart from that, it accounts

for stress-dependency of the stiffness moduli, all stiffness's increase with pressure (all three inputs relate to reference stress, 100kPa). The plastic yield surface is not fixed and can expand due to plastic straining and it accounts dilatancy of soil.

A) Constitutive Equations

The hyperbolic relationship between the vertical strain, ε_1 , and the deviatoric stress, q is the basic idea for the formulation of the hardening soil model. When soils are subjected to a primary deviatoric loading, they tend to show a decrease in the stiffness accompanied by a development of plastic strain.

The constitutive equations developed for hardening soil modeling is based on test results of a standard drained triaxial test. The relationships between deviatoric stress and axial strain, *figure 5.2*, from the test result can be best fitted by a hyperbola curve in a Cartesian coordinate system. The curve can be best described by the following two formulas:

$$\varepsilon_1 = \frac{qa}{2E_{50}} \frac{\sigma_1 - \sigma_3}{qa - (\sigma_1 - \sigma_3)} \quad (5.1)$$

$$q_f = \frac{6\sin\phi_p}{3-\sin\phi_p} (P + C\cot\phi_p) \quad (5.2)$$

$$qf = M (P + C\cot\psi_p) \quad (5.3)$$

$$qa = q_f/R_f \quad (5.4)$$

Parameters C and ϕ_p are from Mohr-Coulomb failure criterion and R_f is the failure ratio. A default value of $R_f=0,9$ is used as $R_f=1$ indicates a plastic yielding.

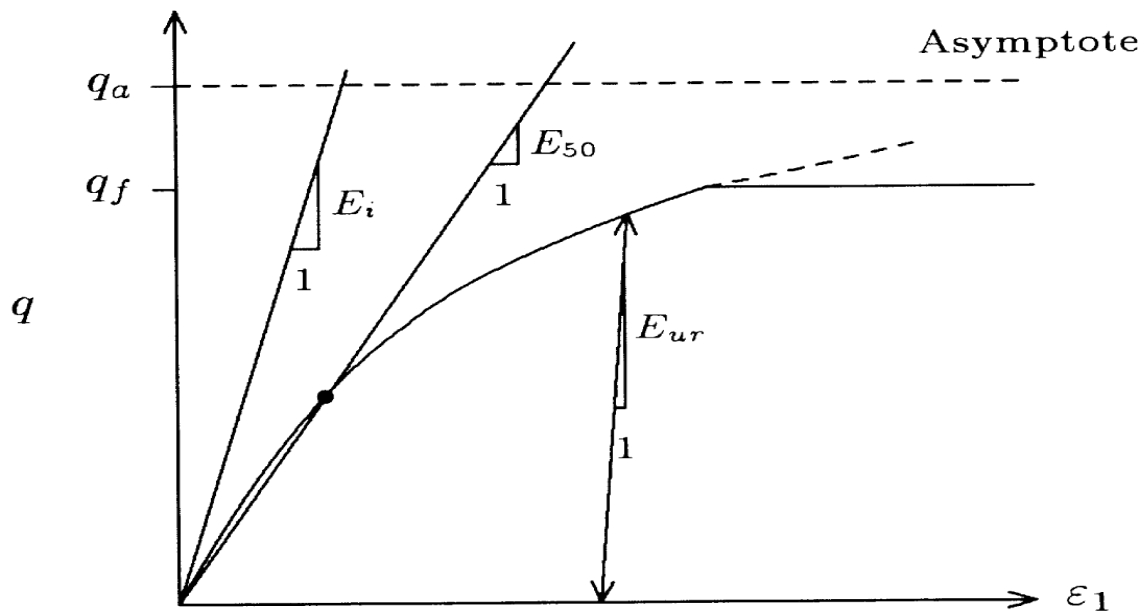


Figure 5.2: Hyperbolic stress-strain relation for primary loading for a standard drained triaxial test

B) Stress dependent stiffness

The stress-strain relationship of vertical loading is highly non-linear. Assigning stiffness parameter for the soil which represents the entire loading conditions is difficult. One stiffness parameter, initial tangent modulus can be used to represent the stiffness of the soil. But, for better representation of the soil unlike the Mohr-Coulomb model which uses a fixed stiffness parameter, the stiffness in HS model is dependent on the confining stress.

$$E_{50} = E_{50}^{ref} \left[\frac{(\sigma_3' + a)}{\sigma_{ref} + a} \right]^m \quad (5.5)$$

σ_{ref} is the reference atmospheric pressure, 100KPa and E_{50}^{ref} is a reference stiffness modulus corresponding to the reference stress, σ_{ref} . The extent of dependency of stiffness on stress is indicated on the m parameter. Usually m= 0,5 and 1 is used for sand and soft clays respectively.

$$E_{ur} = E_{ur}^{ref} \left[\frac{(\sigma_3' + a)}{\sigma_{ref} + a} \right]^m \quad (5.6)$$

In HS-model, the unloading/ loading path is modeled as purely non-linear, elastic and E_{ur} is used for further calculation. Similarly, E_{ur}^{ref} is the value of Young's modulus for unloading/loading part for the reference stress.

$$G_{ur} = \frac{1}{2(1+\nu_{ur})} E_{ur} \quad (5.7)$$

The elastic strains can come from the deviatoric loading and from the first consolidation. The elastic strains in HS-model are calculated using Hook's formula.

$$\varepsilon_1^e = q/E_{ur} \quad \varepsilon_2^e = \varepsilon_3^e = \nu_{ur} q/E_{ur} \quad (5.8)$$

C) Yield Surface

HS-model use isotropic hardening connected to two plastic yield surfaces: cone and cap. The **cone** plastic yield surface is described Mohr - Coulomb criterion. Plastic shear strain, γ^p , is the relevant parameter to the development of the failure surface. For a typical drained triaxial test, the failure conditions can be indicated in a $P^p - q$ diagram.

$$f_{12} = \frac{qa}{E_{50}} \frac{\sigma_1 - \sigma_2}{qa - (\sigma_1 - \sigma_2)} - \frac{2(\sigma_1 - \sigma_2)}{E_{ur}} - \gamma^p \quad (5.9)$$

$$f_{13} = \frac{qa}{E_{50}} \frac{\sigma_1 - \sigma_3}{qa - (\sigma_1 - \sigma_3)} - \frac{2(\sigma_1 - \sigma_3)}{E_{ur}} - \gamma^p \quad (5.10)$$

$$\gamma^p = \varepsilon_1^p - \varepsilon_2^p - \varepsilon_3^p = 2\varepsilon_1^p - \varepsilon_2^p \approx 2\varepsilon_1^p \quad (5.11)$$

By setting equation 5.9 and 5.10 to a value of 0 for constant value of γ_p , we can plot the points in P-q plane until the Mohr-Coulomb failure criteria defined by equation 5.3 is reached. For cone yielding surface we use parameters from triaxial test results such as E_{50}^{ref} and E_{50} .

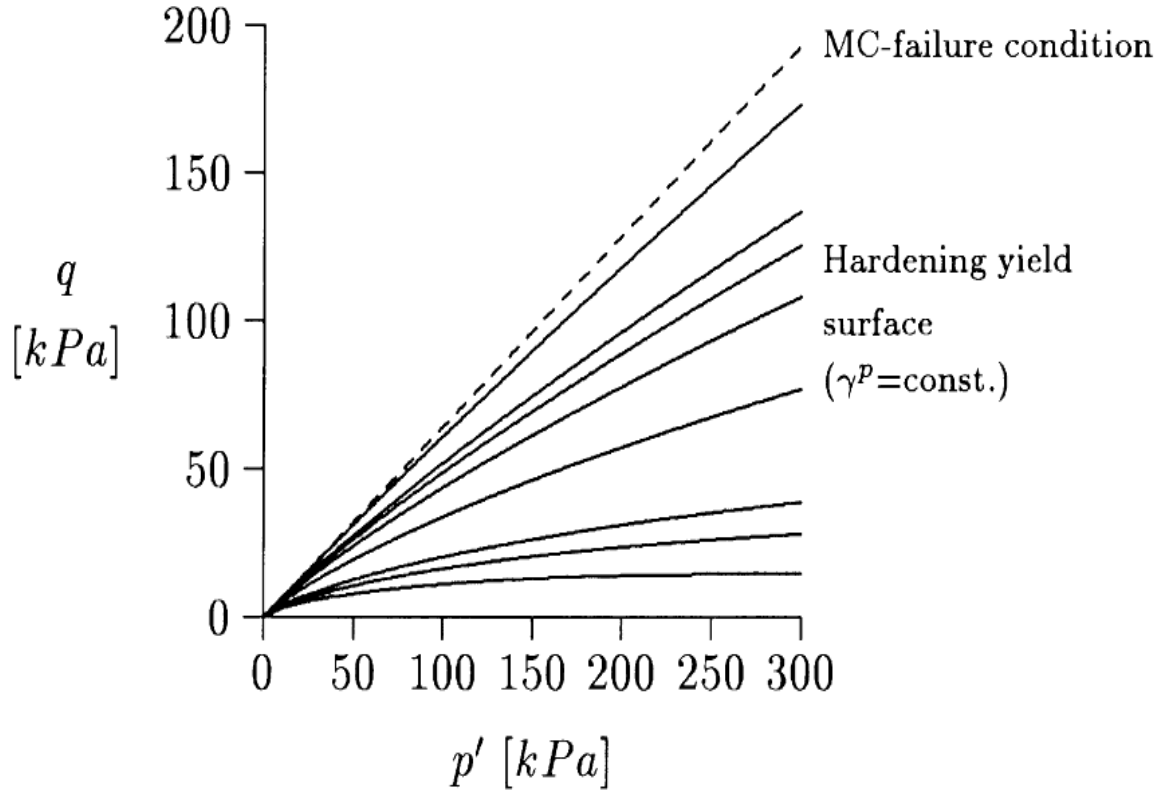


Figure 5.3: Successive values of yield loci for various values of hardening parameter γ_p and failure surface.

Even if volumetric strain is close to zero for coarse grained soils, we cannot essentially say it is zero. Shear yield surfaces indicated on figure 5.3 above do not explain ϵ_v . Therefore, the need for another yield surface to close the elastic region on the p-axis is important. This creates a *cap* yielding surface which is controlled by a preconsolidation stress.

The function of cap yielding surface coincides with the result that we see in oedometer test. Depending on the preconsolidation level, we use oedometer parameters such as E_{oed}^{ref} and E_{oed} .

In HS-model as in every model uses the relationship between volumetric and plastic shear strain rate. Dilatancy parameter is used to connect between the two. The flow rule relation between them is as follows:

$$\dot{\epsilon}_v^p = \sin \psi_m \dot{\gamma}^p \quad (5.12)$$

Dilatancy is connected to the development of plastic strains and related to cone yielding surface only.

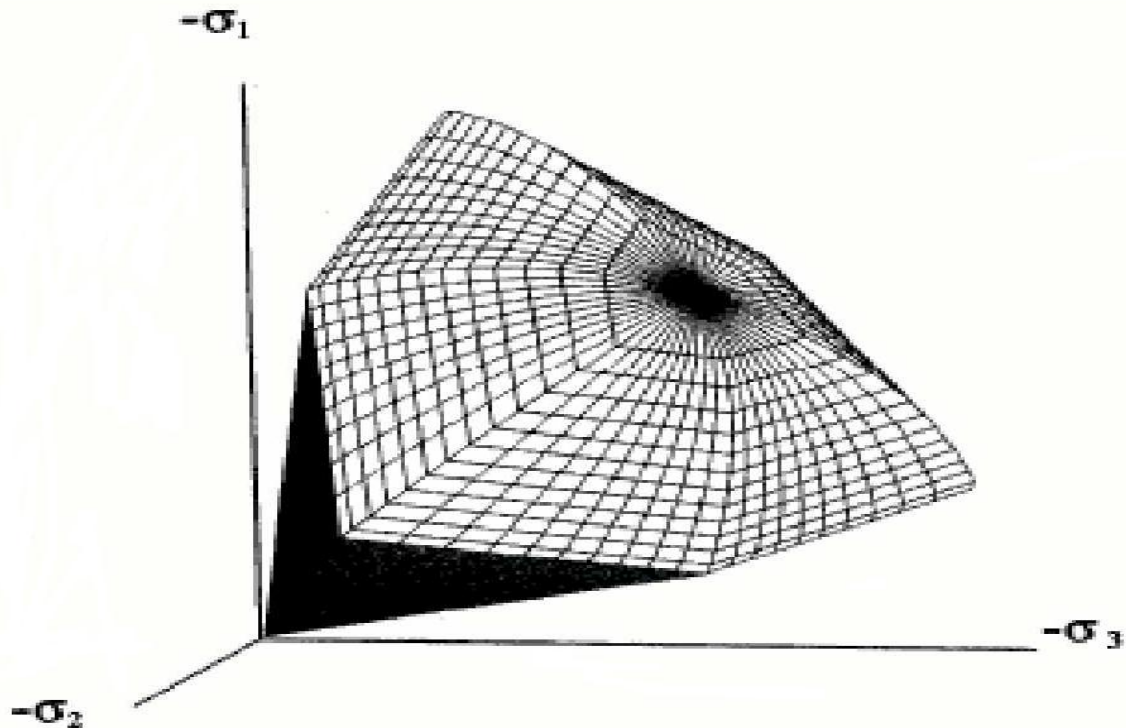


Figure 5.4: Cap yielding surface of hardening soil model

5.2.3 Soft soil creep model

The model was designed for highly compressible soils: peat, nearly normally consolidated clay and clayey silt. It is one of the families in cam clay model which are based on critical state soil mechanics.

A) Main principle

The main principle of soft soil creep model comes from the unique interpretation of oedometer test result. After load application, the pore pressure dissipates and primary then secondary strain starts to accumulate. From recorded stress strain diagram, modulus number for both over and normally consolidated regions are used as an input in PLAXIS after some rearrangement. Unlike HS model in which the modulus depends on some reference modulus and σ_3 , in SSC model modulus number only depends with stress over time. *Figure 5.5* illustrates the development of SSC model for one dimension parameters using oedometer results.

A) Yield surface

The yield surface of SSC model is controlled by the preconsolidation stress, which is the control parameter for plastic strains. An elliptic preconsolidation surface will, for increasing p' , expand and slide along the control line from origin and through the crown of the ellipse as shown in *figure 5.6*.

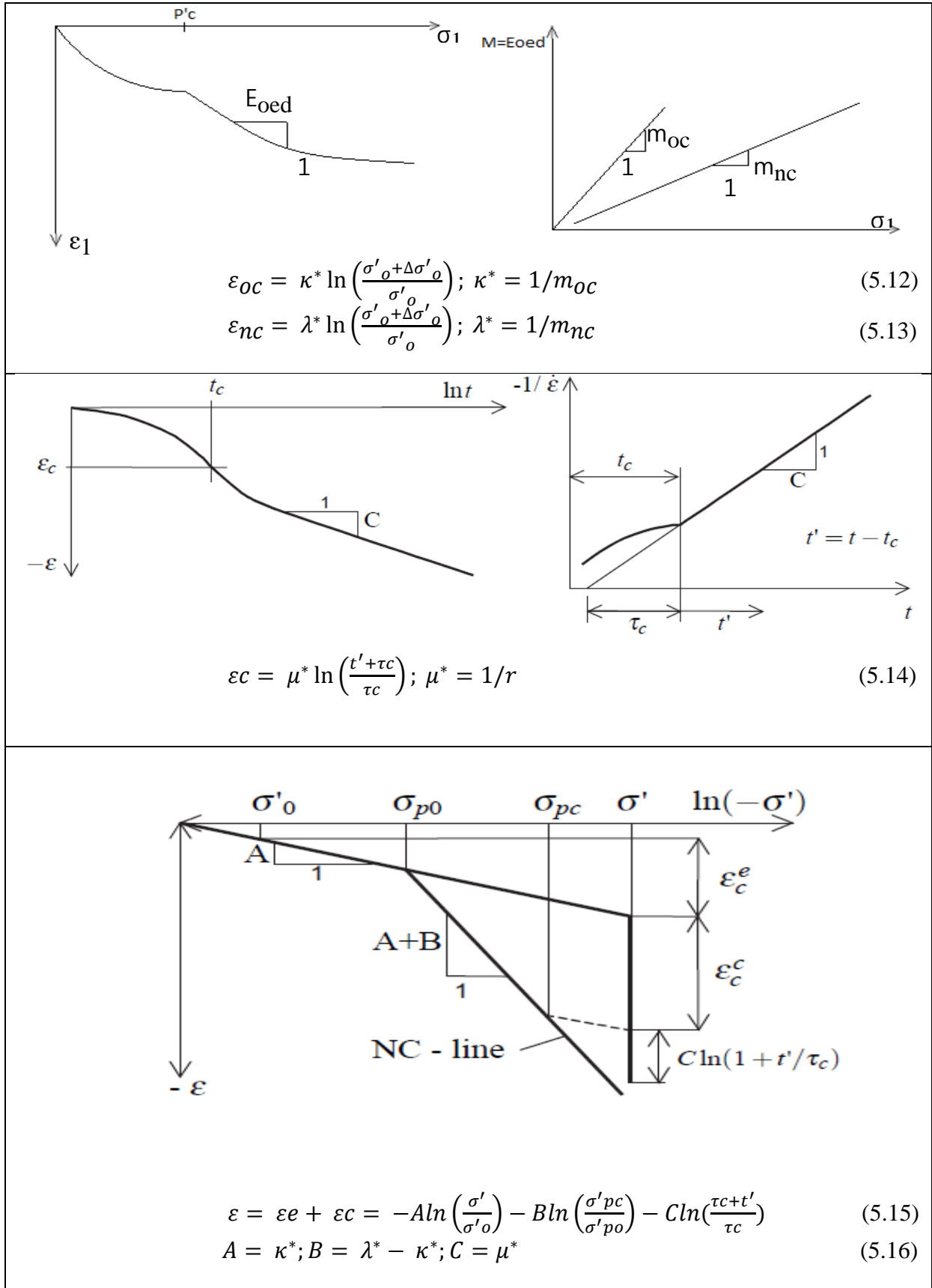


Figure 5.5: SSC model 1D derivation [23&24]

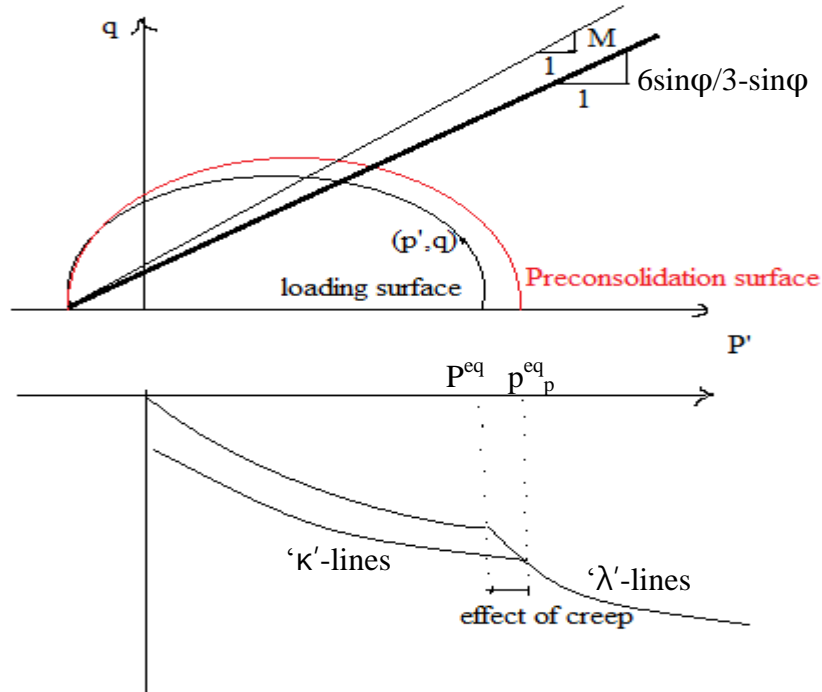


Figure 5.6: Yield surface for SSC model [23]

ε_v

5.2.4 Constitutive models for EPS geofoam

There is a continuous development in modeling EPS geofoams. Earlier times the models were designed to describe the behavior of stress-strain-time. The most famous and practical models include time dependent- Findley model and time independent- preber et al model. But, in this section hyperbolic constitutive models developed from triaxial test results on cylindrical EPS samples ($h=100\text{mm}$ and $\phi=50\text{mm}$) under different confining pressures (0, 20, 40 and 60KPa) and different density materials (15, 20,25,30 Kg/m^3) [25] is discussed.

A constant strain rate of 1%/min was used to load the samples and nonlinear stress strain diagram was developed for different density and confining pressure. But the effect of density on compressive strength and initial tangent modulus were more visible than the confining pressure. In the same test, volumetric strain and principal strain were measured and a linear relationship with a good fit was possible for most of the data.

The hyperbolic model (similar to HS model) has been used to describe stress-strain behavior of the test results for EPS. The mathematical form of the model is represented by the deviator stress and the major principal strain terms with material-dependent constants. In this typical model, the stress strain relationship was made to be a function of confining stress and density. Poisson's ratio was assumed to be dependent on confining stress as well. Subsequent relationships derived from the test are provided as follows:

$$\sigma_1 = \frac{a\varepsilon_1 b(\%)}{c + \varepsilon_1 b(\%)} \quad (5.17)$$

$$a = -60,955 + 9,843\gamma + 0,339\sigma_3 \quad (5.18)$$

$$b = 1,135 + 0,042\gamma - 0,008\sigma_3 \quad (5.19)$$

$$c = -0,437 + 0,102\gamma - 0,002\gamma^2 + 0,011\sigma_3 - 0,00039\gamma\sigma_3 \quad (5.20)$$

Where: γ is the density of EPS geofoam (kg/m^3) and σ_3 the confining stress (kPa).

Also from the derived equations, tangent modulus and poisson's ratio were provided as a function of axial strain as shown in equation 5.21 and 5.22.

$$Et = \frac{\partial \sigma}{\frac{\partial \varepsilon_1(\%)}{100}} = \frac{abc\varepsilon_1(\%)^{(b-1)}}{\varepsilon_1(\%)^{2b+2c\varepsilon b_1(\%)+c2}} * 100 \quad (5.21)$$

$$\nu = \frac{1}{2} \left[1 - \left(\frac{\varepsilon_v}{\varepsilon_1} \right) \right] \approx 0,0967 + 0,00308\gamma - 0,0023\sigma_3 \quad (5.22)$$

It can be seen that the mathematical form of the proposed model is different from the typical hyperbolic function represented by the deviator stress and the major principal strain terms with material-dependent parameters. These parts of difference between the models may be due to the different deformation processes of EPS geofoam and soil. As shown from data outputs, EPS geofoam deforms mostly in major principal strain direction with relatively small lateral deformations. A soil, however, undergoes contraction or dilation processes affected by the soil properties, confining stress, and deviator stress. Therefore, the stress-strain response of EPS geofoam can be effectively represented in terms of major principal stress and strain [25]. Finally, the model was verified using test data under different conditions and a good correlation was found.

5.3 Calibration of EPS parameters using soil models in PLAXIS 2D

Unconfined compressive strength test has been performed in PLAXIS soil test by setting σ_3 to zero under triaxial test tab. Different parameters has been used to develop stress-strain relationship, during which the duration of the test was kept to 1 hr and maximum allowable strain to 20%. Comparison up on results obtained from the two models, hardening soil model and soft soil creep model, with UCS test results obtained from testing 50mm cubical EPS block is presented in this section.

Figure 5.7 and 5.8 illustrates calibration σ - ε relationship obtained from PLAXIS 2D using the two different models and different parameters for each shown in table 5.1. Comparison of output results indicates well correlation between FE output and tested EPS samples. Since both soils and polymers show elastic behavior for small strain at the beginning, initial tangent modulus calculated for stresses between 0 and 1% strain is well captured for both models. Initial modulus in the range of 5 to 6MPa is common for 50mm cubic EPS samples and the same range of values is obtained from FE output for HS model and slightly higher value for SSC model. Compressive strength both at 5 and 10% strain are slightly underestimated in FE output in general. This is attributed to the fact that polymers tend to show a higher resistance because of their viscoelastic nature rather than plasticity as in the soils. Summary of calibrated results are presented in table 5.2.

Table 5.1: Summary of input parameters for calibration in PLAXIS 2D

Material Parameters Used for PLAXIS input										
Parameter	Name	EPS layer								Unit
		HS1	HS2	HS3	HS4	SSC1	SSC2	SSC3	SSC4	
Material Model	Model	HS				SSC				
Type of material behaviour	Type	Dr'd*	Dr'd	Dr'd	Dr'd	Dr'd	Dr'd	Dr'd	Dr'd	
EPS unit weight	γ	0,2	0,2	0,2	0,2	0,2	0,2	0,2	0,2	KN/m ₃
Young's Modulus	E_{50}^{ref}	6000	5000	4000	6000	-	-	-	-	KN/m ₂
	E_{oed}^{ref}	6000	5000	4000	6000	-	-	-	-	KN/m ₂
	E_{ur}	1800 0	1500 0	12000	1800 0	-	-	-	-	KN/m ₂
Flexibility coefficients	λ^*	-	-	-		0,125	0,125	0,125	0,125	-
	κ^*	-	-	-		0,03	0,03	0,03	0,03	-
	μ^*	-	-	-		0,005	0,004	0,005	0,005	-
Poissons's Ratio	ν	0,1	0,1	0,1	0,1	-	-	-		-
Poissons's Ratio un/reloading	ν_{ur}	0,1	0,1	0,1	0,1	0,1	0,1	0,15	0,1	-
Friction Angle	ϕ	27	27	27	30	27	27	27	30	°
Cohesion	C	35	35	35	35	35	35	35	35	KN/m ₂
Dilancy angle	ψ	0	0	0	0	0	0	0	0	
Compressive strength	σ_{comp}	100	100	100	100	100	100	100	100	KN/m ₂

*Dr'd= drained

Table 5.2: Calibrated test results using HS and SSC model in PLAXIS 2D

HS 1		SSC 2		Sample 1	
Parameters	Value	Parameters	Value	Parameters	Value
E50ref	6MPa	λ^*	0,125	ν	0,1
Eoed ref	6MPa	κ^*	0,03	ϕ	27
Eur	18MPa	μ^*	0,004	ψ	0
ν	0,1	ν	0,1	$\sigma_{1\%}$	49,49
ν_{ur}	0,1	ν_{ur}	0,1	$\sigma_{5\%}$	107
C	35	C	35	$\sigma_{10\%}$	121
ϕ	27	ϕ	27	Eti	4949
ψ	0	ψ	0		
$\sigma_{1\%}$	46,6947	$\sigma_{1\%}$	62,0365		
$\sigma_{5\%}$	83,6212	$\sigma_{5\%}$	94,0282		
$\sigma_{10\%}$	104,494	$\sigma_{10\%}$	94,1432		
Eti	4669,47	Eti	6203,65		

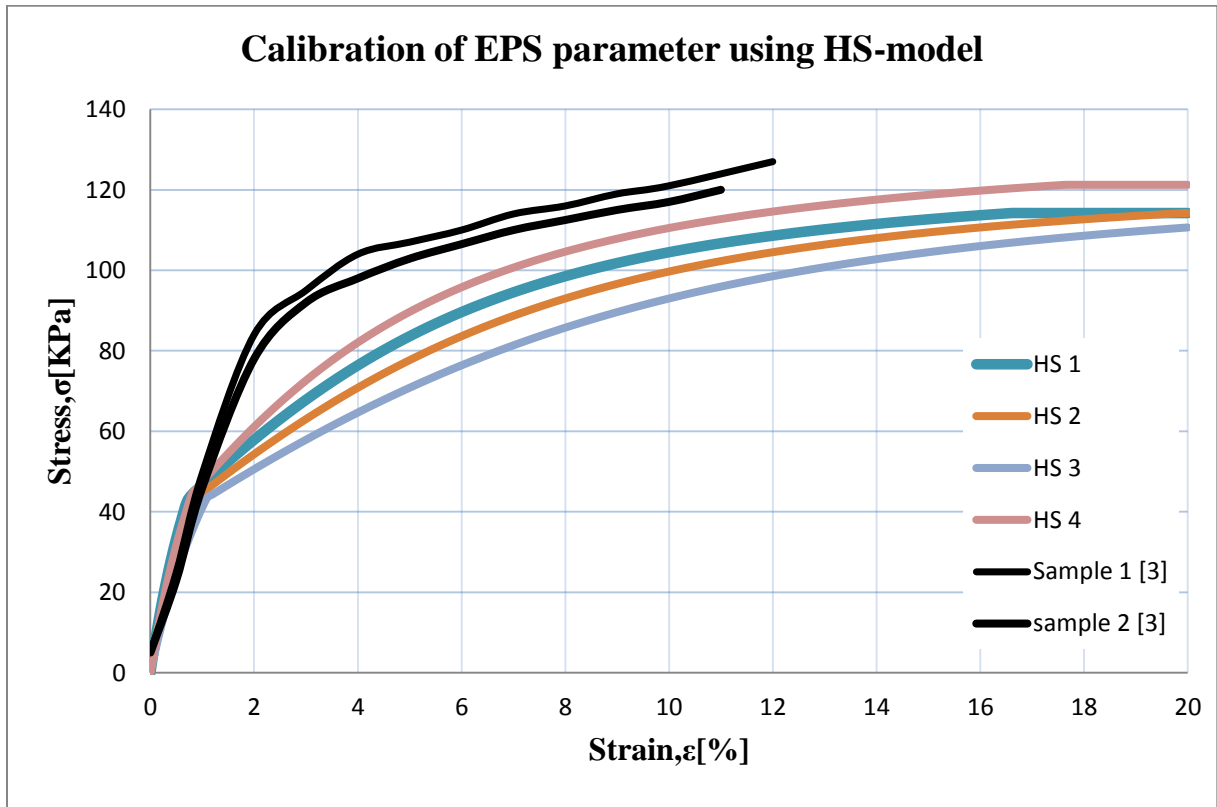


Figure 5.7: Calibration of EPS parameters using HS-model in PLAXIS 2D

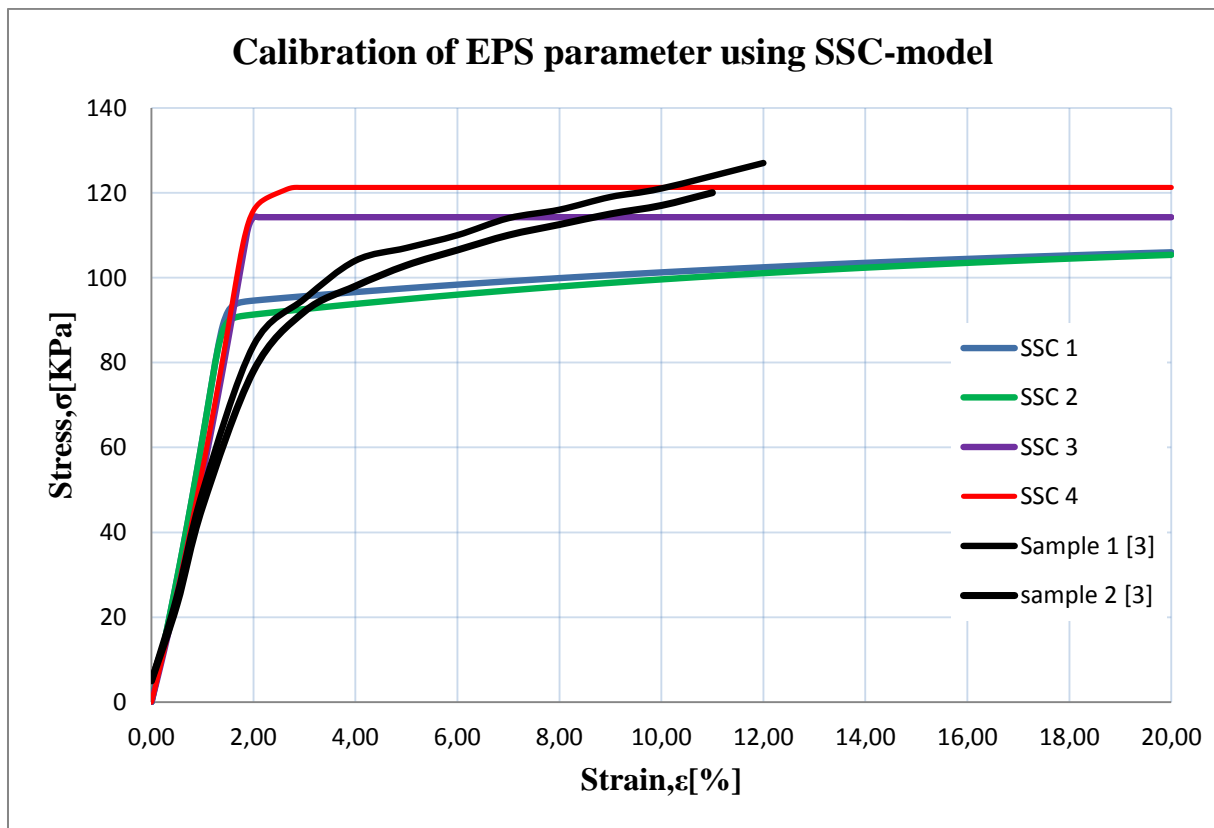


Figure 5.8: Calibration of EPS parameters using SSC-model in PLAXIS 2D

5.4 FE simulation of a full scale creep test using PLAXIS 2D

Models that exist in PLAXIS are mainly developed to capture the behavior of the soil as close as possible. Unlike the soils which need to be designed for many components, the main area of concern in EPS geofabric design is deformation or creep. A good proximity result can be achieved for this if we use the proper material parameters on PLAXIS.

5.4.1 Full scale laboratory creep test on EPS geofabric

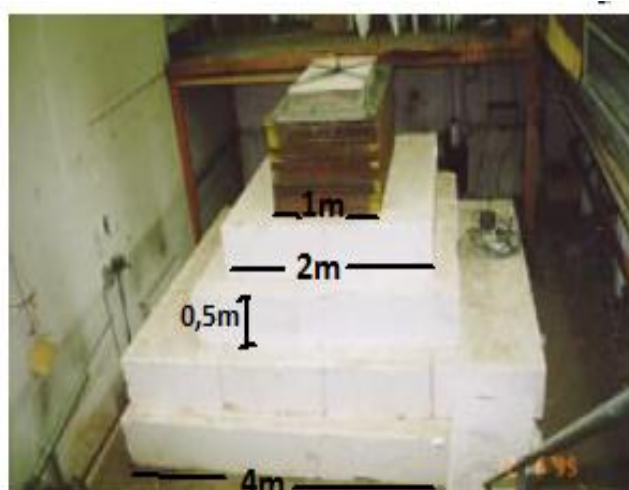
A full scale creep test was carried out at the Norwegian Road Research Laboratory (now called the Road Technology Department) by Roald Aabøe in 1993. The main aim of the test was to study the time dependent property of an EPS geofabric structures. Duration of the test was 1270 days and during which stress distribution and long term creep deformation was measured.

Test layout

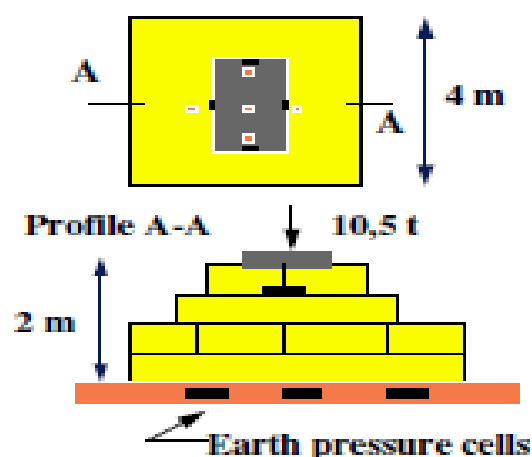
Individual EPS blocks of dimension 1,0m X 1,5m X 0,5 m and compressive strength of 100KPa are staggered to form a 4m X 4m in plan at the bottom of the fill. The fill increases to its 2m height with an approximate of 2:1 side slope to form a 2m X 2m in plan at the top of the fill (*figure 5.9*).

Load application and instrumentation

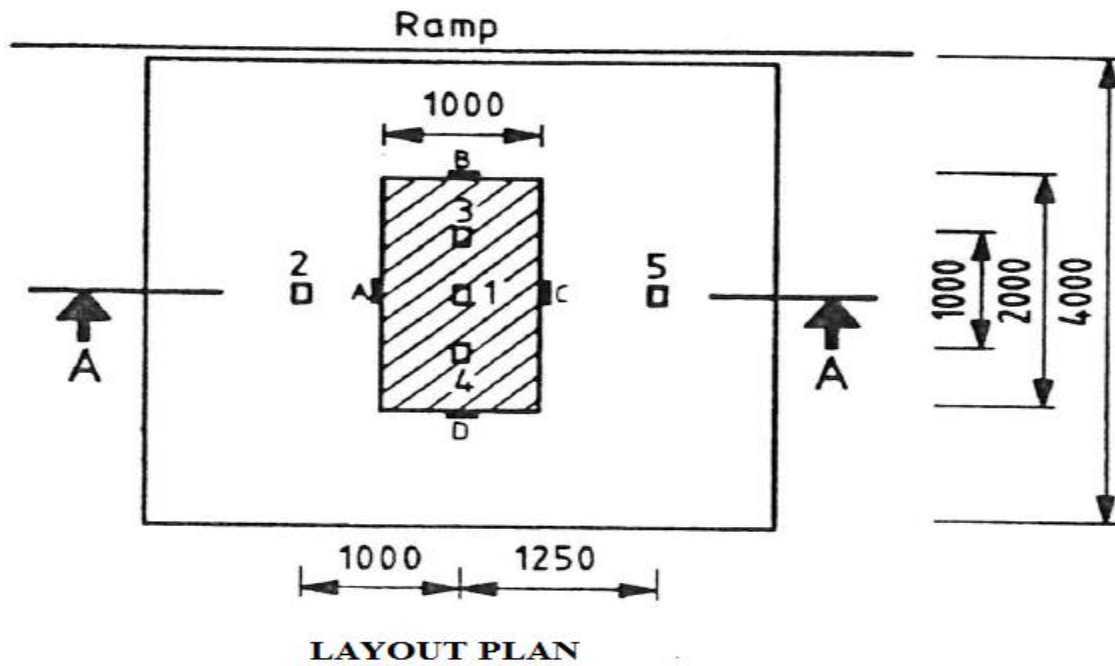
A stress of 52,5KPa is applied using 105KN load through a 2m X 1m steel plate on top of the fill. Four pressure cells were installed on the bottom of the fill to capture the stress distribution caused within the fill (*figure 5.9b*). A digital level (model-NA 3000) was used to measure the deformation at 4 points on the lowest steel plate and average value is taken as the deformation of the fill. The points were small brackets which were screwed to the edges of the plate and marked as from A - D (*see figure 5.9 c*).



a) 3D overview of the test



b) Cross sectional view of the test



c) Layout plan of the test

Figure 5.9: Full scale creep test at NRRL (Aabøe, 1993), [5]

Test results

At the end of the test, an approximate value of 1,1% of strain over a period of 1270 days is registered and among which 64% of the strain has been registered within the first two days. From pressure cell readings, an average of 7,8KPa stress is measured at the bottom of the fill. Which makes a 1:1,8 approximate stress distribution since the load at the top is 52,5KPa and a fill height of 2m.

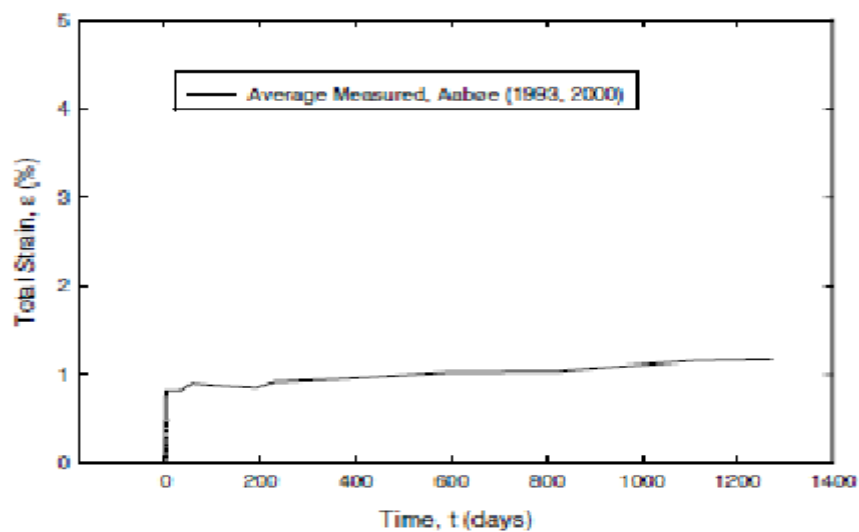


Figure 5.10: Total strain registered for full scale creep test at NRRL (Aabøe, 1993) [5]

5.4.2 PLAXIS 2D simulation of full scale test

In this section, the full scale creep test performed by Aabøe in 1993 is analyzed using PLAXIS 2D. The same geometry and load step is used as that of the full scale test. EPS Parameters is obtained from the simulation by adjusting the output from PLAXIS until a reasonable fit is obtained to the full scale test result. Soft soil creep model is used to model the test. Summary of input parameters and output are shown below.

Input parameters

Table 5.3: Input parameters for long term deformation in PLAXIS 2D

Material Parameters Used for PLAXIS input					
Parameter	Name	EPS layer			Unit
		Trial 1	Trial 2	Trial 3	
Material Model	Model	SSC			
Type of material behaviour	Type	Drained	Drained	Drained	
EPS unit weight	γ	0,2	0,2	0,2	KN/m ³
Flexibility coefficients	λ^*	0,1	0,13	0,125	-
	κ^*	0,02	0,03	0,03	-
	μ^*	0,005	0,005	0,004	-
Poissons's Ratio	ν	-	-	-	-
Poissons's Ratio un/reloading	ν_{ur}	0,1	0,1	0,1	-
Friction Angle	ϕ	30	30	27	°
Cohesion	C	35	35	35	KN/m ²
Dilintancy angle	ψ	0	0	0	
Compressive strength	σ_{comp}	100	100	100	KN/m ²

Geometry and mesh input

A 4m by a 2m high embankment as shown in *figure 5.11* is used as a geometry input. Plain strain condition with a fine mesh producing 3829 nodes of 15-noded triangular element is applied for the simulation. Mid-point of the loading plate is used to get the strain output.

Parameters from back calculation

Table 5.4: Parameters from back calculation for SSC model

Parameters	Value
λ^*	0,125
κ^*	0,3
μ^*	0,004
ν	0,1
ν_{ur}	0,1
ϕ	27
C	30

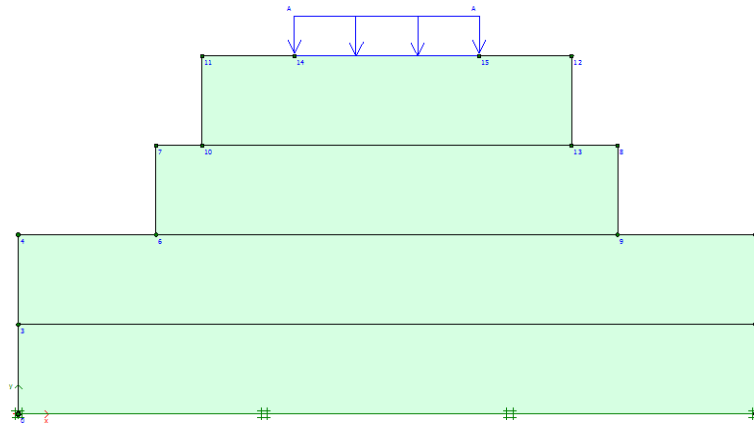


Figure 5.11: Input geometry

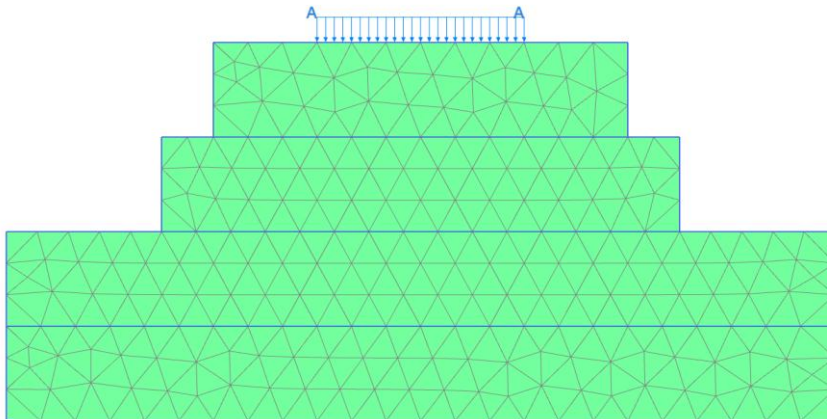


Figure 5.12: Generated mesh

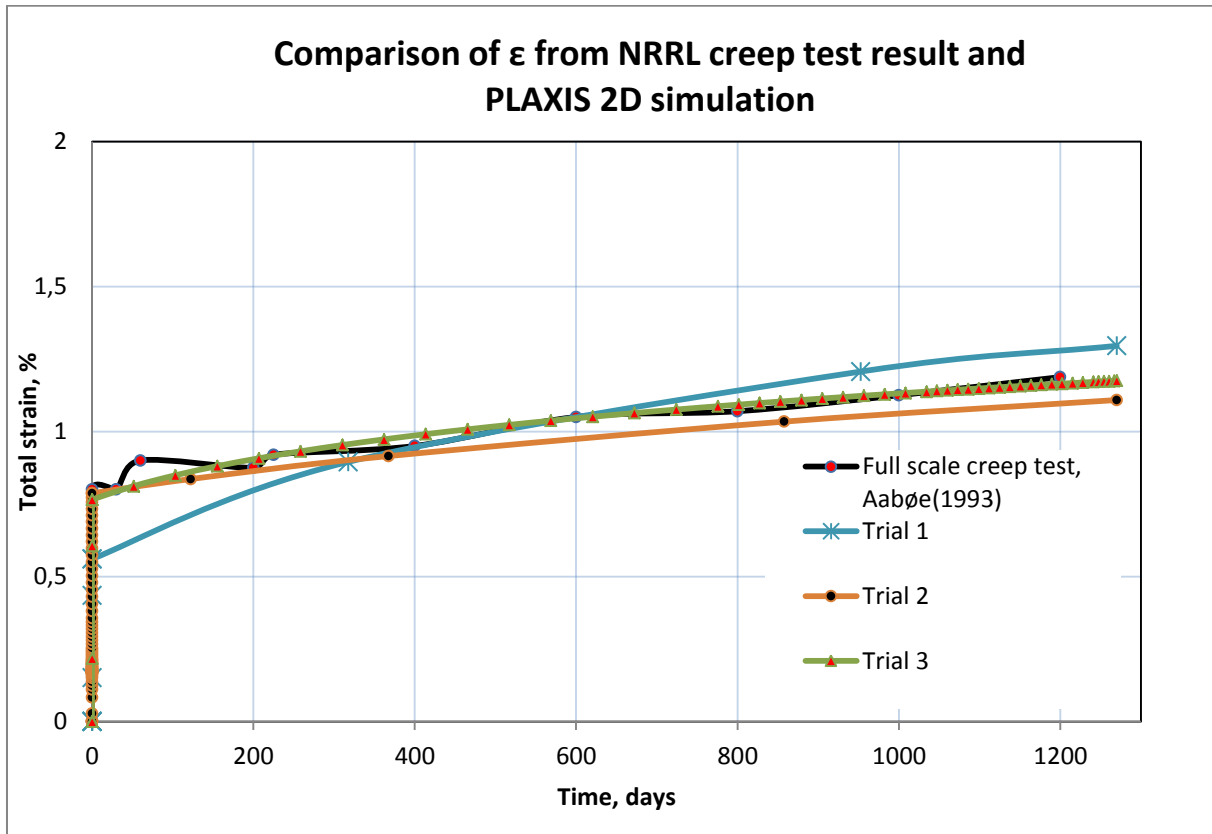


Figure 5.13: Comparison of full scale test result and SSC model PLAXIS 2D output

FE output using SSC model gives good fit with the average measured value. Stiffness parameter calculated using the stress at 1% strain provides 6MPa which is the same as modulus of elasticity value given in European standard but slightly overestimates to the average tangential modulus observed from sample testing.

5.5 Conclusion

Finite element analysis of EPS gefoam embankment using soil models should be treated carefully because of the difference in logic how the constitutive equations for soils and polymers made of. For that matter, some soil parameters may not give any meaning for EPS like that of cohesion. But, one can calibrate and use soil parameters for EPS because of the similarity of stress strain relationship up on loading.

With sufficient accuracy, one can use to simulate laboratory tests for EPS using HS model in PLAXIS to calibrate some outputs and for further analysis. SSC model on the other hand gives good estimate of longterm deformation if used the appropriate parameters as shown in table 5.4.

Chapter 6

Creep Modeling

6.1 Introduction

Since 1960's, different researches has been carried out to investigate the engineering properties of geofoam, one of the eight member families of polymeric material. The polymeric nature of the materials makes it highly durable under heavy loads. Its use in civil engineering, merely on road construction, has been growing since 1970's due to this property in addition to its insulation capacity. However, long term deformation of the polymeric material in general has been the core focus for design purposes.

The deformation tendency of materials under a relatively constant stress below the yield strength has been one of the main areas of practical importance. Several constitutive models describing the creep behavior of different materials are proposed throughout the years. Since 1940's, the time dependent behavior of polymeric materials especially tensile creep behavior took the primary focal point. But with time and experience, compressive creep and relaxation for non-planar geosynthetics like that of geofoams, tensile relaxation of planar geosynthetics such as geogrids, geomembranes and geotextiles has been deeply investigated [16].

Under a constant compressive load coming from the pavement structure, EPS geofoam as a part of a light weight fill embankment undergoes through deformation in its design life. As explained in the earlier chapters, polymer materials including EPS undergo through three stages of creep, primarily, secondary and tertiary. The amount of the load the EPS bearing, the duration of loading and the temperature can affect how the creep develops. EPS can be at any stages of creep at a particular time. Different empirical equations and mathematical models for prediction of the performance of creep have been suggested throughout the years. But, for practical engineering design use, EPS has been designed for its 50% strength value to limit the time dependent strain within 2% based on experience and test data.

Different kinds of time dependent constitutive creep models exist. Depending on the basis for the derivation of the model, they can be categorized in to two broad conceptual categories [16]: empirical and deterministic approaches. The empirical approaches use the allowable stress, which is a reduced value from the strength of material, as a basis for determination of the time dependent deformation. Whereas, the deterministic approaches such as Findley equation, model using isochrones, models with creep strain rate and models using weibull distribution use some form of a mathematical model to estimate the time dependent strain. In this chapter, Findley equation, the general power rules and LCPC equations and their parameters are discussed. Comparison of calculation results from full scale laboratory test and finite element code, PLAXIS, are discussed. Creep models using isochrones is discussed briefly as well. Overall discussion on the mechanical time-dependent characteristics of EPS geofoam under normal compressive stress is presented.

6.2 Empirical models

6.2.1 Findley equation

Since the start of using polymer materials for civil and other engineering practices, predicting the general trend of strain under different loading conditions has been a continuous focal point. Unlike the immediate strain which can be gathered with sufficient accuracy from short term tests, predicting the time-dependent behavior has not been always easy. There were times the time dependent strain of polymeric materials especially geofoam blocks had been ignored in the design. But, as durability is one of the major criteria for design of long term stability, knowledge basis of material as time dependency is important.

Mathematical equations using a power law function to model the time dependent creep strain of polymer materials in tension has been suggested by Findley in 1950's and it is called Findley equation[16]. The basic components of the Findley equations are two: immediate strain, ε_0 , which is the initial strain within the first hour of loading and the time dependent strain or creep part, ε_c . Findley uses an assumption to model the creep part by using a power law mathematical equation as shown below in equation 2.

$$\varepsilon = \varepsilon_0 + \varepsilon_c \quad (6.1)$$

$$\varepsilon = \varepsilon_0 + m \left(\frac{t}{t_0} \right)^{n_F} \quad (6.2)$$

Where: ε_0 is the immediate strain up on stress application,

ε_c is the time dependent strain,

t is time after stress application, hrs

t_0 is dimension parameter, 1hr

n_F is a dimensionless Findley parameter,

Findley uses five material dependent parameters (n_F , m'_F , ε'_{oF} , σ_{eF} , σ_{mF}) to define the creep component of the total strain and gives a specific relationship for ε_0 and m as shown in equation 3 and 4.

$$\varepsilon_0 = \varepsilon'_{oF} \sinh\left(\frac{\sigma}{\sigma_{eF}}\right) \quad (6.3)$$

$$m = m'_F \sinh\left(\frac{\sigma}{\sigma_{mF}}\right) \quad (6.4)$$

Where: m'_F is a dimensionless Findley material parameter

σ is applied stress

ε'_{oF} is a dimensionless Findley material parameter

σ_{eF} is a Findley material parameter with dimensions of stress

σ_{mF} is a Findley material parameter with dimensions of stress

As stated from several triaxial and uniaxial compressive strength tests performed on test specimens of EPS geofoam, the “elastic” region is between 0-1% strain and linear can be assumed. However, the stress strain relationship is actually non-linear elsewhere. Therefore, calculation for determination of Findley parameters should be preceded carefully by stating the stress range they are evaluated and the temperature.

Throughout the year after the proposal of Findley equation, simplification and adjustments are made to the original formula to include some facts from test results [16]. Findley (1960) and Chambers (1984) visualize that simplification to the original formula can be made if the ratio of applied stress to the dimensionless Findley parameter is less than one and the formula is called the simplified Findley equation.

$$\text{For } \left(\frac{\sigma}{\sigma_{eF}}\right) \leq 1, \sinh\left(\frac{\sigma}{\sigma_{eF}}\right) \cong \left(\frac{\sigma}{\sigma_{eF}}\right) \quad (6.5)$$

$$\text{For } \left(\frac{\sigma}{\sigma_{mF}}\right) \leq 1, \sinh\left(\frac{\sigma}{\sigma_{mF}}\right) \cong \left(\frac{\sigma}{\sigma_{mF}}\right) \quad (6.6)$$

Therefore, the simplified Findley equation is:

$$\varepsilon = \varepsilon'_{oF} \left(\frac{\sigma}{\sigma_{eF}}\right) + m'_{mF} \left(\frac{\sigma}{\sigma_{mF}}\right) t^{nF} \quad (6.7)$$

Chambers rearrange the parameters and defined another formula as:

$$\varepsilon = \frac{\sigma}{E_{oF}} + \frac{\sigma t^{nF}}{E_{cF}}; E_{oF} = \frac{\sigma_{eF}}{\varepsilon'_{oF}} \& E_{cF} = \frac{\sigma_{mF}}{m'_{mF}} \quad (6.8)$$

$$\varepsilon = \frac{\sigma}{E_{vF}}; E_{vF} = \left(\frac{1}{\frac{1}{E_{oF}} + \frac{t^{nF}}{E_{cF}}}\right) \quad (6.9)$$

Where E_{vF} is a time-dependent secant young's modulus.

The other noticeable formula in the determination of creep for polymeric material is the one proposed by Horsely. It is derived by assuming the initial strain to be zero in the Findley equation.

$$\varepsilon = m'_H \sinh\left(\frac{\sigma}{\sigma_{mH}}\right) t^{nH} \quad (6.10)$$

Where: m'_H is dimensionless Horsely parameter

n_H is dimensionless Horsely parameter

σ_{mH} is Horsely material parameter with dimensions of stress

From experience, it has been indicated that Findley equation gives comparably a good result on the estimation of creep for EPS geofoam. But, in order to get best fit Findley parameters, data from a long term creep measurements with different stress conditions and material

property shall be considered. In the previous chapter, comparative analysis based on the principles of soil and EPS constitutive models has been presented. How much the time dependent strain property of geofam materials can be picked up by soil models is investigated. In this section however, Findley parameters are calculated using output data from FEM simulation, PLAXIS.

Full scale laboratory creep test performed by Roald Aabøe in 1993 is modeled using PLAXIS, FEM simulation. The test layout and geometric description is as documented in chapter 5, section 5.4.1. Soft soil creep model has been introduced to capture the creep of the fill within the testing period. A plain strain with a fine mesh, a refined cluster of 10cm in each side of the end of loading plate and 20cm below the surface is used for finite element simulation. A total of 16105, 15- noded triangular elements are generated during the process.

Approximately the same points at which the deformations were measured during the full scale test are used to do the same for the FE simulation. Average strains from three points, at the two edges and mid-point of distributed load, are used to develop ϵ -t curves (*see appendix D*). Three sets of stresses (52,5KPa, 40KPa and 30KPa) and seven different durations (1hr, 5, 7, 100, 500, 1000 and 1270days) are used to gather data for long term strain for EPS. The stresses are selected to be with in the expected load limit the EPS faces as a light weight fill material in road construction.

Table 6.1: Input parameters for PLAXIS

Material Parameters Used for PLAXIS input			
Parameter	Name	EPS layer	Unit
Material Model	Model	SSC	
Type of material behaviour	Type	Drained	
EPS unit weight	γ	0,2	KN/m ³
Flexibility coefficients	λ^*	0,125	
	κ^*	0,03	
	μ^*	0,004	
Poissons's Ratio un/reloading	ν_{ur}	0,1	
Friction Angle	ϕ	27	
Cohesion	C	35	KN/m ²
Dilitancy angle	ψ	0	
Compressive strength	σ_{comp}	100	KN/m ²

As shown in *figure 6.1* the total strain at the end of 1270days for a stress of 52,5KPa is 1,12% which is nearly the same as the measured value 1,187%. But the development of the strain for the lower stresses, 30 and 40KPa, is much lower. *Figure 6.2* is one of the different ways of plotting the creep test results suggested by Hovrath(1998). The depiction of the figure suggests, not only strain is related with the power function of time but also logarithmic functions can be used into mathematical models.

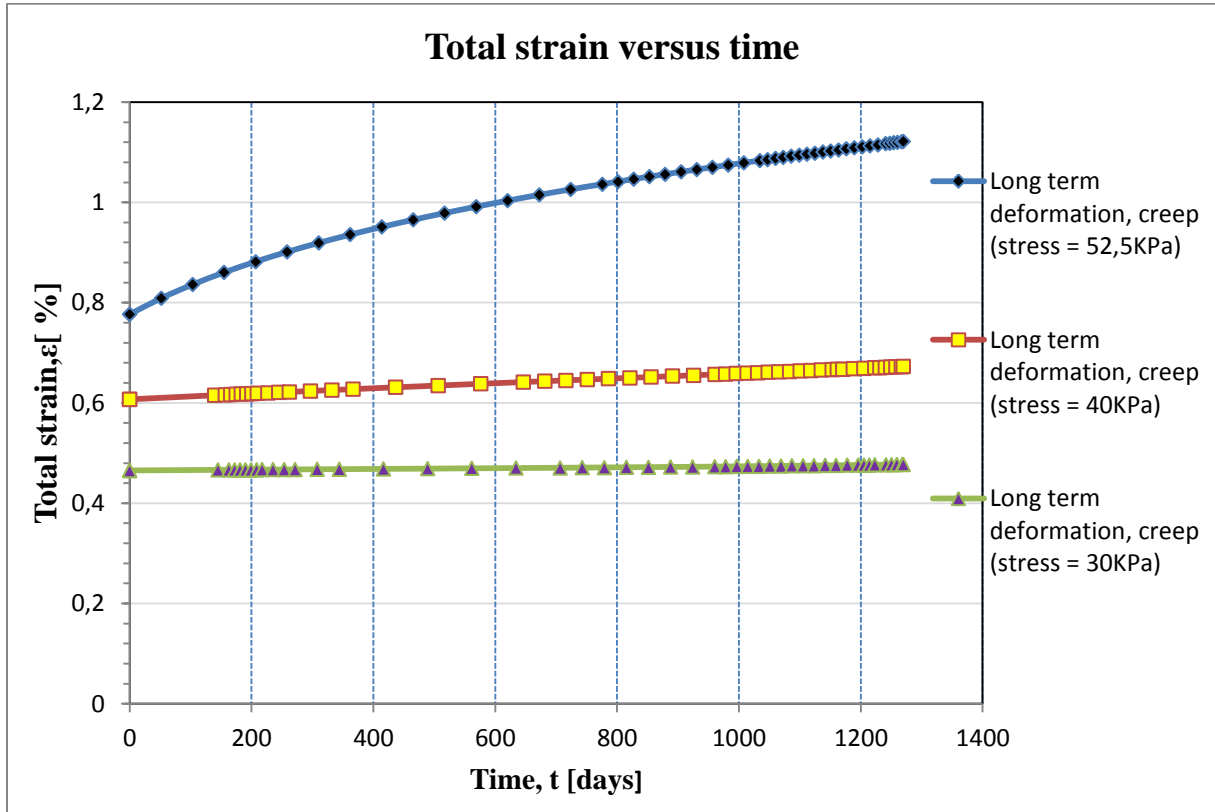


Figure 6.1: Creep test result output from PLAXIS

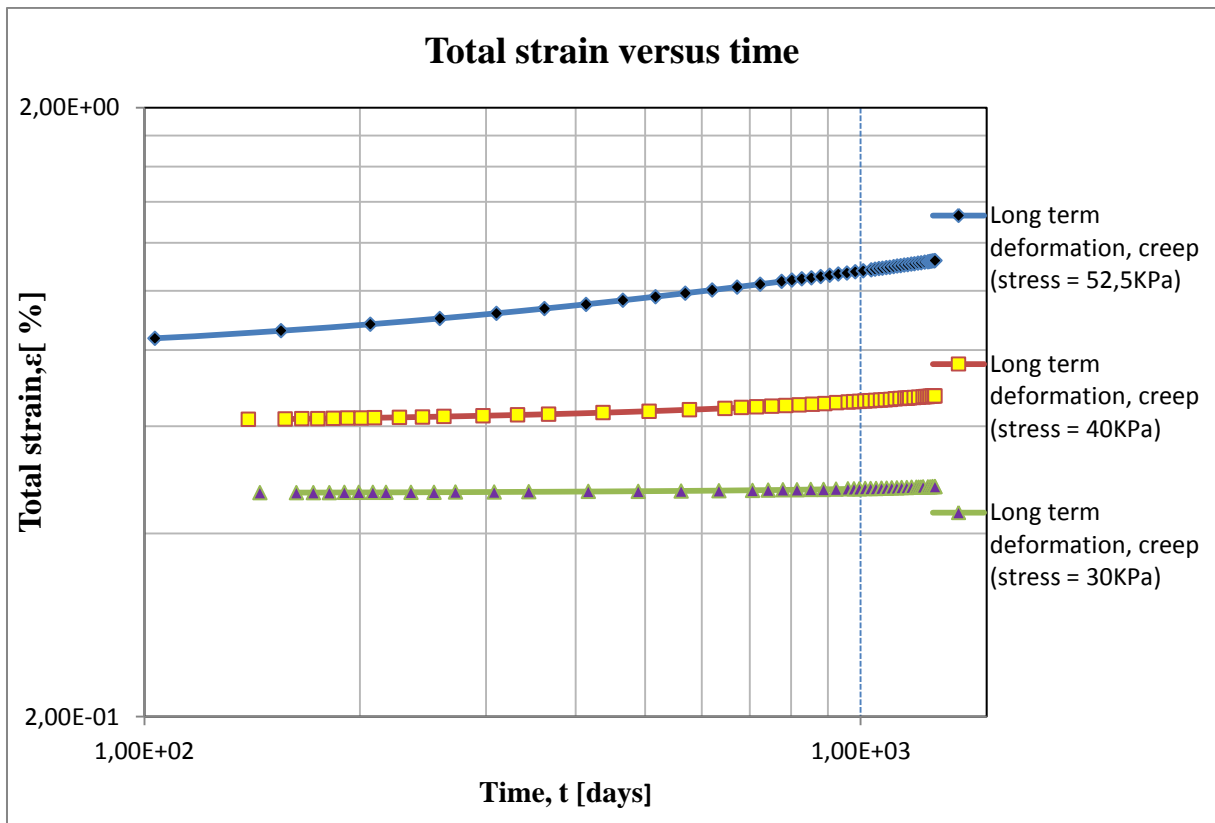


Figure 6.2: Log10 total strain vs Log10 time result output from PLAXIS

Determination of Findley parameters needs at least two different sets of stress applications on the same material or model. For this study, a range of three different stresses are used on the same model to get output. Simultaneous equations on both equations 6.3 and 6.4 will give us 4 Findley parameters (m'_F , ε'_{oF} , σ_{eF} and σ_{mF}) whereas n_F can be found from a special plot of the creep test results as shown in figure 6.3. Most polymeric material shows a linear curvature when only the time dependent strain, ε_c , of the material plots against time and both are in logarithmic base 10 scale (Findley and Kholsa 1956). Therefore, n_F is the slope of the linear line.

For plotting of figure 6.3, two ways can be followed as presented by Findley and Chambers. Findley suggests optimizing the best fit line before selecting ε_o whereas Chambers suggests the benefit of selecting ε_o from an independent rapid loading test on the same material and fit the lines next. In this study both procedures are followed and reasonably close results are collected.

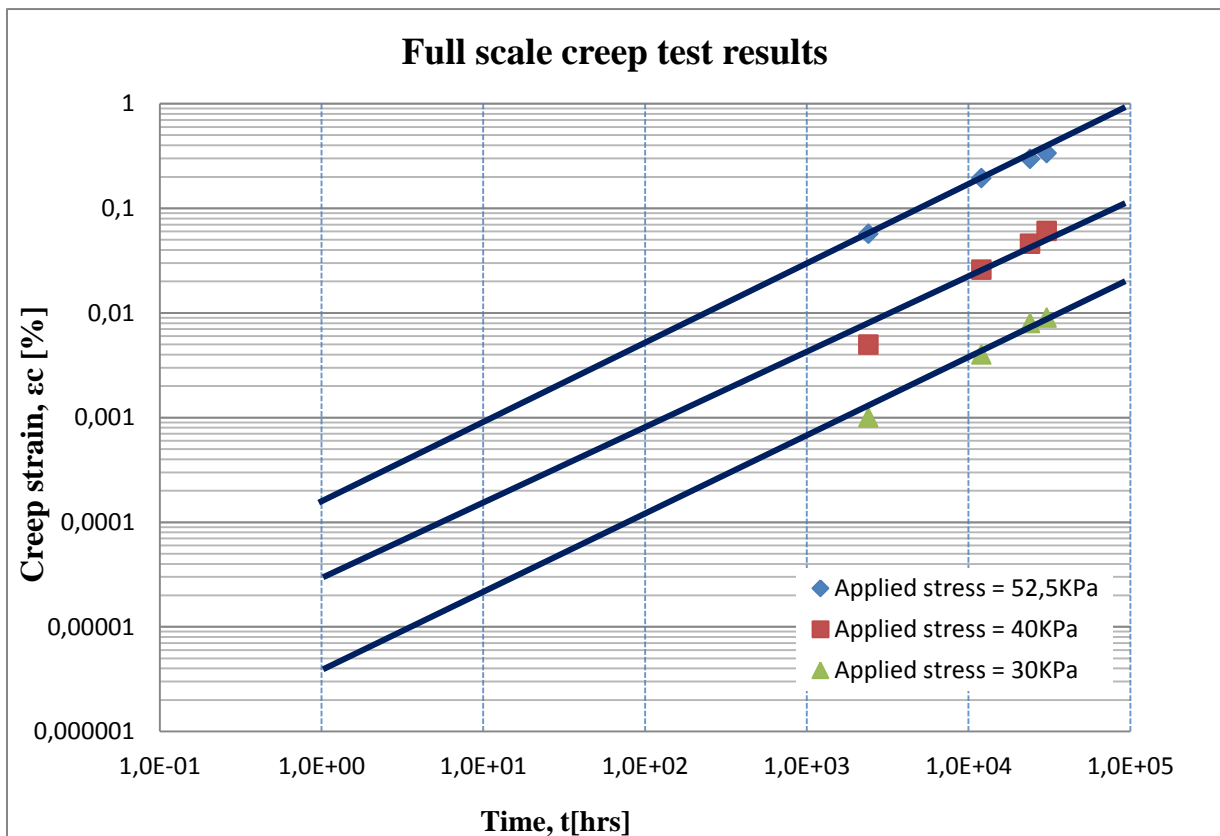


Figure 6.3: Log10 creep vs Log10 time result output from PLAXIS

Rapid loading test is carried out using the soil lab test tab in the PLAXIS model to generate results of immediate strain of the EPS geofoam used for the full scale model. Unconfined compressive strength test is performed using the triaxial test by setting σ_3 to zero. Since it is recommended that axial strain data be obtained immediately up on stress application and frequently for the first hour after load application to better estimate ε_o [12], the test in PLAXIS was run only for an hour. Figure 6.4 shows the output result from the soil test lab in PLAXIS. Stress- strain data are collected and for the intended stresses a relatively close value is obtained from both procedures.

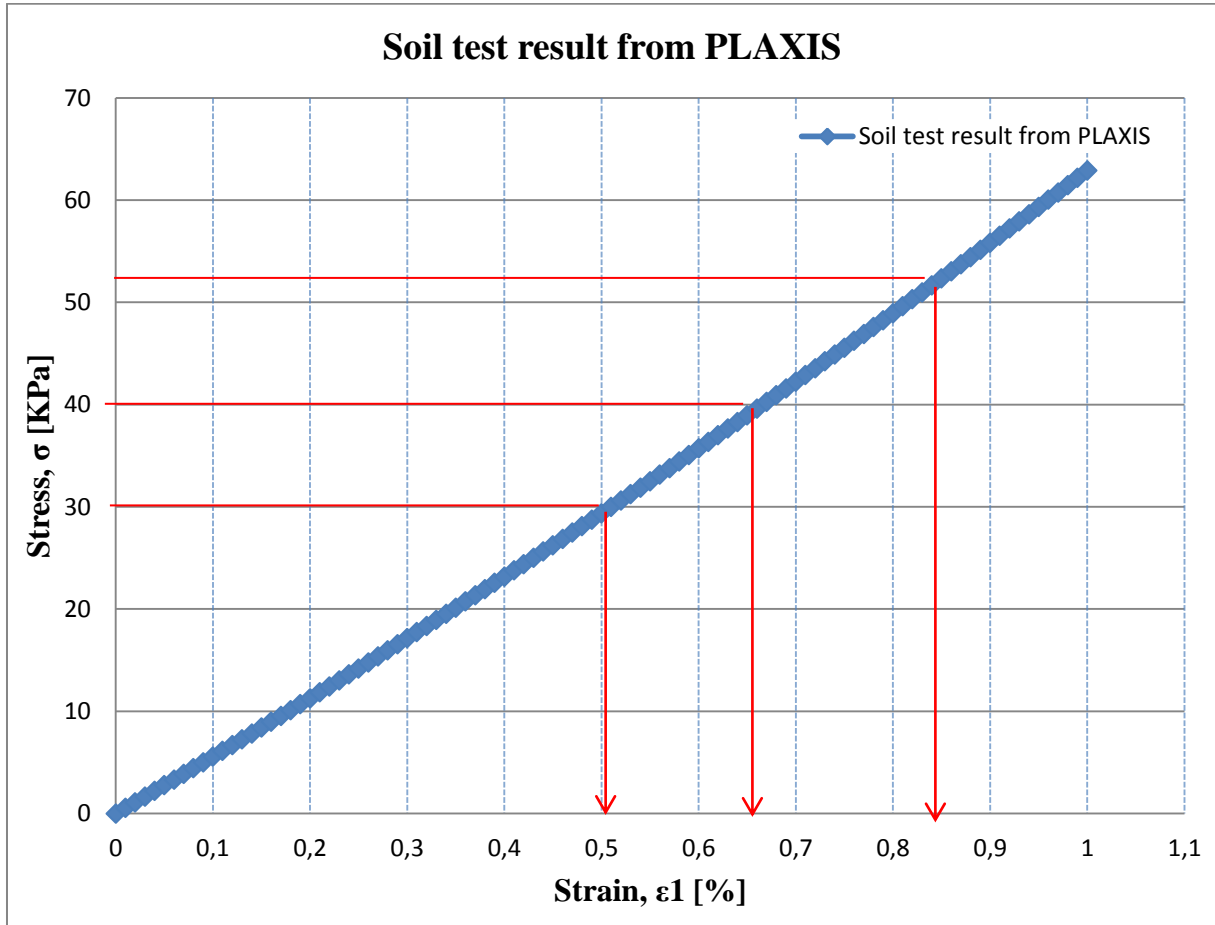


Figure 6.4: Stress-strain output from PLAXIS

Table 6.2: Initial strain and initial tangent calculated using Findley and Chambers approach

Applied stress, σ [Kpa], C1	Initial strain, E_o , C2	Initial strain, ϵ_o from rapid loading test, C3	Initial tangent Young's modulus, E_{ti} , $C4=C1/C2$	Initial tangent Young's modulus, E_{ti} , $C5=C1/C3$
30	0,00468	0,0051	6410,26	5882,35
40	0,00612	0,00665	6535,95	6015,03
52,5	0,00783	0,0085	6704,98	6176,47

One of the Findley parameter, n_F is found from by averaging the slope of the three linear best fit lines in figure 6.3. The other four parameters are calculated using trial and error method in excel by using equation 6.3 and 6.4. Findley parameters are summarized in table 6.3 below.

Table 6.3: Findley equation parameters calculated from PLAXIS output

Findley equation parameters	
n	0,71
ϵ'_{oF}	0,009
σ_{eF}	58
m'_F	0,000000004
σ_{mF}	7,80

Findley parameters can be checked based on what they are representing. For example as stated by Findley, the parameter ε'_{oF} should be in the range of the elastic limit strain for EPS geofoam blocks which is around 0,01 and σ_{eF} would be the corresponding stress in the range of 50 to 60KPa(*see table 2.4 type EPS VIII*). The young's modulus resulting from $\sigma_{eF}/\varepsilon'_{oF} = 58/0,009 \approx 6400\text{KPa}$ is nearly similar to the one found in table 6.2. The Findley parameter σ_{mF} corresponds to the magnitude of the stress below which the creep is negligible and it is defined as the stress corresponding to 0,005 strain. It is expected to be in the range of 25 – 30KPa. But, during this calculation a relatively lower value is obtained due to the sensitivity of evaluating σ_{mF} and m'_F parameters and the number of data used to fit the linear curves.

Substituting all Findley parameters in to the main equation 6.2 and for EPS with density of 20Kg/m^3 :

$$\varepsilon = 0,009 \sinh\left(\frac{\sigma}{58}\right) + 0,000000004 \sinh\left(\frac{\sigma}{7,8}\right) t^{0,71} \quad (6.11)$$

6.2.2 General power-law equation

It is one of the derivatives of Findley equation with the general form shown in equation 6.12 below.

$$\varepsilon = \varepsilon_0 + mt^n; \varepsilon_0 = \sigma/E_{ti} \quad (6.12)$$

The most widely used general power-law equation is the one reported by Magnan and Serratrice in 1989. Based on a number of test results performed by Laboratoire Central des Ponts et Chaussées (LCPC, France) on different density EPS geofoam specimens, they developed an empirical formula for the coefficients m and n.

$$m = 0,00209 \left(\frac{\sigma}{\sigma_y}\right)^{2,47} \quad (6.13)$$

$$n = -0,9 \log_{10} \left[1 - \left(\frac{\sigma}{\sigma_y}\right)\right] \quad (6.14)$$

Where σ is the applied stress in KPa and σ_y is the yield/plastic stress of the EPS in KPa. Plastic/yield stress is the stress when the strain in the EPS geofoam is nearly 1,5%. The main purpose of introducing such parameter is to normalize the applied stress in equation 6.14 while producing stress strain model for the EPS [16].

$$\sigma_y = 6,41\rho - 35,2 \quad (6.15)$$

$$E_{ti} = 479\rho - 2875 \quad (6.16)$$

Substituting equations 6.13 to 6.16 in to the parent equation 6.12 will provide the LCPC general power law equation as shown below.

$$\varepsilon = \left(\frac{\sigma}{479\rho - 2875}\right) + 0,00209 \left(\frac{\sigma}{6,41\rho - 35,2}\right)^{2,47} t^{\{-0,9 \log_{10} [1 - \left(\frac{\sigma}{6,41\rho - 35,2}\right)]\}} \quad (6.17)$$

Where: ε is the total strain in decimal.

General power law equation parameters, m and n , are determined using PLAXIS and equations provided by LCPC (Magnan and Serratrice) in table 6.4 below.

Table 6.4: Comparison of general power law equation parameters from PLAXIS output and LCPC method

General power law equation parameters				
Applied stress, σ [Kpa]	PLAXIS output		LCPC	
	m	n	m	n
30	0,00000004	0,725	0,000128	0,152
40	0,00000003	0,715	0,000260	0,220
52,5	0,00000015	0,708	0,000509	0,325

Based on the above analysis, comparison is presented in *figure 6.5* between Findley equation, simplified Findley equation, general power law equation, LCPC equation and average measured value for the full scale laboratory creep test. Findley and general power law equation parameters obtained from tests performed by BASF in Ludwigshafen, Germany in 1987 also included as reported in Hovrath (1998) (*see appendix E.1*). Test results from BASF tend to give an overestimated result which reaffirms small scale test results overestimate the total deformation.

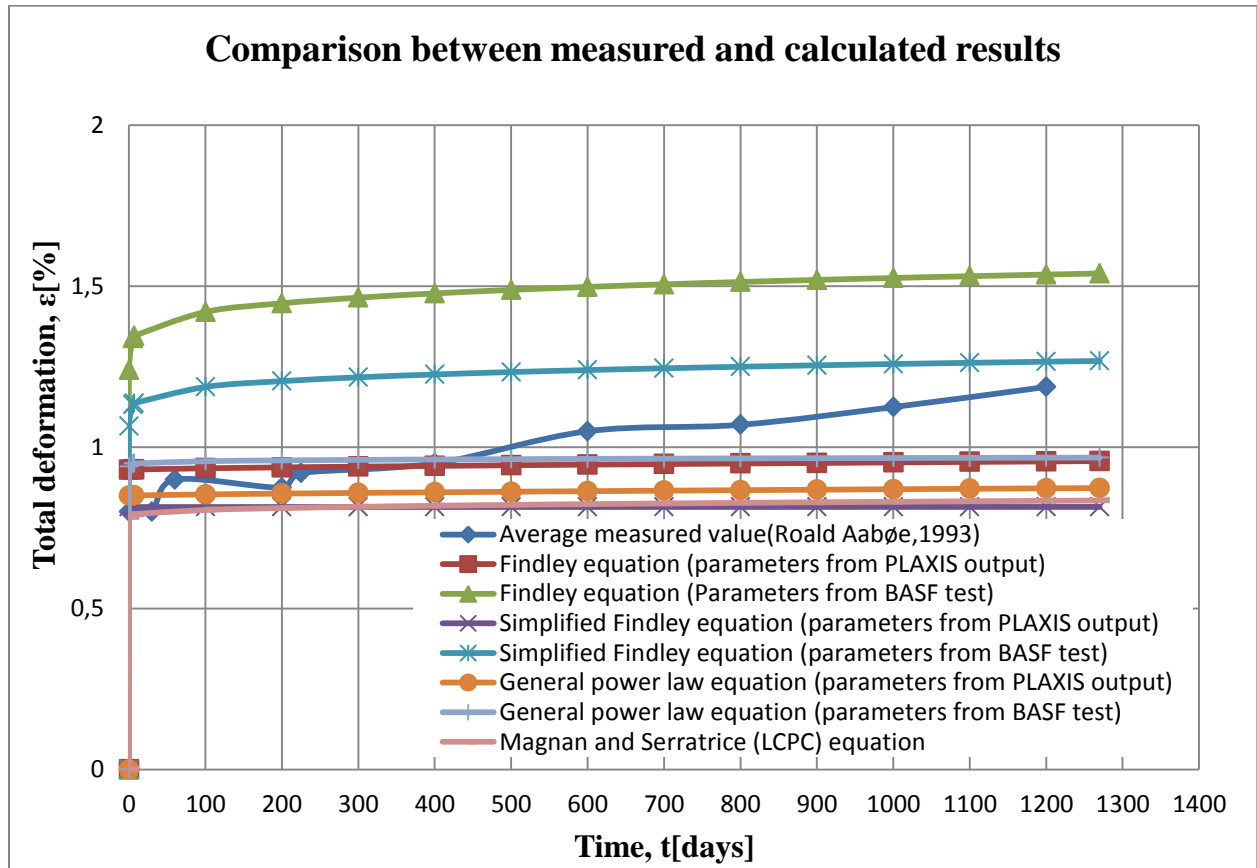


Figure 6.5: Comparison between measured and calculated total deformation results

6.2.3 Other empirical equations

Empirical equations relating strain with logarithmic function of time was proposed in 1943 by Leaderman. However, the method utilizing the empirical equations was only applicable to the linear relationship between strains and log time [9]. Results obtained from test data and this empirical equation has shown good agreement among them.

$$\varepsilon = A \log t + Bt + C \quad (6.18)$$

6.3 Model using isochronous stress-strain curves

EPS geofom material as other engineering materials depicts time related strain, creep, under constant load application. The best graphical way to explain the process is by using isochronous stress-strain curves (ISSC). *Figure 6.6* shows ISSC indicating the time dependency of creep strain with constant stress application. For a constant stress σ_0 , strain increases from ε_0 to ε_{10000} as the time elapses from 0 to 10,000hrs.

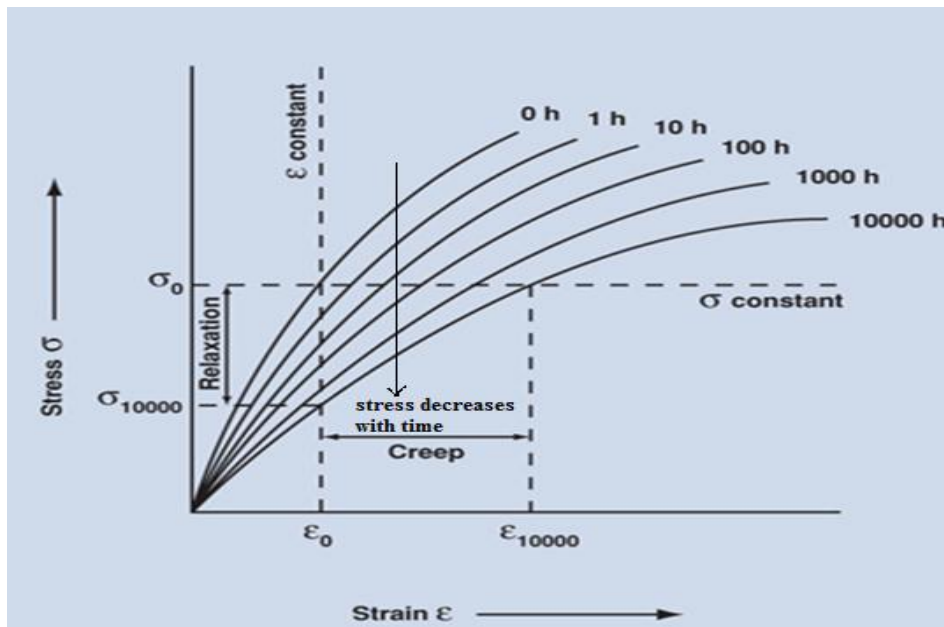


Figure 6.6: ISSC curve [19]

ISSC curve also explains stress relaxation which is a corollary phenomenon to creep. If the deformation is constant, the stress resisting that deformation will decrease with time. The physical mechanism that causes a plastic to undergo creep also applies to the phenomenon of stress relaxation. *Figure 6.6* also illustrates that at a fixed strain, the stress decreases with the elapsed time [18].

Similar approaches have been taken to develop ISSC curves for EPS geofom and to established relationship between applied stress and total strain. Missirlis, Papastylianou, Atmatzidis and Chrysikos performed compressive and creep test on specimens cut-out from 2,5x1x0,5m EPS blocks. The principle of time-temperature superposition (ASTM, 1997) was applied to predict the creep behavior of EPS geofom. For the creep test, cylindrical samples of diameter 100mm and height / diameter ratio of 2.0 is used.

Based on the data they obtained through synthesis of results from time-temperature superposition principle, they create isochronous curves for each type of EPS products they used as shown in *figure 6.7*. It was observed that the behavior of all types of EPS Geofam varied after 100 to 180 days only for higher values stress application. The slope of the linear lines in the isochronous curves is correlated with the power function of time to describe the viscoelastic nature of the EPS [20].

$$\sigma_n = \frac{\sigma}{\sigma_{c10}} = [59,374 - 5,982 \left(\frac{t}{t_0}\right)^{0,167}] \varepsilon_{tot} \quad (6.18)$$

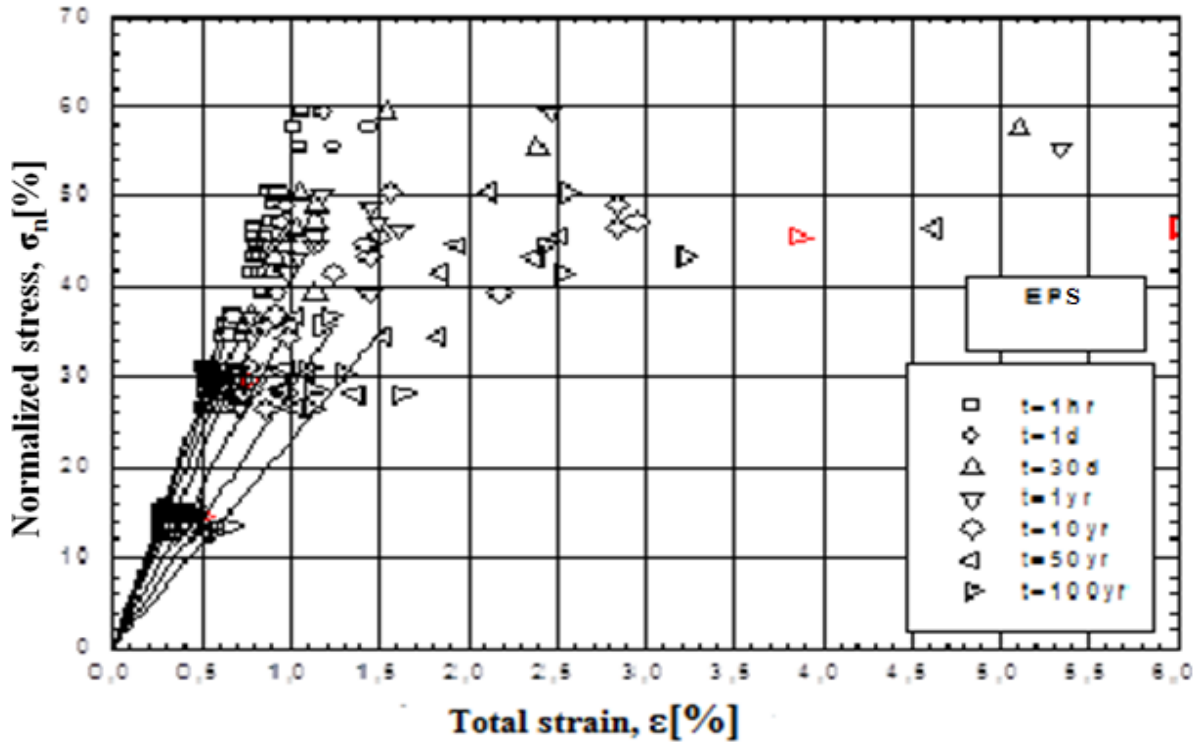


Figure 6.7: Normalized isochronous curves [20]

The same full scale laboratory test performed by Roald Aabøe is used to study the isochronous stress strain curves produced from PLAXIS. Three different stresses (30, 40 and 52,5 KPa) are applied on the model and average strain on the top surface of the fill using three points (at either end and mid point of the loading plate) is obtained (*see appendix D*). *Figure 6.8* illustrates ISSC produced from loading time periods of 1hr, 5, 7, 100, 500, 1000 and 1270 days for the three stresses. For stresses less than 30 KPa, insignificant change in permanent strain is shown throughout the periods. But as the stresses increase from 40 to 52,5 KPa, a marginal increase in creep is shown as the period of loading increases.

The E-modulus of the fill started to increase in linear form for the stress range up to 40 KPa as the loading increases. A linear correlation coefficient of $R^2 > 0,99$ is obtained for σ - ε curve within stress range of 40 KPa (*see appendix E.2*). Nonetheless, E-modulus decreases as the time of loading increases as shown in *figure 6.9*. Linear relationship is shown for $E(t)$ in the lower range of stress but a power function can describe better as the stresses increase. This indicates the viscoelastic nature of EPS.

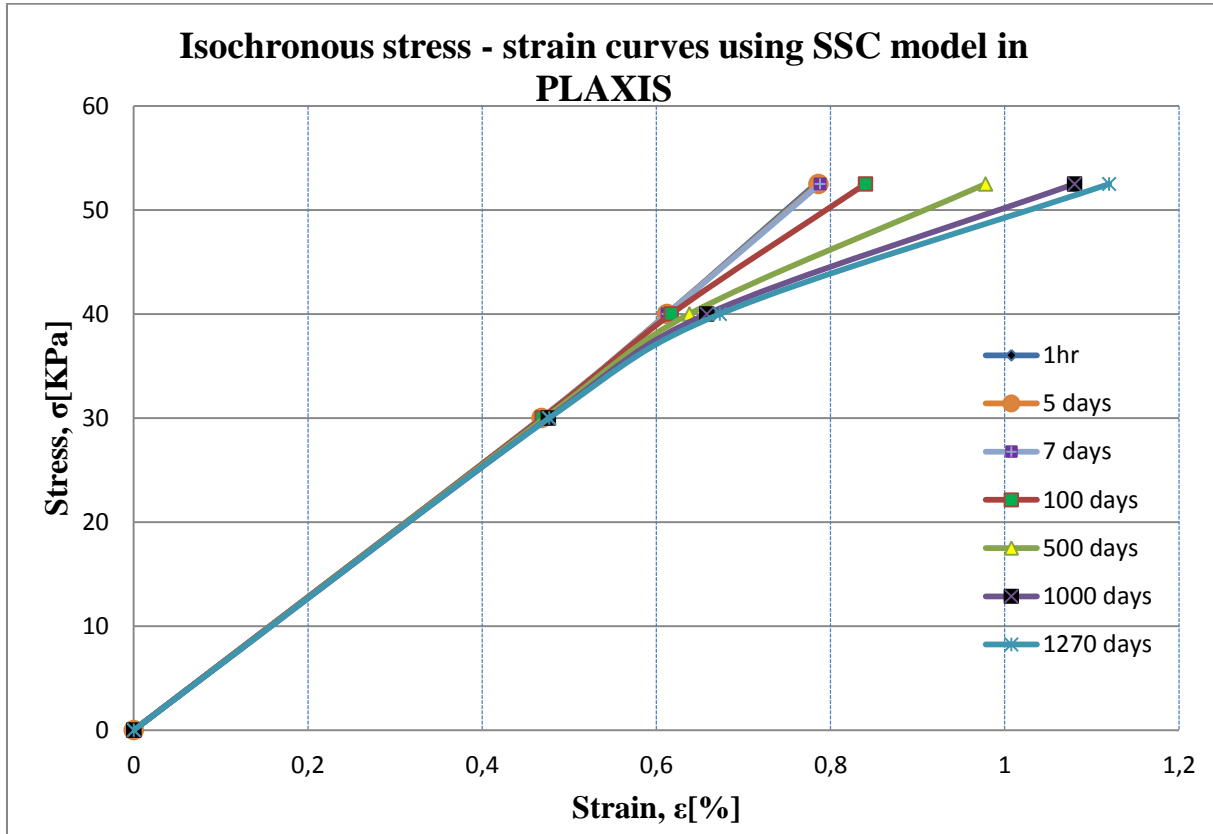


Figure 6.8: Normalized isochronous curves for full scale laboratory creep test, 1993

For this case a power function is used to represent E as a function of time using trial and error. With average R^2 value of 0,8957, an empirical function of $E(t)$ is shown in equation 6.19 as follows:

$$E(t) = 76 - 5,1 * t^{0,22} \quad (6.19)$$

Using the above characterization of E -modulus, we can formulate the total strain for EPS geofoam as follows:

$$\varepsilon_{tot} = \sigma / E(t) \quad (6.20)$$

$$\varepsilon_{tot} = \sigma / (76 - 5,1 * t^{0,22}) \quad (6.21)$$

Figure 6.10 illustrates comparison between average measured total strain value for the full scale creep test with PLAXIS output and empirical formula derived from ISSC (equation 6.21). A reasonably close estimation is found from the empirical formula. Most importantly, the initial deformation is well captured.

6.4 Models using creep strain rate, Sherby dorn plot

The models in this group allows for the prediction of the creep for plastic materials in general by expressing the strain rate as a function of time and material constants. One simple example for this could be found by deriving the ε_{tot} in Findley equation with respect to time as shown below in equation 6.23 after substitution.

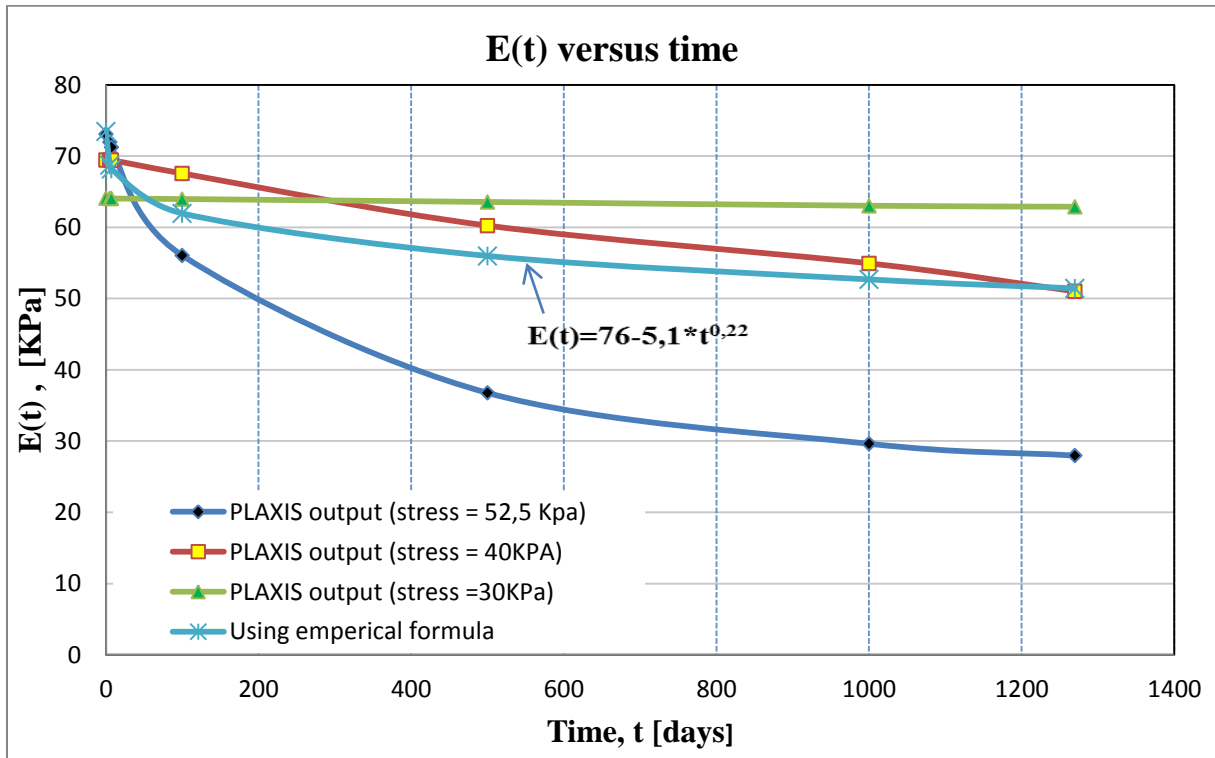


Figure 6.9: E(t) versus time for full scale laboratory creep test, 1993

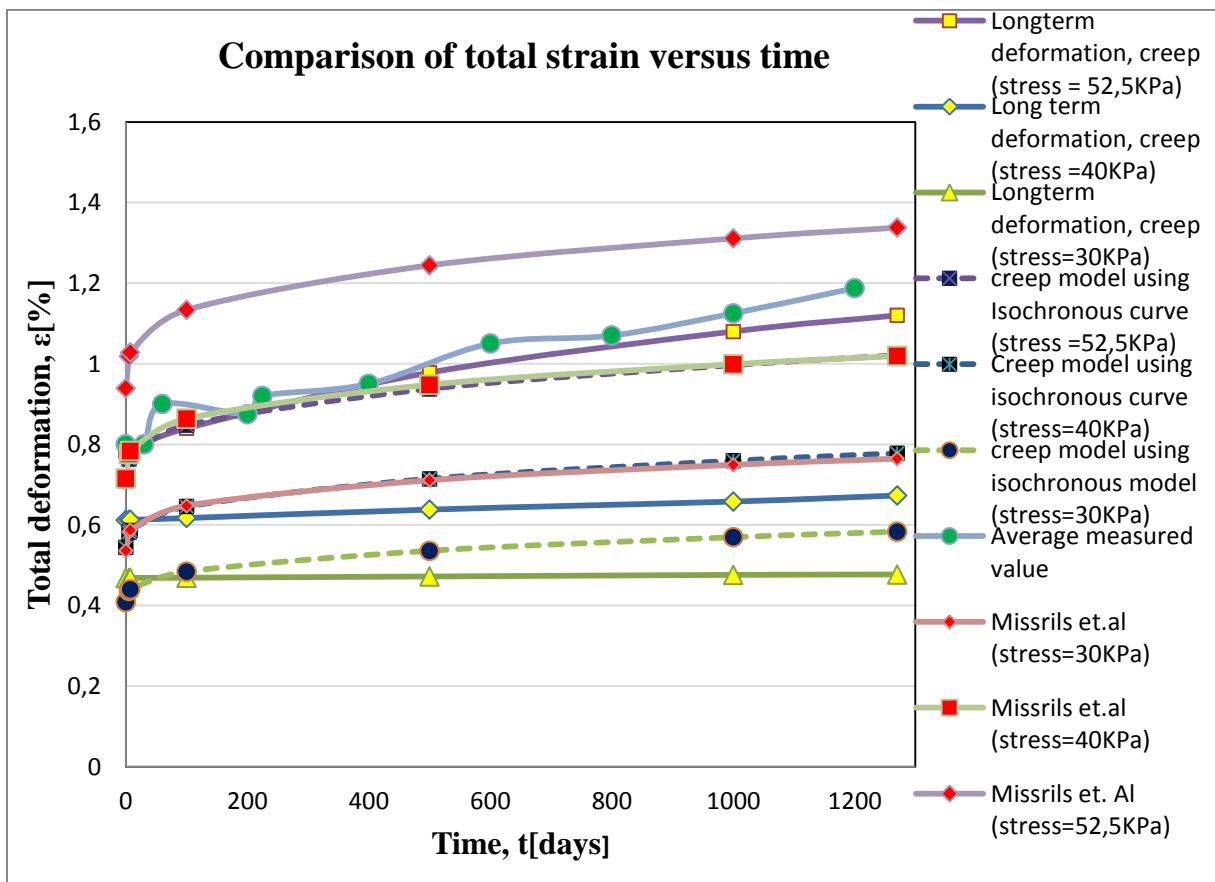


Figure 6.10: Comparison of results from empirical formula, PLAXIS output and average measured total deformation with time.

$$\partial \varepsilon_{tot} / \partial t = \partial (\varepsilon_0 + m \left(\frac{t}{t_0}\right)^{n_F}) / \partial t \quad (6.22)$$

$$\dot{\varepsilon} = m * n_F \sinh\left(\frac{\sigma}{\sigma_{mF}}\right) t^{(n_F - 1)} \quad (6.23)$$

Another way of illustrating the creep behavior of plastic materials is by using Sherby - Dorn plots as shown in figure 6.11. It gives a visual impression at which creep stage is our loaded material.

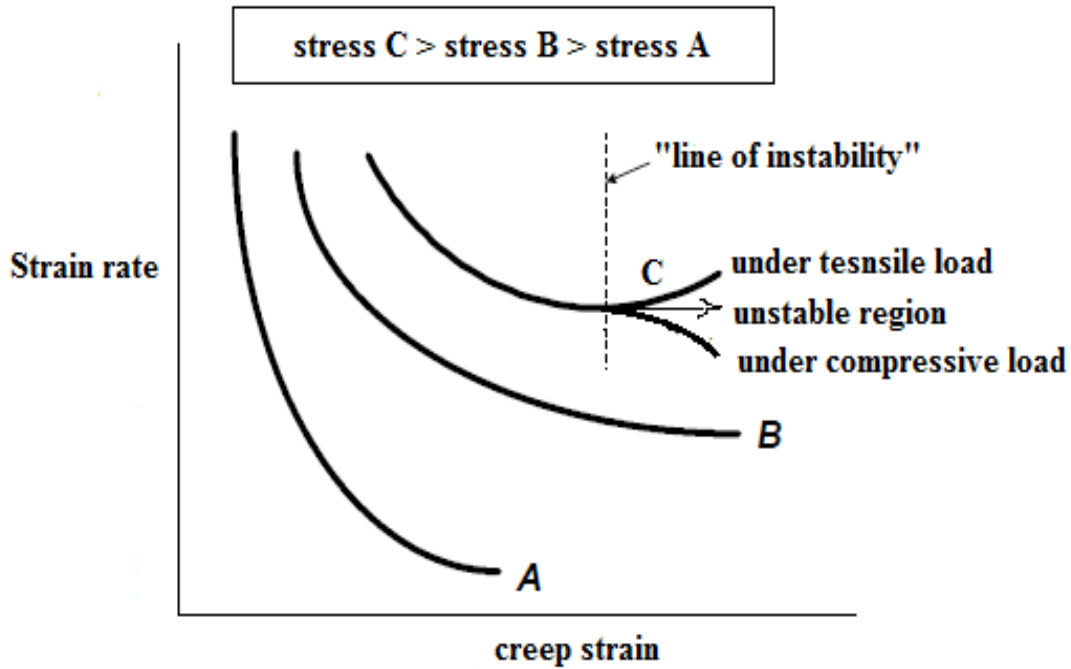


Figure 6.11: Sherby-Dorn plot [amended from [16]]

Sherby-Dorn plot for the full scale laboratory test is established using output from PLAXIS as shown in figure 6.12 and 6.13. It is clear that PLAXIS output and Findley equation gives a good prediction towards 52,5KPa applied stress and the fill was still in the range of stable region. Even if the number of samples taken is small, figure 6.13 still demonstrates the difference in the curvature of the curves as the applied stress varies. It can be demonstrated from the results shown in figure 6.12 that FE output using PLAXIS gives a lower strain rate than Findley equation at the start of the loading but a higher strain rate as time progresses.

Other known creep prediction formulas using creep strain rate had been developed for other families of plastic such as geomembrane by Merry and Bray (1987). The model was based on the method developed by Singh and Mitchel (1986) for modeling the creep rate of soils [9].

The formula has three parameters in its mathematical model and it is proved to represent well the creep at the primary level.

$$\dot{\varepsilon} = Ae^{\alpha D} \left(\frac{t}{t_0}\right)^m \quad (6.24)$$

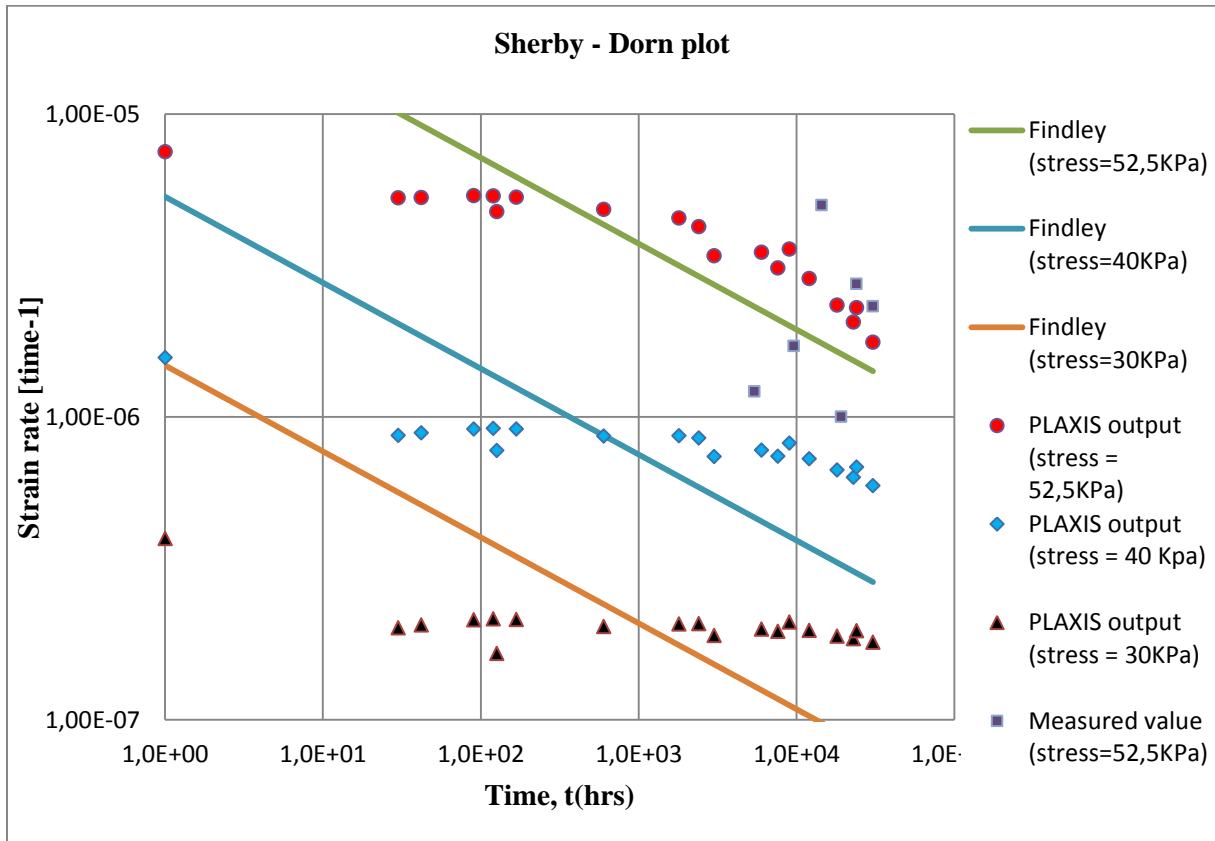


Figure 6.12: Sherby-Dorn plot (strain rate versus time)

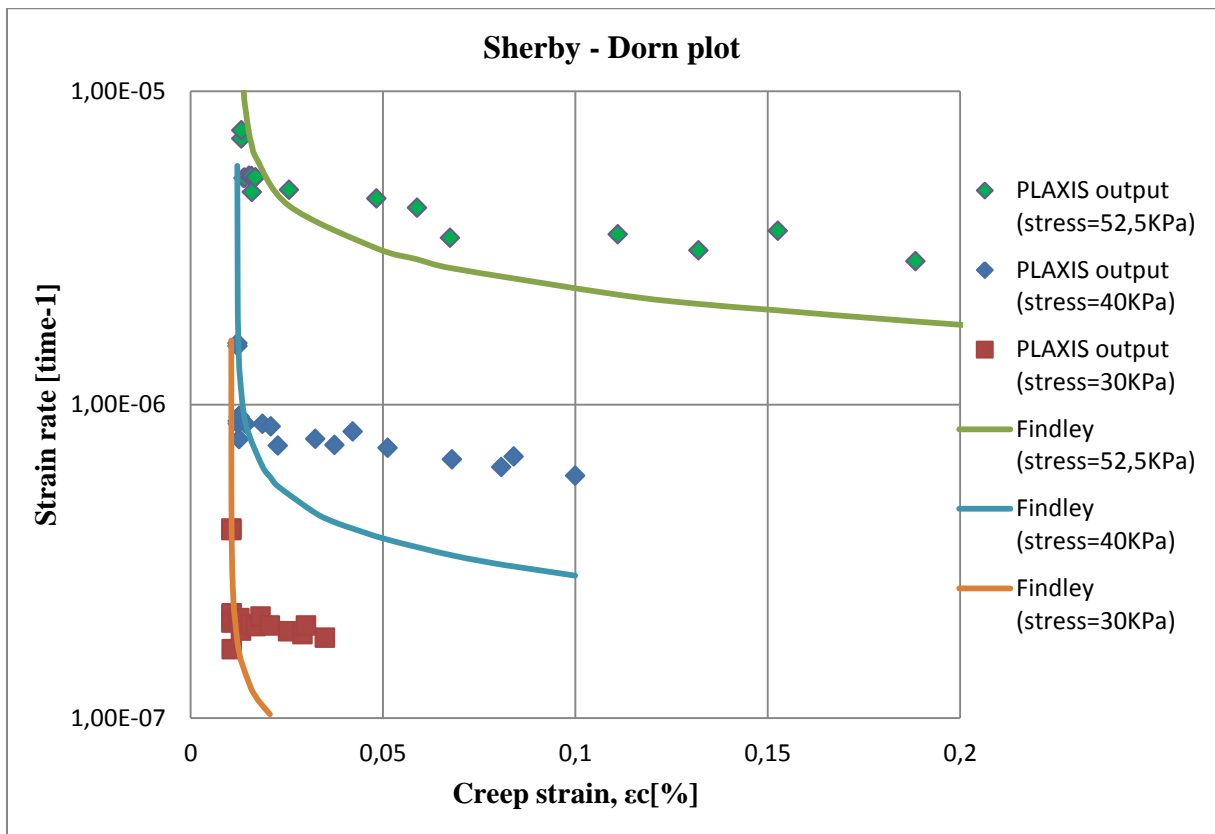


Figure 6.13: Sherby-Dorn plot (strain rate versus creep strain)

Where:

$\dot{\epsilon}$ = creep strain rate,

t, to = value of unit time;

D = deviator stress; and

A, α , and m = constant found by fitting of experimental results.

6.5 Other creep models

6.5.1 Mechanical models

These models try to formulate the creep behavior by using dashpot and spring to characterize the viscoelastic behavior of polymers in general. From simple to complicated different arrangements of spring and dashpot can be followed to define a specific component in creep. For example a series (Maxwell model) or parallel (Voigt or Kelvin model) arrangement of spring and dashpot can be used to define stress relaxation and creep/recovery condition respectively. More advanced models such as a series connection of Kelvin or Voigt model are mostly used to define the creep characteristics of polymers in general. *Figure 6.14* illustrates Kelvin model and a series of Kelvin models.

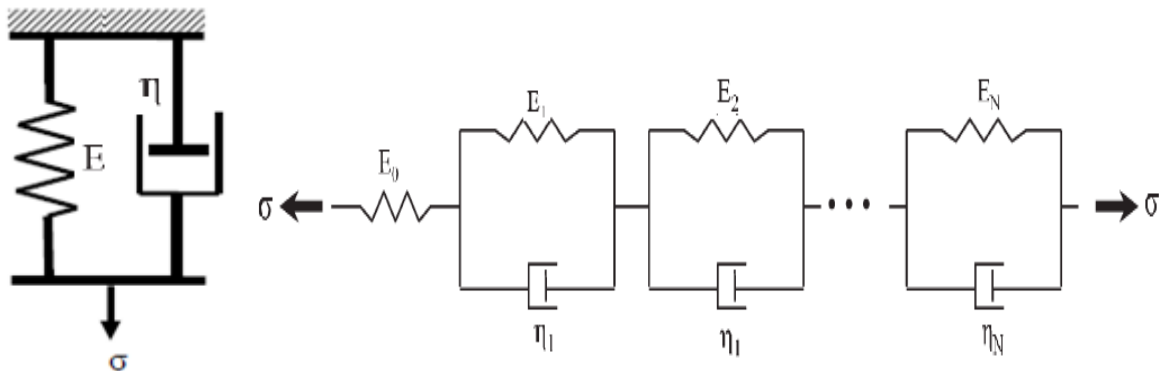


Figure 6.14: A) Basic Kelvin Model [9] B) Multi-Kelvin Model [21]

The Kelvin model can be expressed by equation 6.27 as follows:

$$\epsilon(t) = \sigma_0 \psi(t); \psi(t) = \psi_e + \psi_v(t) \quad (6.25)$$

$$\psi(t) = \frac{1}{E_0} + \sum_{i=1}^n \frac{1}{E_i} \{1 - \exp(-\frac{t}{\tau_i})\} \quad (6.26)$$

$$\epsilon(t) = \frac{\sigma_0}{E} [1 - \exp(-\frac{t}{\tau_i})] \quad (6.27)$$

Where:

$\psi(t)$ is the creep compliance function of time (t).

ψ_e stands for the instantaneous elastic part of the compliance, and

ψ_v is the viscous part of the compliance

E is the modulus to account for the resistance of the spring elements

τ_i accounts for the viscous response of the dashpots

E_0 is the elastic modulus of the spring, and

E_i is the modulus corresponding to each Kelvin element.

$1/E_0$ term denotes the single spring element in Fig. 6.13,

n denotes the number of Kelvin element in series.

The main aim of material modeling after setting up these formulas should be therefore, to find the best function for $\psi(t)$ which describes the stress-strain relationship from the creep test [21].

Based on equation 6.26 using three Kelvin elements, Joy J. Cheng, Maria Anna Polak and Alexander Penlidis found a good result for high density polyethylene material using both linear and non-linear assumptions for τ_i .

6.5.2 Weibull distribution

Weibull distribution is one of the most widely used lifetime distributions in reliability engineering. It is a versatile distribution that can take on the characteristics of other types of distributions, based on the value of the shape parameter, β . It is one of the famous statistical based formulas which define the failure criteria of materials. The most widely used Weibull function is the three-parameter equation shown in equation 6.28.

$$f(t) = \frac{\beta}{\eta} \left(\frac{t-\gamma}{\eta} \right)^{\beta-1} e^{-\left(\frac{t-\gamma}{\eta} \right)^{\beta}} \quad (6.28)$$

Where:

η is scale parameter,

β is shape parameter (or slope),

γ is location parameter

t is time

In creep model however, Weibull distribution is used mostly because it resembles the distribution from test data. Therefore, Weibull distribution is used to fit the data and further analysis and predictions follow as needed. Equation 6.29 is the most widely used Weibull distribution formula to predict the total deformation for polymer materials in general.

$$\varepsilon_{tot}(t) = \varepsilon_i + \varepsilon_c [1 - \exp(-\left(\frac{t}{\alpha} \right)^{\beta})] \quad (6.29)$$

For the creep behavior of polymeric materials, Fancey (2001) employed the model to predict the creep behavior of Nylon 6.6, polypropylene, and polyether-etherketone (PEEK) [9] whereas Kevin S. Fancey (2005) determined the creep, recovery and relaxation of nylon 6.6.

6.6 A real case history – Løkkeberg bridge

6.6.1 Løkkeberg bridge

In this section, comparison of long term deformation in EPS filled light weight embankments from theoretical modeling outputs as well as average measured results from long term monitoring projects is presented. Performance of EPS filled embankments which are constructed at either end of the Løkkeberg Bridge is considered as a base for discussion.

Løkkeberg bridge is one of the many bridges along the E6 motorway road between Norway and Sweeden to the southwest direction of Norway. It is 36,8m long single span acrow steel bridge across the E6 to facilitate the traffic flowing in that direction temporarily. The bridge was built in 1989. Due to the soft soil deposit of 16m below the abutment and low bearing capacity expectancy, it was decided to use EPS embankment as an abutment to carry the deck of the bridge as an alternative to end bearing pile.



Figure 6.15 Location of Løkkeberg bridge

6.6.2 Dimension and material quality

Løkkeberg bridge is 36,8m long and 5,5m high from the ground, single lane bridge. In order to support the traffic and dead load coming from the bridge deck, a 5m and 4,5m high EPS fill embankment was used at either ends of the bridge. Three types of EPS have been used for this project, EPS240 on the first layer immediately below the bridge, EPS180 until halfway through and the rest was filled with EPS100.

6.6.3 Stress distribution

As a part of investigation, stress distribution in the EPS embankment was measured using 10 hydraulic earth pressure cells 10 years after construction. A consistent data was obtained one

year after installation of the cells. *Figure 6.17* illustrates the consistency of measured data on EPS blocks after 10 years of operation. However, lower stresses than expected is measured at the central part of the fill which might be explained by the arch effect brought by the settlement of the underlying sub soil as well as higher stress to the left side of the embankment.

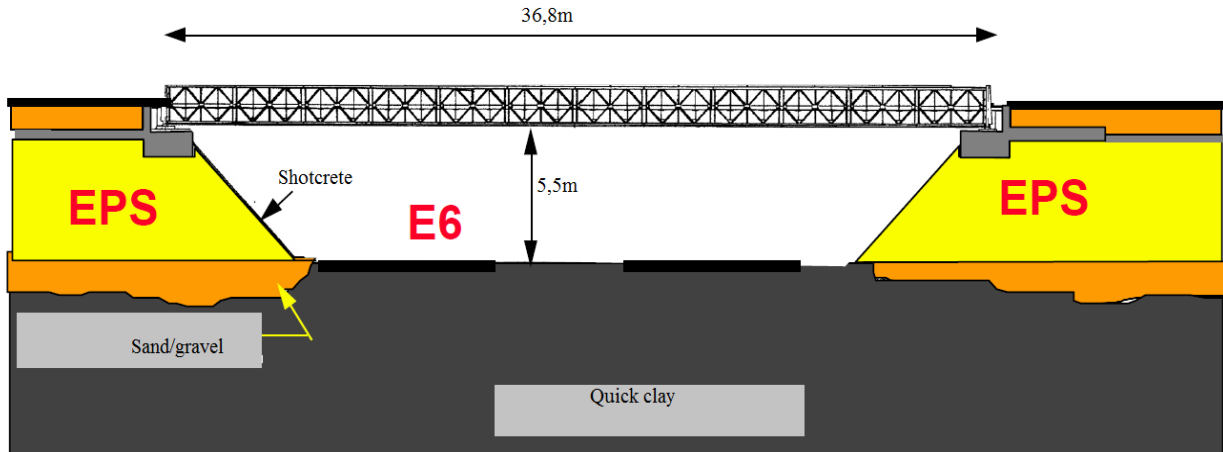


Figure 6.16: Geometry of Løkkeberg bridge

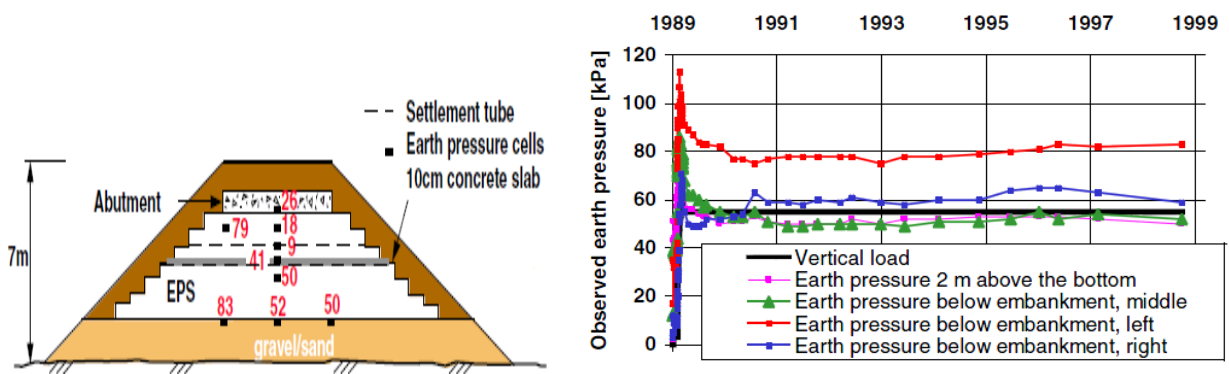


Figure 6.17: Observed stress distribution at Løkkeberg bridge after 10 years in to operation

6.6.4 Measured deformation

Total deformation measured 12 years after operation is nearly 6cm which accounts 1,3% of the EPS thickness. Average creep measured for 10 years at the bottom layer of EPS accounts for 6,5% of the thickness. On practical point of view, satisfactory results were obtained.

6.6.5 Comparison between observed and calculated deformation

For practical engineering design of EPS fill embankments, Findley and LCPC equations have been used considerably as discussed in the previous sections. But in this section, comparisomal analysis based on results from measured deformation on the EPS fill embankment and Findley, LCPC as well as their families output derived from PLAXIS 2D will be presented below.

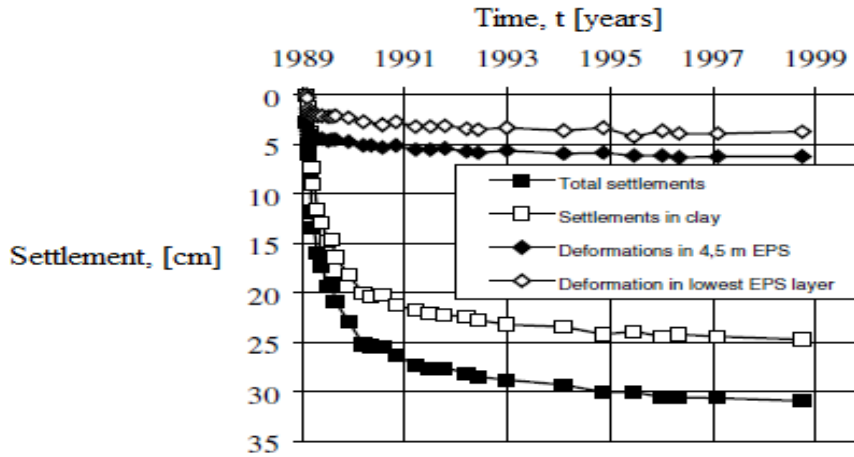


Figure 6.18: Measured total deformation at Løkkeberg bridge

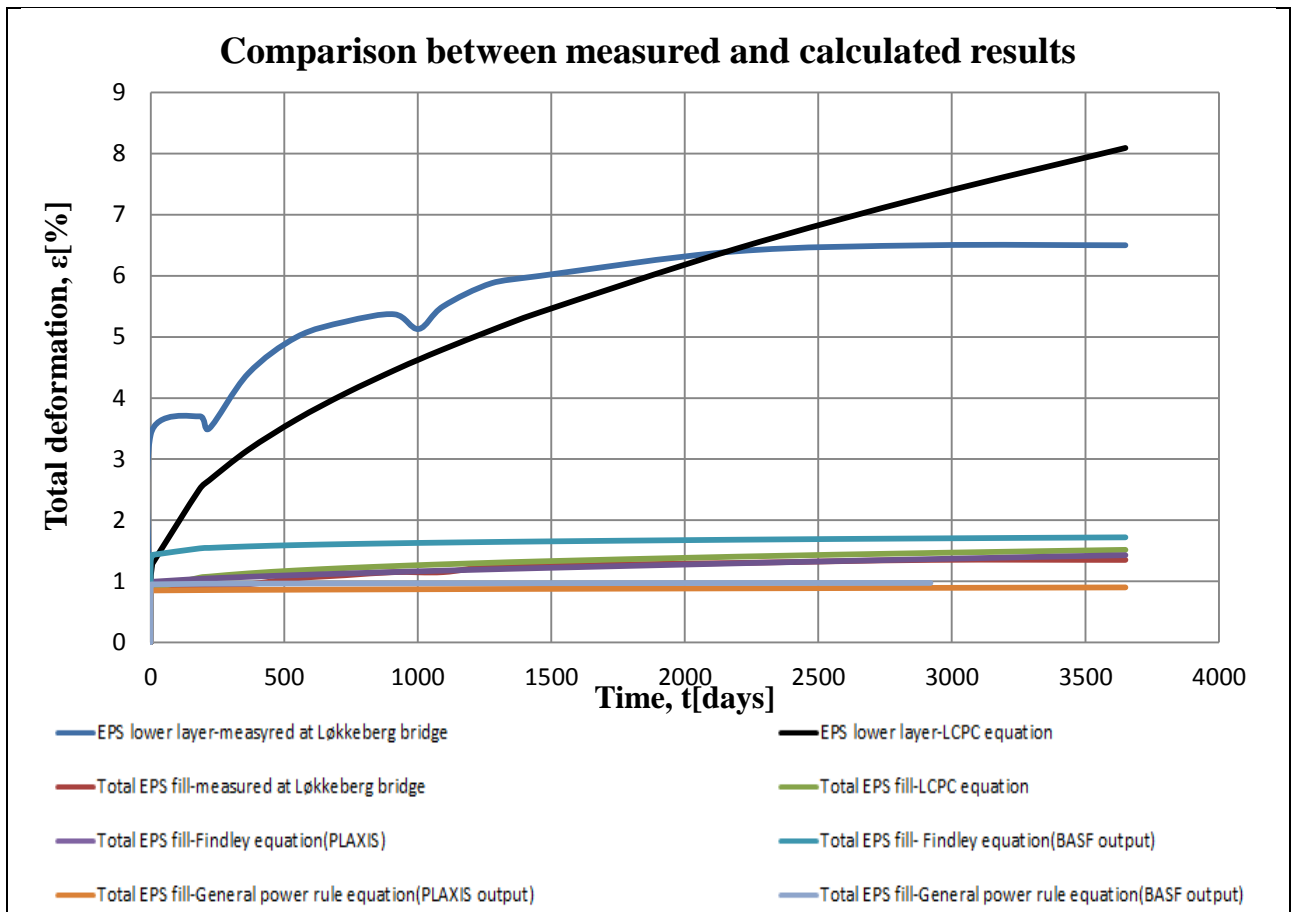


Figure 6.19 Comparison and calculated values of EPS total deformation at Løkkeberg brige

As illustrated in figure 6.19 LCPC equation (Magnan and serratrice) tend to overestimate the total deformation as time increases considerably while Findley equation gives relatively a reliable estimation. In general, general power law equation tends to underestimate the total deformation. In addition, results based on PLAXIS tend to give a better estimation than BASF. Perhaps, this might be explained to the fact that output results from PLAXIS are based on full scale test unlike BASF in which the output was obtained from small samples which overestimate deformation.

6.7 Conclusion

In this chapter, overall presentation about creep modeling for EPS geofaom in different methods is presented. Particularly, focus on the application of FE methods, PLAXIS, for EPS blocks are investigated. Even if the constitutive models of soil is different from polymer materials, the overall stress-strain relationship calibrated from PLAXIS can be used for EPS blocks with good accuracy.

Determination of Findley parameters is highly sensitive on the accuracy at which immediate strain is calculated. Stress range and duration of the test has also a direct impact on determination of Findley parameters. Findley parameters calculated from PLAXIS output is in general different from the values obtained from lab tests. As for any FE output, the values obtained in this chapter can be changed as the size of mesh and soil parameters differ.

A slightly overestimation of elastic modulus and hence immediate strain is noticed on FE, PLAXIS calculation. But, for the overall duration of the full scale test under study, PLAXIS output gives good estimation. Creep calculated from parameters obtained in BASF test tend to overestimate which confirms results from small size test samples tend to do that way.

Empirical formulas to determine creep of EPS geofaom based on ISSC curves merely depend on the accuracy of establishing relationship between E-modulus with time. Polymer materials tend to show viscoelastic nature under loading and a power function can relate the development of modulus with time much better. A good estimation of creep is obtained from ISSC curve obtained from PLAXIS output.

In general, results obtained from FE simulation in this chapter gives a good estimation for total deformation and it can always be changed as parameters in FE code changes.

Table 6.5: Summary of formulas for prediction of total deformation

Name	Formula
Findley equation (parameters from PLAXIS output)	$\varepsilon=0,009*\sinh(\sigma/58)+0,000000004 *\sinh(\sigma/7,8)t^{0,71}$
Findley equation (parameters from BASF test)	$\varepsilon=0,011 *\sinh(\sigma/54,2)+0,000305* \sinh(\sigma/33)t^{0,20}$
Simplified Findley equation (parameters from PLAXIS output)	$\varepsilon=0,009 *(\sigma/58)+0,000000004 *(\sigma/7,8)t^{0,71}$
Simplified Findley equation (parameters from BASF test)	$\varepsilon=0,011* (\sigma/54,2)+0,000305* (\sigma/33)t^{0,20}$
General power rule equation (parameter from PLAXIS output)	$\varepsilon=0,0085+0,0000015 t^{0,708}$
General power rule equation (parameter from BASF test)	$\varepsilon=0,0094+0,000666 t^{0,202}$
Magnan and Serratrice (LCPC) equation	$\varepsilon=0,00783+0,000509 t^{0,325}$
Formula using ISSC (PLAXIS output)	$\varepsilon= \sigma/ (76 -5,1t^{0,22})$
Formula using ISSC (Missrils et.al)	$\varepsilon= \sigma/ (59,4 -5,98t^{0,17})$

Chapter 7

Summary and Conclusions

7.1 Summary

This investigation aimed at the parametric study of EPS as a light weight fill embankment in road construction. Both short and long term deformation characteristics as well as mechanical parameters of EPS are discussed based on laboratory test outcomes and literature reviews. Up on this study some conclusions are arrived and stated as follows.

Literature reviews on parametric study of EPS suggested scattered results on mechanical parameters specially poisson's ratio and elastic modulus. Laboratory and research results on EPS parameters are summarized and presented in chapter 2 including suggested parameters indicated in AASHTO and Eurocode design manuals.

Parametric studies of EPS under short term loading were studied and presented in chapter 3 of this document. Laboratory tests were carried out on EPS100 block of density 30Kg/m³ to determine the effect of specimen size and shape, loading rate as well as temperature on the outcome of mechanical parameters of EPS. An increase in elastic modulus as well as compressive strength is shown when the specimen size increases. In addition, disc shaped samples tend to give stiffer material parameters with respect to cylindrical and cube shaped samples. A 30% increase in stiffness for 5°C temperature difference is shown for tests carried out in the lower temperature range (-20 – 20 °C). Consequently, higher compressive strength is indicated as the temperature of the specimen depressed. Overall, an average stiffness value of nearly 5MPa and compressive strength $\sigma_{10\%}$ of 115KPa ($\sigma_{5\%} = 93\text{KPa}$) was found. Scattered and non-uniform results were found from test outputs and trend between parameters were improbable to produce.

In chapter 4, long term deformation of EPS was studied based on laboratory test outcomes on small size samples and literature reviews. A 5days creep test on EPS100 showed the influence of decreasing the total deformation as the specimen size increases. Deformation value of 1%, 0.85 and 0.55% for 50mm, 100mm and 150mm cube samples respectively and a much lower values recorded in full scale tests. Disc shaped samples produce lesser immediate deformation rather than cube and cylindrical shaped samples, however, the rate of deformation in disc shaped samples are higher and therefore produce highest deformation as time passes by. The effect of temperature on the creep, subsequently on total deformation, is studied in this chapter as well. As temperature risen from -20 to -10 and -5 °C, the total deformation decreased, leading to a reverse effect. Since the scatter of results were high during laboratory test of EPS, less number of tests as well as the uncertainties related with loading the samples are mentioned for the unexpected result. Overall, higher total deformation were registered during this tests than what is obtained in literatures and field measurements.

Finite element analysis of EPS geofam embankments are studied in chapter 5. Design criteria of EPS geofam embankment, discussion of soil models with respect to the

characteristics of EPS are studied. Constitutive equations of hardening soil model and soft soil model are briefly discussed and compared with some of the models used for EPS. Finally, calibration of EPS parameters using hardening and soft soil models in PLAXIS 2D is performed and compared with some of the outputs obtained from laboratory test of EPS. A workable fit is obtained and lead to the conclusion: one can calibrate and use soil parameters for EPS because of the similarity of stress strain relationship up on loading. Parallely, full scale EPS embankment test carried out by Roald Aabøe in 1993 is simulated using PLAXIS 2D and total deformation outcomes were compared with the measured ones and satisfactory results were obtained. But, slight overestimation of elastic modulus and hence immediate strain is noticed on FE, PLAXIS calculation.

In chapter 6, creep models for EPS geofoam are discussed. Empirical equations, creep models using isochronous stress-strain curves, creep strains using strain rate and mechanical creep models are discussed. Findley equation as a part of empirical equation was dealt in detail and coefficients for the equation are calculated using the output from PLAXIS 2D simulation of the full scale creep test performed in 1993 by Roald Aabøe. Rather different coefficients were obtained from what is calculated using BASF test results on 50mm samples. Nevertheless, good prediction was found when used to estimate the long term deformation of the Løkkeberg bridge EPS embankment. Similar calculations were performed to develop coefficients for Missrils equation developed using isochronous stress-strain curves and satisfactory results are obtained. Equations obtained as a result of this study are summarized at the end of chapter 6.

7.2 Conclusion

1. Even if EPS geofoam blocks are manufactured in controlled process, both physical and mechanical parameters of the material obtained in tests are scattered due to the non-uniformity of pre-puffs (beads) in molding stage of production. Therefore, sampling is very important.
2. An initial tangent (secant) modulus of 5MPa can be used for preliminary design of EPS embankment if EPS100 is used. Nevertheless, tests should be carried out to for the exact material to be used in the actual construction phase and change accordingly, if needed.
3. Poisson's ratio of 0,1 is highly recommended but for special uses of EPS, as buffer to vibration, precise tests should be carried.
4. Special attentions should be given while using FE calculations using soil models for EPS embankments. Parameters calibrated using HS-model gives slight overestimation in stiffness and SSC model predicts the total deformation very well.
5. Loads under 50% of the compressive strength of EPS produce less than 2% total deformation. In addition, Findley equation can estimate the deformation of EPS well within a practical range.

Chapter 8

Recommendations

Based on the outcome of this study the following suggestions are made:

1. Local measurement of deformation for EPS samples are necessary to obtain accurate parameters needed for small strain application. Stress measuring cells of between 1 – 2KN is recommended to be used for EPS100 blocks.
2. More accurate performance characteristics of EPS can be obtained by doing long term deformation tests in temperature chambers where the temperature can fluctuate from lower ranges up to high up on constant loading.
3. Empirical equations for determination of total deformation should include time-stress-temperature parameters. Test results obtained from recommendation 2 can be used to fill the temperature dependent parameter on some of the existent equations, e.g Findley equation, to give it more accuracy.

Chapter 9

References

1. NCHRP Project HR 24-11 report 529, “*Guidelines for Geofoam Applications in Embankment Projects*”, transportation research board (TRB), 2004, USA, pp 1- 70
2. Lars-Marius B. Andersen, Jon Andreas Tjernsbekk, Tiril A. Stang and Kari Lindqvist “*Ekspandert polystyren i norsk vegbygging*”, bachelor thesis at Høgskolen i Østfold, June 2011
3. Ahmed Fouad Elragi, “Selected Engineering Properties and Applications of EPS Geofoam”, 2006: (<http://www.softoria.com/institute/geofoam/index.html>)
4. I. J. Gnip, V. I. Kersulis, and S. I. Vaitkus, “*Predcting thr deformability of Expanded polystyrene in long term compression*”, Mechanics of Composite Materials, Vol. 41, No. 5, 2005
5. Norwegian public road administration, “*Publication no.100: Light-weight filling materials for road construction*”, Oslo, December 2002, pp.11-25
6. Hans Tepper,” *EU product standard for EPS and performance requirements*”, EPS conference 2011, Lillstrøme, Norway, pp. 5.
7. T. Schanz, P.A Vermeer and P.G Bonnier, “ *The hardening soil mode: Formulation and verification*”, 1999 Balkelma, Rotterdam, pp. 1-16
8. PLAXIS user manual, chapter 8, pp. 85-88
9. PHd thesis sang sik yo, “*Evaluation of Creep Behavior of Geosynthetics Using Accelerated and Conventional Methods*”, Ph.d thesis at Drexel University, August 2007
10. European Manufacturers of EPS EUMPS, “ *EPS White blocks, Background Information on standardization of EPS*”, 2011, pp-18
11. Ivan Gnip, Vladislovas Kersultis, Saulius Vaitkus, Sigita Vejelis, “*Assessment of Strength under Compression of Expanded Polystyrene (EPS) Slabs*”, Institute of Thermal Insulation, Vilnius Gediminas Technical University, Linkmenu 28, LT-08217 Vilnius, Lithuania , ISSN 1392–1320 material sciences (MEDŽIAGOTYRA). Vol. 10, No. 4. 2004
12. David Arellano, Roald Aabøe, Timothy D. Stark “ *Comparison of existing EPS – block geofoam creep models with field measurements*”, EPS geofoam 3rd international conference, December 2001, Salt Lake city, Utah
13. Srirajan, D. Negusse and N. Anasthas, “*Creep behavior of EPS geofoam*”, Syracuse University, NY, USA pp. 1-12
14. European standard for EPS manufacturing:(<http://www.scribd.com/doc/73740765/BS-EN-13163-2001>)
15. Styropoor-technical information, “*highway construction/ground insulation:Styropor foam as a lightweight construction material for road base-courses*”, june 1991/September 1993, pp 1-10.
16. John S. Horvath, “*Mathematical Modeling of the Stress-Strain-Time Behavior of Geosynthetics Using the Findley Equation: General Theory and Application to EPS-*

- Block Geofam*”, Manhattan College School of Engineering, Civil Engineering Department-Bronx, New York 10471-4098, U.S.A, May 1998.
17. John S. Horvath, “*Manufacturing Quality Issues for Block-Molded Expanded Polystyrene Geofam*”, Manhattan College School of Engineering, Civil Engineering Department-Bronx, New York 10471-4098, U.S.A, February 2011.
 18. Santa Clara University Engineering Design Center:
(http://www.dc.engr.scu.edu/cmdoc/dg_doc/develop/material/property/a2200002.htm#210458)
 19. Bright science bright living (DSM) material quality investigation:
(http://www.dsm.com/en_US/html/dep/design_pressfits.htm)
 20. Missirlis, Papastilianou, Atmatzidis and Chrysikos, “*Behavior of EPS Geofam in Compression*”
 21. Joy J. Cheng,¹ Maria Anna Polak,² Alexander Penlidis¹,” *An Alternative Approach to Estimating Parameters in Creep Models of High-Density Polyethylene*”, Polymer Engineering & Science Volume 51, Issue 7, Article first published online: 4 NOV 2010, pp 1227-1235
 22. Kevin S. Fancey, “*A mechanical model for creep, recovery and stress relaxation in polymeric materials*”, Journal of material science, 08 July 2005
 23. Steinar Nordal, “*Advanced geotechnical engineering*”, literature book at Norwegian university of science and technology
 24. PLAXIS user manual
 25. Byung Sik Chun, Hae-Sik Limb, Myung Sagongc and Kyungmin Kima, “*Development of a hyperbolic constitutivemodel for expanded polystyrene (EPS) geofam under triaxial compression tests*”, Geotextiles and Geomembranes Volume 22, Issue 4, August 2004, Pages 223-237
 26. Edwin Theodorus Jacobus Klompen, “*Mechanical properties of solid polymers: Constitutive modelling of long and short term behavior*”, Technische Universiteit Eindhoven, 2005. Proefschrift. - ISBN 90-386-2806-4 NUR 971, pp 4
 27. Sujan E. Bin Wadud, “*Time-Temperature Superposition Using DMA Creep Data*”, TA Instruments, Inc., 109 Lukens Drive, New Castle, DE 19720, pp. 1
 28. D.S. Matsumotuo, “*Time-Temperature Superposition and Physical Aging in Amorphous Polymers*”, Polymer Physics and Engineering Laboratory Corporate Research and Development General Electric Company Schenectady, New York 12301, pp.1-2
 29. K.G.N.C. Alwis and C.J. Burgoyne, “*Stepped Isothermal Method for Creep Rupture Studies of Aramid Fibres*”, pp. 183-184

Chapter 10

Appendix

Appendix A European standard

A.1 European Standard classification of EPS products (EN 13163:2001)

EPS- products are divided into types as shown in Table A.1 and A.2. Type EPS T has specific impact sound insulation properties. Each type, except EPS S, which is not used in load bearing applications, shall satisfy two different conditions at the same time in order to ensure adequate product performances.

Table A.1: Classification of EPS products

Type	Compressive stress at 10 % deformation kPa	Bending strength kPa
EPS S	–	50
EPS 30	30	50
EPS 50	50	75
EPS 60	60	100
EPS 70	70	115
EPS 80	80	125
EPS 90	90	135
EPS 100	100	150
EPS120	120	170
EPS 150	150	200
EPS 200	200	250
EPS 250	250	350
EPS 300	300	450
EPS 350	350	525
EPS 400	400	600
EPS 500	500	750

Table A. 2: Classification of load bearing EPS products with acoustical properties

Type	Compressibility	Dynamic stiffness
EPS T	Level taken from Table A. 4	Level taken from Table A.3

Table A.3: Levels of dynamic stiffness

Level	Requirement MN/m³
SD50	≤ 50
SD40	≤ 40
SD30	≤ 30
SD20	≤ 20
SD15	≤ 15
SD10	≤ 10
SD7	≤ 7
SD5	≤ 5

Table A. 4: Levels of compressibility

Level	Imposed load on the screed kPa	Requirement mm	Tolerance mm
CP5	≤ 2,0	≤ 5	≤ 2 for $d_L < 35$ ≤ 3 for $d_L ≥ 35$
CP4	≤ 3,0	≤ 4	
CP3	≤ 4,0	≤ 3	
CP2	≤ 5,0	≤ 2	≤ 1 for $d_L < 35$ ≤ 2 for $d_L ≥ 35$

A.2 Factory Production control (EN 13163:2001)

A.2.1 Testing frequencies

Table A.5: Minimum product testing frequencies

Clause		Minimum testing frequency ^a		
No	Title	Direct testing	Indirect testing	
			Test method	Frequency
4.2.1	Thermal resistance and thermal conductivity ^b	1 per 24h or 1 per 3 month or 1 per 3 month 1 per year	-	-
			And weight per moulded item or density (using a manufacturer correlation)	1 per 2hr
			And other test method for thermal conductivity	1 per week
			And density (using the correlation given in Fig A.2)	1 per 2 hr
4.2.2	Length and width	1 per 2 hr	-	-
4.2.3	Thickness	1 per 2hr	-	-
4.2.4	Squareness	1 per 4 hr	-	-
4.2.5	Flatness	1 per 8 hr	-	-
4.2.6	Dimensional stability	ITT ^c	-	-
4.2.7 and 4.3.6	Bending strength	1 per day or 1 per 3 month	-	-
			And manufacturers method	1 per day
4.2.8	Reaction to fire	See table A.2		
4.3.2	Dimensional stability under specified compression load and temperature conditions	ITT ^c	-	-
4.3.3	Deformation under specified compression load and temperature conditions	ITT ^c	-	-
4.3.4	Compressive stress at 10% deformation	1 per day or 1 per 3 month or 1 per year	-	-
			And weight per moulded item or density (using a manufacturer correlation)	1 per 2hr
			And weight per moulded item or density (using the correlation given in figure A.1)	1 per 2hr
4.3.5	Tensile strength perpendicular to faces	1 per week or 1 per 3 month	-	-
			And bending strength	1 per day
4.3.8	Compressive creep	ITT ^c	-	-
4.3.9.1	Long term water absorption by immersion	ITT ^c	-	-

4.3.9.2	Long term water absorption by diffusion	ITT ^c	-	-
4.3.10	Freeze and thaw resistance	ITT	-	-
4.3.11	Water vapour transmission	ITT	-	Tabulated values
4.3.12	Dynamic stiffness	1 per week	-	-
4.3.13	Thickness, d Compressibility	1 per day 1 per week	- -	- -
4.3.15	Release of dangerous substances ^d	-	-	-

^a The minimum testing frequencies expressed in test results shall be understood as the minimum for each production unit line under stable conditions. In addition to the testing frequencies given above, testing of relevant properties of the product shall be repeated when changes or modifications are made that are likely to affect the conformity of the product.

^b For factory production control one measurement shall always be one test result.

^c ITT, see EN 13172.

^d Frequencies are not given, as test methods are not yet available.

Table A.6: Minimum product testing frequencies for the reaction to fire characteristics

Clause		Minimum Testing frequency ^a								
No	Title	Direct testing ^{b,c}		Indirect testing ^{d,e}						
4.2.8	Reacti on to fire class			Product		Components ^{f,g}				
						Substantial(EPS)		Non- substantial(Layers)		
		<i>Test method</i>	<i>Frequen cy</i>	<i>Test method</i>	<i>Freq uenc y</i>	<i>Test method</i>	<i>Frequ ency</i>	<i>Test method</i>	<i>Frequency</i>	
A1	prEN ISO 1182 and prEN ISO 1716 (and prEN ISO 13823)	1 per 2 years and Indirect testing	-	-	Loss on ignition	1 per 4 hr	Loss on ignition or calorific potential	1 per 4 hr		
					Apparent density	1 per 1 hr	Weight unit per area	1 per 1 hr		
A2	prEN ISO 1182 or prEN ISO 1716 (and prEN ISO 13823)	1 per 2 years and Indirect testing	-	-	Loss on ignition	1 per 4 hr	Loss on ignition or calorific potential	1 per 4 hr		
					Apparent density	1 per 1 hr	Weight unit per area	1 per 1 hr		
B,C,D	prEN ISO 13823 and prEN ISO 11925-2	1 per month Or 1 per 2 years and indirect testing	-	-	-	-	-	-		
					prEN ISO 11925-2	1 per day ^h	Apparent density and thickness	1 per 2 hr	Weight unit per area	1 per day
					-	-	-	-	-	-
E	prEN ISO 11925-2	1 per day ^h	-	-	-	-	-	-		
F	-	-	-	-	-	-	-	-		

^a The minimum testing frequencies, expressed in test results, shall be understood as the minimum for a product or product group for each production unit/line under stable conditions. In addition to the testing frequencies given given above, testing of relevant properties of the product shall be repeated when changes or modifications are made that are likely to affect the conformity of the product.

^b Direct testing can be conducted either by third party or the manufacturer.

^c Direct testing may also be the referencescenario room-corner test ISO 9705:1993 Fire test – full scale room test for service products.

^d Indirect testing is only possible in the case of products falling within the system 1 of conformity of reaction to fire, or by having a notified body verifying the correlation between the direct testing.

^e Indirect testing can be either on the product or its components

^f Definition as given in Euroclasses decision 2000/147/EC:

Substantial component: a material that constitute a significant part of a non- homogeneous product. A layer with a mass per unit area $\geq 1,0\text{Kg/m}^2$ or a thickness $\geq 1,0\text{mm}$ is considered to be a substantial component.

Non substantial component: A material that does not constitute a significant part of a non-homogeneous part. A layer with a mass per unit area $\leq 1,0\text{Kg/m}^2$ or a thickness $\leq 1,0\text{mm}$ is considered to be a non substantial component.

^g Incase of a certified component, the frequency is once per delivery of the component.

^h Incase of certified raw material the frequency is once per week.

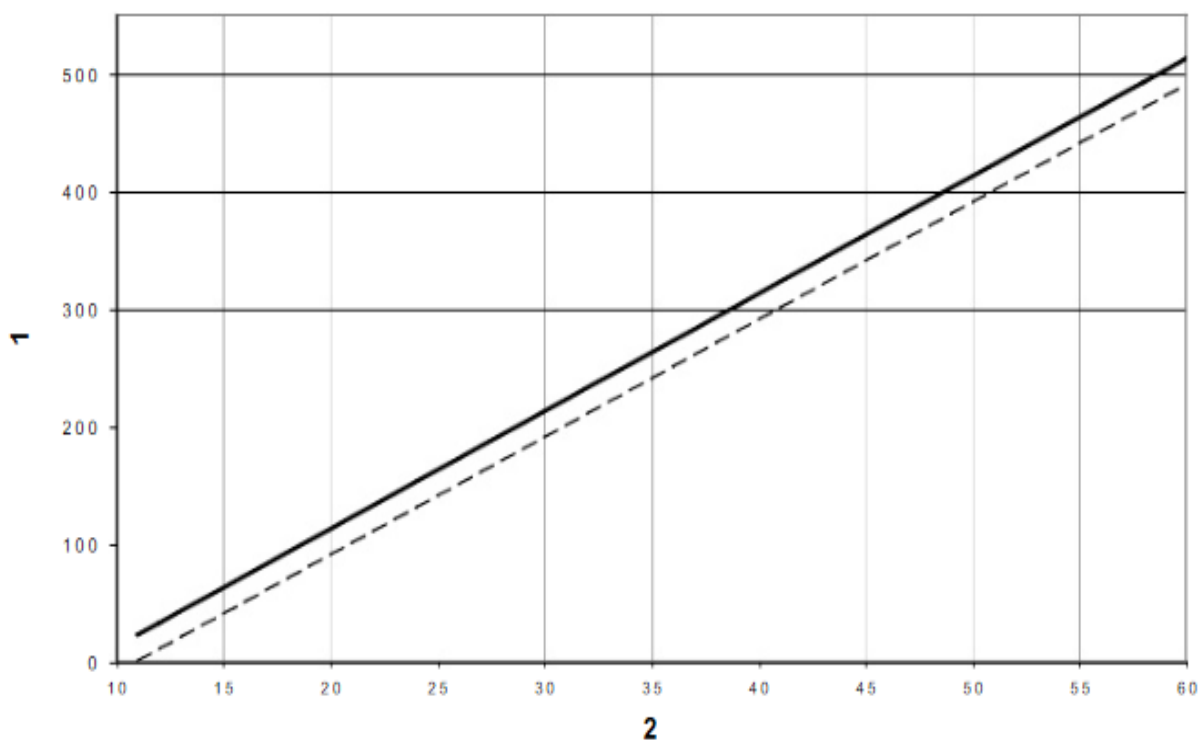
A.2.2 Indirect testing

A.2.2.1 General

If indirect testing is used, the correlation between the directly tested and the indirect property shall be known and the approach shall be calculated on a one sided 90 % prediction interval.

NOTE In this context compressive stress by 10 % deformation and thermal conductivity may be evaluated indirectly using the apparent density and its established mathematical correlation to these properties. For the relationship between compressive stress at 10 % deformation and apparent density and thermal conductivity and apparent density there is a large amount of data collected in Europe. The curves in Figures A.1 and A.2 have been calculated on this European data to which every manufacturer may refer. If a manufacturer wants to use his own data, he has to calculate and to record the approach for a prediction interval, $1-\alpha$, of 90 %.

A.2.2.2 Compressive stress at 10 % deformation



Key

1 Compressive stress 10[kPa]

2 Apparent density Pa [kg/m³]

_____ Compressive stress

----- Predicted compressive stress

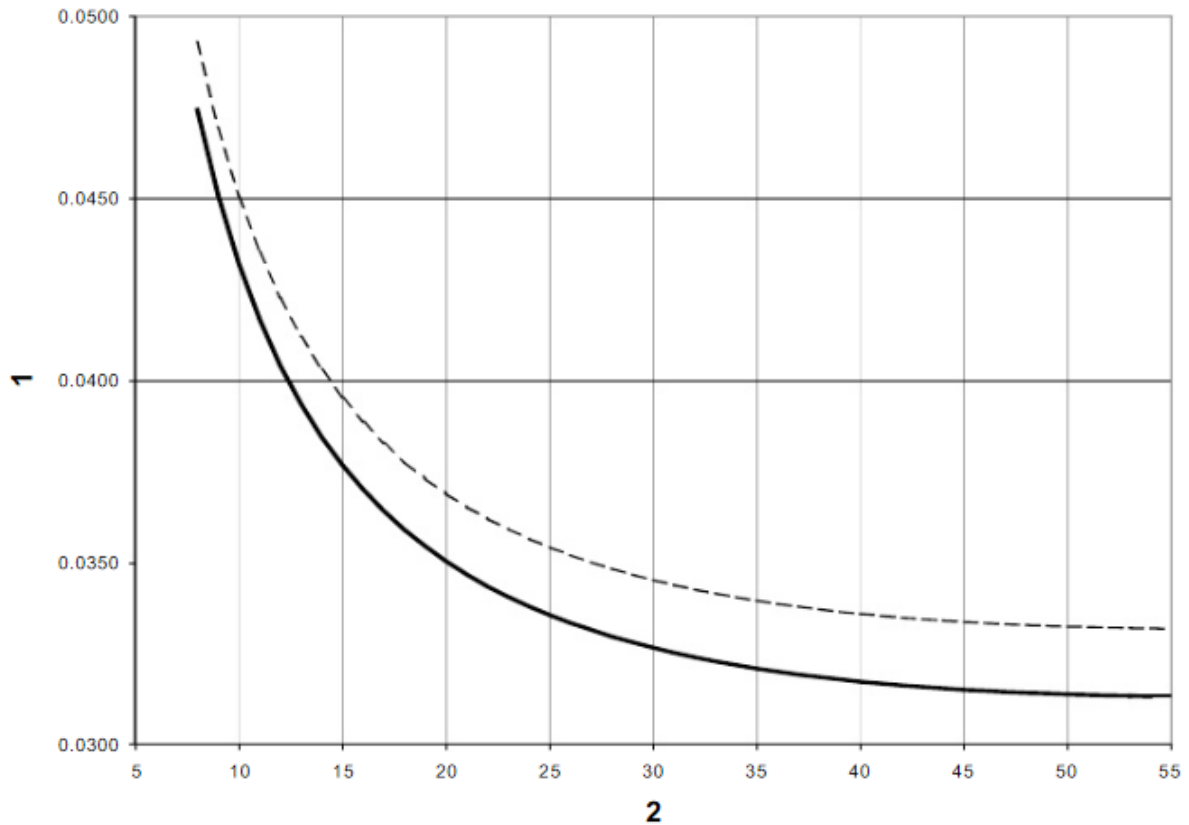
Figure A.1 — Relationship between compressive stress at 10 % deformation and apparent density for indirect testing; $1 - \alpha = 0,9$; $n = 495$

Regression of $\rho_a \geq 11 \text{ kg/m}^3$

$\sigma_{10, \text{mean}} = 10 \text{ Kpa.m}^3/\text{Kg} \times \rho_a - 81 \text{ Kpa} [\text{Kpa}]$

$\sigma_{10, \text{pred}} \approx 10 \text{ Kpa.m}^3/\text{Kg} \times \rho_a - 109,1 \text{ Kpa} [\text{Kpa}]$

A.2.2.3 Thermal conductivity



Key

1 Thermal conductivity λ [W/m·K]

2 Apparent density ρ_a [kg/m³]

————— Mean thermal conductivity

----- Predicted thermal conductivity

Figure A.2 — Relationship between thermal conductivity (at 50 mm reference thickness and 10 °C mean temperature) apparent density for indirect testing; $1 - \alpha = 0,9$; $n = 3873$

Regression for $8 \text{ kg/m}^3 \leq \rho_a \leq 55 \text{ kg/m}^3$:

$$\lambda_{\text{mean}} = 0,025314 \text{ W/(m·K)} + 5,174 \cdot 3 \times 10^{-5} \text{ Wm}^2/(\text{kgK}) \times \rho_a + 0,173606 \text{ Wkg}/(\text{m}^4\text{K}) / \rho_a$$

[W/(m.K)]

$$\lambda_{\text{pred}} \approx 0,027 \cdot 174 \text{ W/(m·K)} + 5,174 \cdot 3 \times 10^{-5} \text{ Wm}^2/(\text{kgK}) \times \rho_a + 0,173 \cdot 606 \text{ Wkg}/(\text{m}^4\text{K}) / \rho_a$$

[W/(m·K)]

A.2.2.4 Thickness effect

For boards of a thickness of 50 mm with a declared thermal conductivity equal or less than 0,038 W/(m·K) the thickness effect is negligible.

To assess the relevance of the thickness effect, a conversion of the measured thermal conductivity, λ_i' , or the thermal resistance, R_i' , into the values λ_i or R_i has to be carried out according to the following equations:

$$\lambda_i = \lambda_i' / L$$

$$R_i = R_i' / L$$

Table A.7 : Thickness effect parameter, L , for the determination of the declared thermal conductivity, λ_0

Declared thermal conductivity λ_0 at reference thickness of 50 mm W/(m·K)	Thickness of the test specimen d mm	Thickness effect parameter L 1
0,046	20	0,90
	30	0,92
	40	0,93
	50	0,95
	100	0,98
	200	1,00
0,043	20	0,91
	30	0,93
	40	0,94
	50	0,97
	100	1,00
0,040	20	0,92
	30	0,95
	40	0,96
	50	0,97
	100	1,00
0,038	20	0,93
	30	0,96
	40	0,97
	50	0,99
	100	1,00
0,035	20	0,94
	30	0,97
	40	0,98
	50	1,00
	100	1,00
0,032	20	0,96
	30	0,97
	40	0,98
	50	1,00
	100	1,00

Parameters shall be obtained from linear interpolation(s) for intermediate values of thermal conductivity and/or thickness.

NOTE

The values in Table A.7 are taken from measured values from Forschungsinstitut für Wärmeschutz e.V. (FIW), Munich and Laboratoire Nationale D'Essais (LNE), Paris.

A.2.2.5 Dynamic stiffness

Dynamic stiffness is dependent upon the thickness of a product.

$$E_{\text{dyn}} \approx S' \times d_B \text{ (} d_B \text{ for the purpose of this equation is given in metres)}$$

If a certain product is provided with different levels of dynamic stiffness at different thicknesses, it is sufficient to control the dynamic stiffness at that thickness which gives in conjunction with the dynamic stiffness the lowest value of the dynamic elasticity modulus, E_{dyn} . If the requirement of the most stringent combination of thickness and dynamic stiffness is fulfilled, all other combinations of the same product are covered, too.

NOTE If a product is manufactured under stable conditions with e.g. the following parameters:

Db	S'	E_{dyn}
20 mm	20 MN/m ³	400 KN/m ²
30 mm	15 MN/m ³	450 KN/m ²
35 mm	10 MN/m ³	350 KN/m ²

Appendix B Laboratory test on EPS geofoam block

B.1 Laboratory test description

- *Objective*

The objective of this test is to determine:

Test – A. Uniaxial compressive strength test on samples of EPS blocks

Test – B. Long term deformation test on samples of EPS blocks

Note: All the tests will be performed on EPS100. One EPS 100 geofoam block (2m X 1m X 0,5m) is required for this test.

- *General*

Elastic modulus calculated from compressive strength test provides different values on cubical, cylindrical and disc shaped small size samples of EPS. Recorded values of Elastic modulus in literatures have shown that sample size has an effect on determination of parameters. In this test, UCS will be performed on the three different shapes to see the development of σ - ϵ curves. Compressive strength values obtained from this test will be compared with literature values and parameters obtained from back calculation.

EPS during its service life time may be subjected to temperature fluctuations. Due to this, sensitivity of EPS parameters towards temperature is necessary to be checked. Uniaxial compressive strength tests performed on EPS sample blocks within a temperature range of 20 – 48°C showed a variation in elastic modulus and compressive strength. The intention of this test is to check and establish the temperature dependency of the short term compressive strength and elastic modulus within the temperature range of -20 to 20°C with 10°C temperature increment. A commonly used 50mm cubic sample block of EPS is used.

B.2 Test – A Uniaxial compressive strength test on samples of EPS blocks

Uniaxial compressive strength test on samples of EPS blocks with different size and shape as well as uniaxial compressive strength test on samples of 50mm cubic EPS blocks at different temperature has been conducted.

- *Specimen Preparation*

The EPS block to be tested should be seasoned (at least 72 hrs after production and stored at room temperature). Recommended sampling technics from literatures including HB274 is followed. Different shape and dimensions of specimens are prepared as shown in *figure B.1* below.

Temperature controlled ice lab is used to set the temperature of the specimens as needed and UCS is performed on them. To check the repeatability of the test all tests are carried twice.

Table B.1 Number and type of specimens used for UCS test

Sample type	No of sample	size
Cubic	6	50X50X50 mm
Cubic	2	100X100X100 mm
Cubic	2	150X150X150 mm
Cylindrical	2	$\Phi = 50\text{mm}$, $h= 50\text{mm}$
Disc	2	$\Phi = 50\text{mm}$, $h=25\text{mm}$

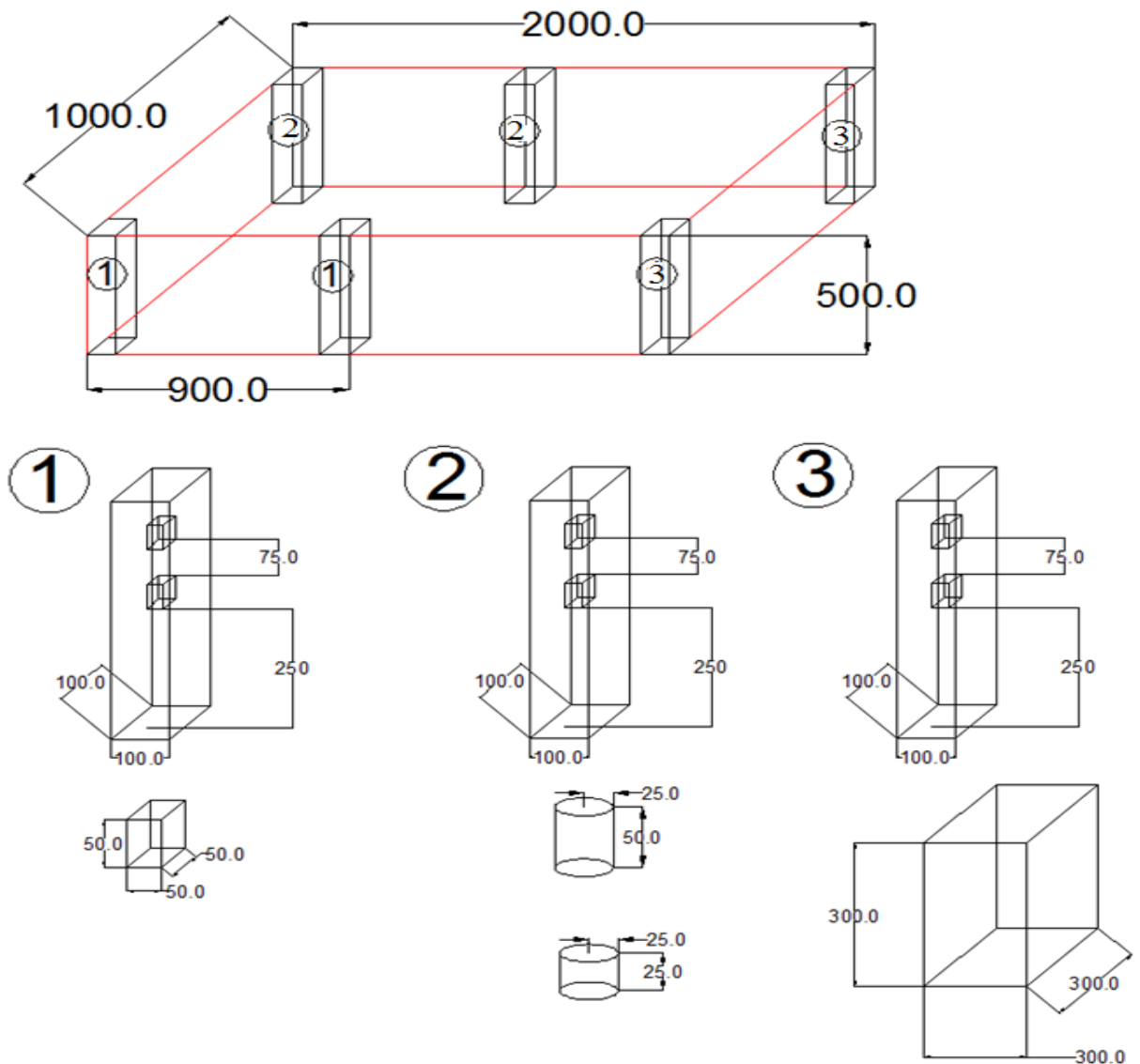


Figure B.1 Technic of sample preparation

- **General Testing Procedure**
 1. Prepare the sample as described in the *figure B.1* above using vertical saw.
 2. Place the sample under the testing machine, UCS machine.
 3. Apply the load at a strain rate of 4mm/min (Literature)
 4. Stop the test when the strain reaches 50%
- **Dimensions of specimens used for the test**

Table B.2 Data of specimens used for UCS test

Shape	Cube								
Sample	S002	S003	S005	S017	S018	S021	S019	S020	S022
mass	3,4	3,8	3,4	3,6	4	3,7	4	3,9	4
hi	50,22	50,27	49,27	50,05	50,17	50,16	50,33	50,32	50,34
l	51,9	50,3	50,88	50,33	50,71	50,35	50,5	50,42	50,79
w	51,09	51,35	47,23	49,74	50,27	49,41	51,08	51,52	50,6
ρ	25,53	29,27	28,72	28,73	31,28	29,65	30,81	29,84	30,92
Load cell	5KN	5KN	20KN	5KN	5KN	5KN	5KN	5KN	5KN
load rate	5mm/min	5mm/min	5mm/min	3mm/min	3mm/min	3mm/min	1mm/min	1mm/min	1mm/min

Shape	Cylinder		Disc	
Sample	S001	S002	S001	S002
mass	3,2	3,5	1,7	1,8
hi	50,38	50,18	25,51	24,88
$\phi 1$	51,15	51,26	51,17	50,63
$\phi 2$	50,71	49,84	49,52	49,83
$\phi 3$	53,36	54,14	51,09	52,16
$\phi 4$	53,03	54,88	50,3	53,29
ϕ_{avg}	52,06	52,53	50,52	51,48
ρ [kg/m ³]	29,84	32,18	33,24	34,76
Load cell	5KN	5KN	5KN	5KN
load rate	5mm/min	5mm/min	5mm/min	5mm/min

Shape	Cube			
Sample	S027	S028	S030	S031
mass	31,2	21	88,9	82
hi	99,5	100	149,5	151
l	99	101	151,5	148,5
w	99	105	146	153,5
ρ	31,99	19,80	26,88	23,82
Load cell	5KN	5KN	5KN	5KN
load rate	5mm/min	5mm/min	5mm/min	5mm/min

Shape	Cube								
Sample	S007	S008	S009	S012	S013	S014	S015	S016	S032
mass	3,3	3,5	2,4	3,8	3,7	4,3	3,61	4,08	2,2
hi	49,61	50,24	50,02	49,91	49,95	49,9	50,43	50,58	50
l	47,06	49,61	49,95	50,2	50,61	50,58	50,58	50,95	49,5
w	50,53	50,86	50,06	50,26	49,71	51	49,71	51,02	48,5
ρ	27,97	27,61	19,19	30,18	29,44	33,41	28,47	31,03	18,33
Load cell	5KN	5KN	5KN	5KN	5KN	5KN	5KN	5KN	5KN
load rate	5mm/min	5mm/min	5mm/min	5mm/min	5mm/min	5mm/min	5mm/min	5mm/min	5mm/min
Temperature	-5	-5	-5	-10	-10	-10	-20	-20	-20

D) Initial tangent modulus, E_{ti}

- Effect of strain rate on initial tangent modulus, E_{ti}

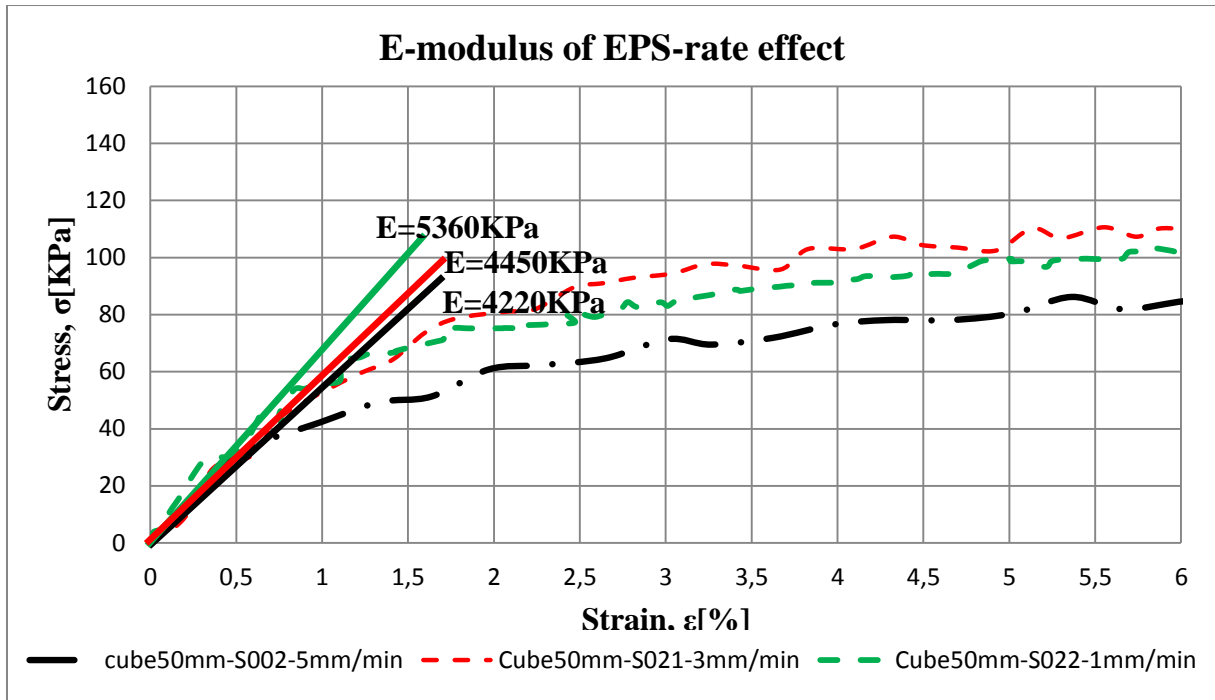


Figure B.2 E-modulus of EPS-rate effect

- Effect of specimen shape on initial tangent modulus, E_{ti}

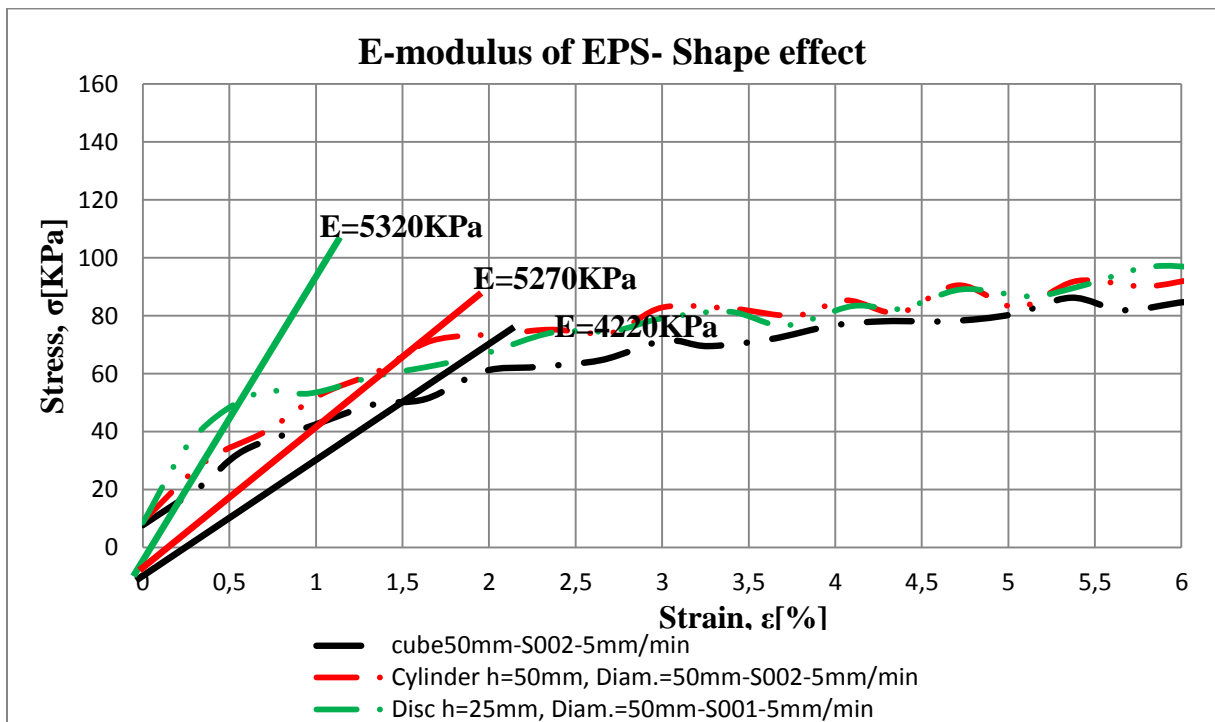


Figure B.3: E-modulus of EPS-shape effect

- Effect of specimen size on initial tangent modulus, E_{ti}

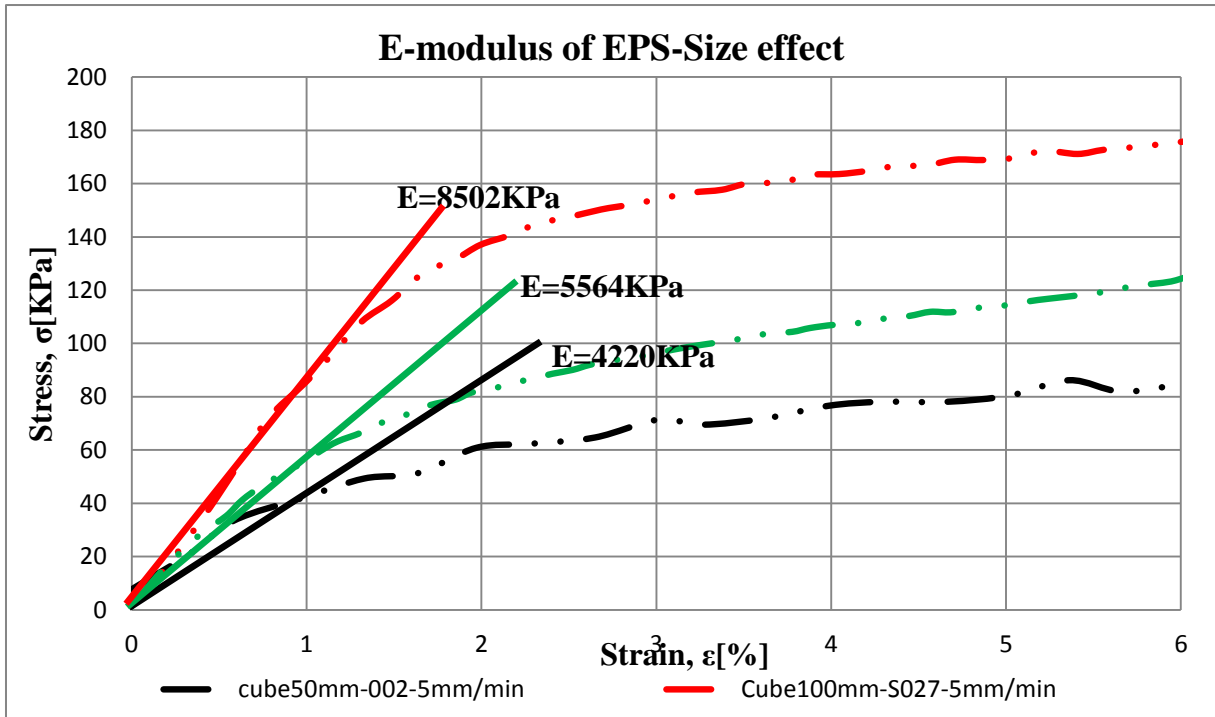


Figure B.4: E-modulus of EPS-size effect

- Effect of specimen temperature on initial tangent modulus, E_{ti}

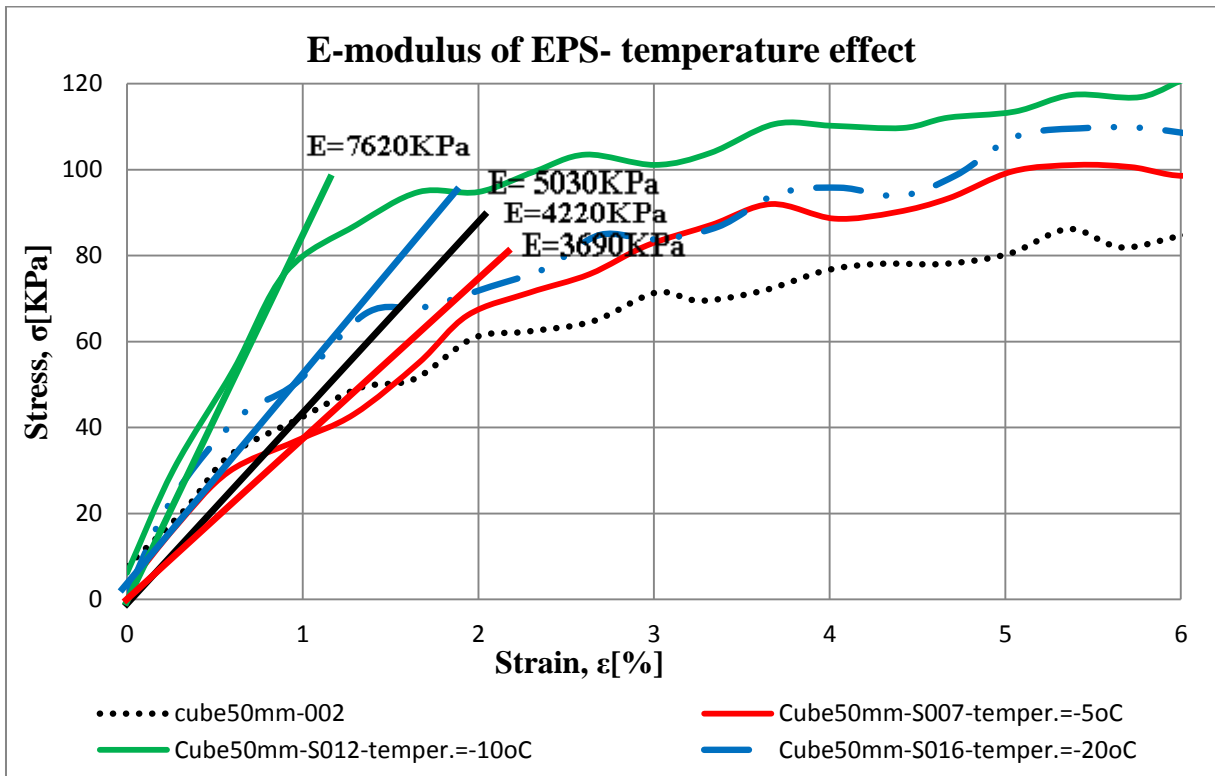


Figure B.5: E-modulus of EPS-temperature effect

II) Short term unconfined compressive strength, σ

- *Effect of strain rate on UCS*

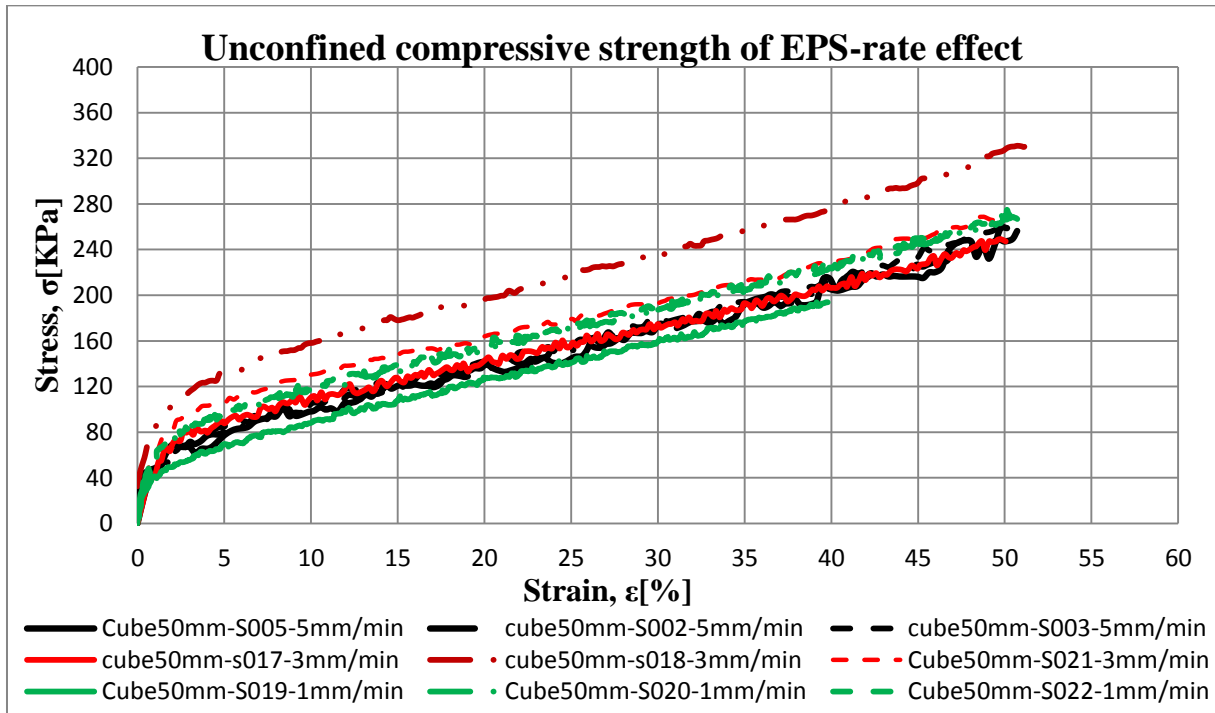


Figure B.6: Unconfined compressive strength of EPS-rate effect

- *Effect of specimen shape on UCS*

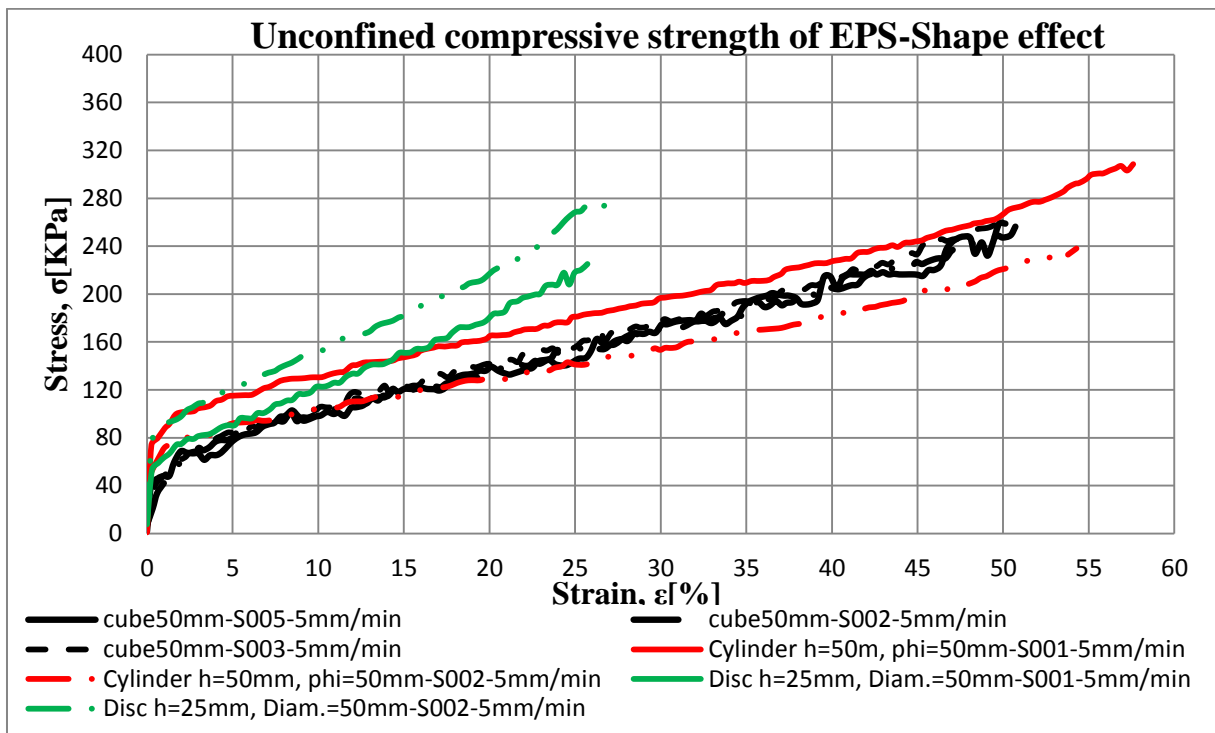


Figure B.7: Unconfined compressive strength of EPS-shape effect

- Effect of specimen size on UCS

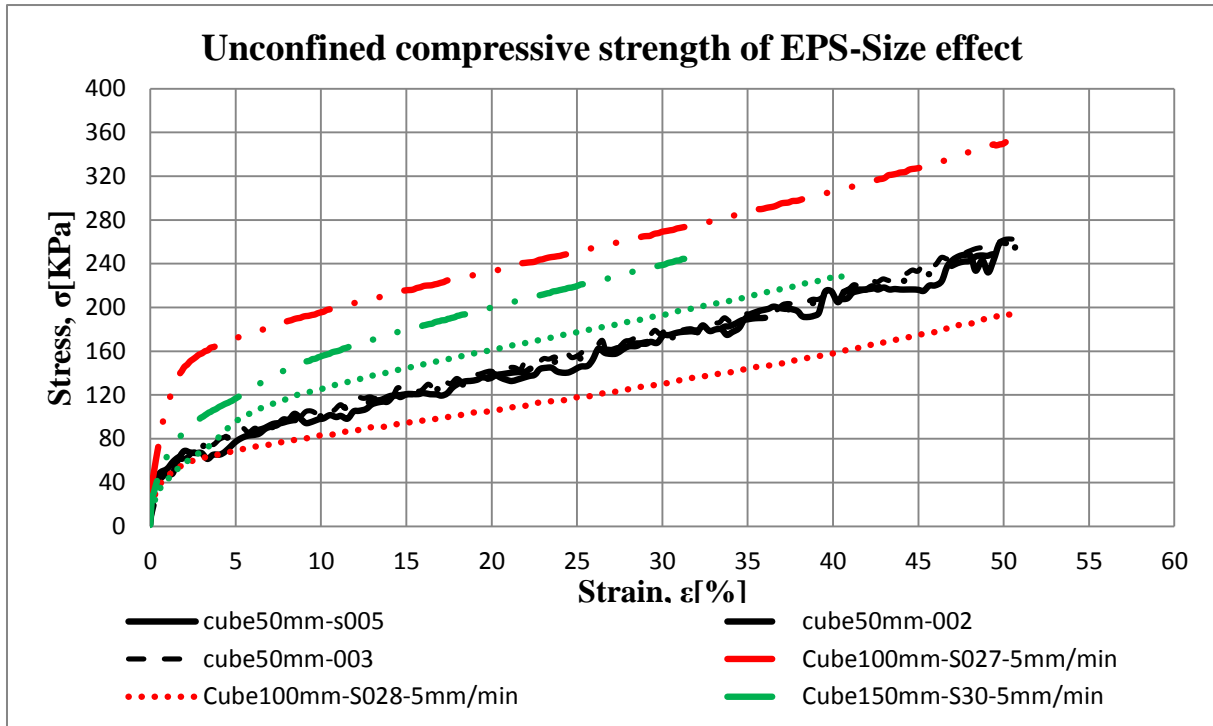


Figure B.8: Unconfined compressive strength of EPS-size effect

- Effect of specimen temperature on UCS

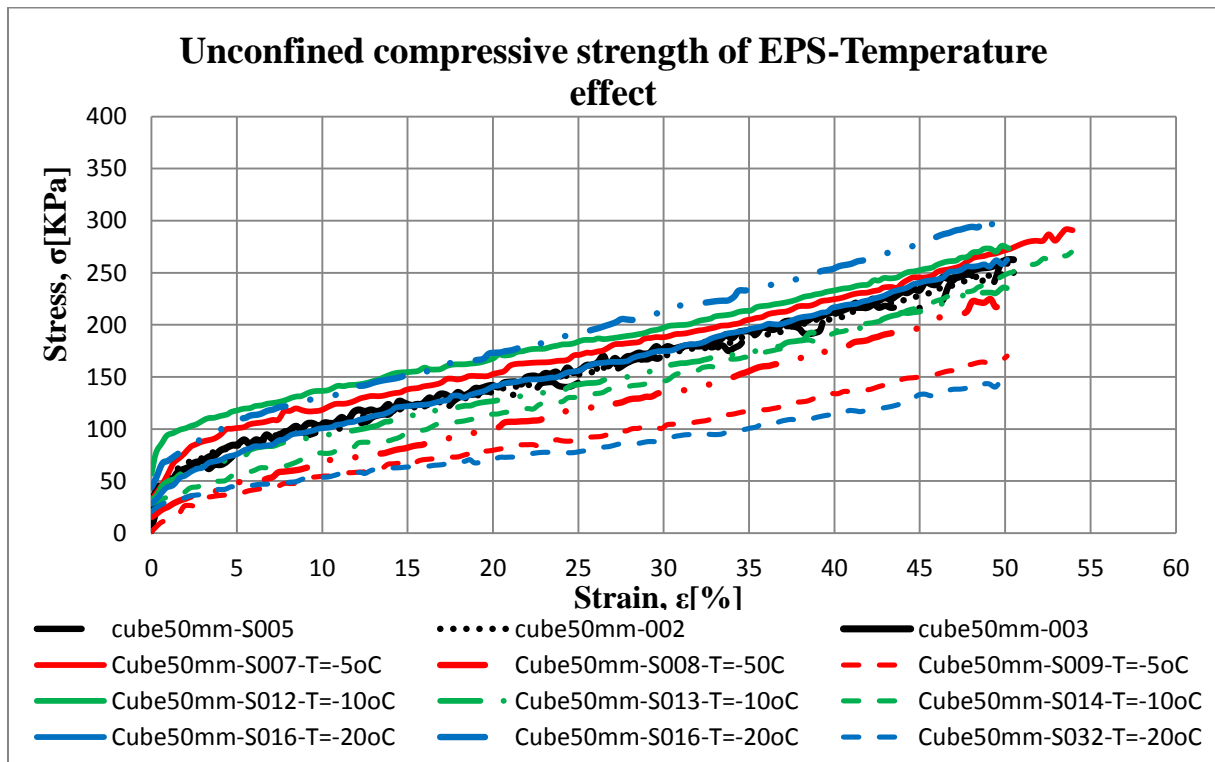


Figure B.9: Unconfined compressive strength of EPS-temperature effect

B.3 Test – B Long term deformation test on samples of EPS blocks

Long term deformation of EPS geofoam block samples with different size and shape has been conducted. A 5 days total deformation is recorded for a constant loading of 30Kpa.

- *Specimen Preparation*

The same sample preparation as in test A and figure B.1 is followed

Table B.3 Number and type of specimens used for long term deformation test

Sample type	No of sample	size
Cubic	2	50X50X50 mm
Cubic	2	100X100X100 mm
Cubic	2	150X150X150 mm
Cylindrical	2	$\Phi = 50\text{mm}$, $h= 50\text{mm}$
Disc	2	$\Phi = 50\text{mm}$, $h=25\text{mm}$

- *General Testing Procedure*

1. Prepare the sample as described in the *figure B.1* above using vertical saw.
2. Place the sample under the testing machine, *figure B.2*.
3. Place the loading rod just on the surface of the sample
4. Start the run button on the computer programme where the data from the Mitutoya is recorded
5. Stop the test after 5 days

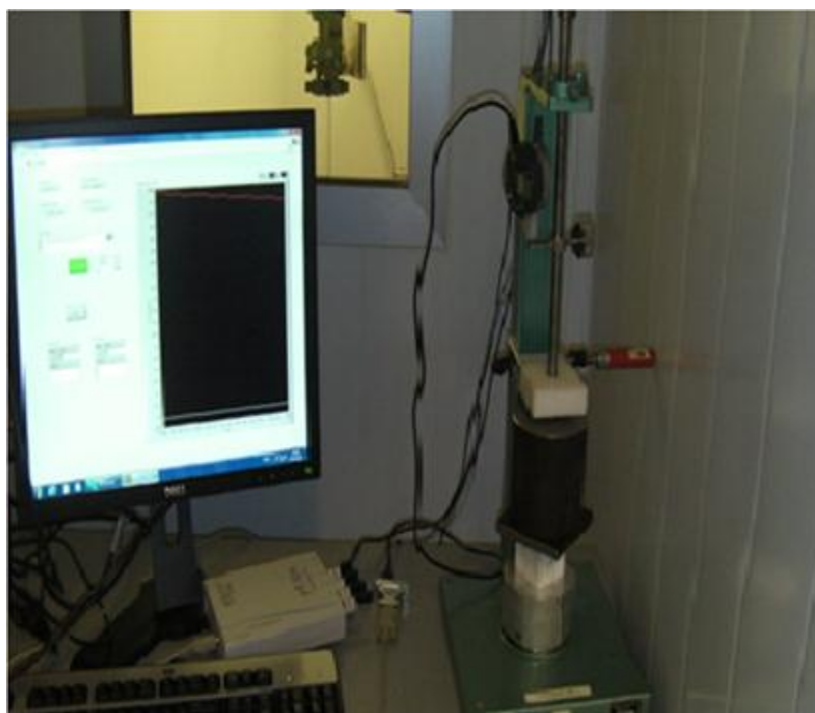


Figure B.10 Test machine used to measure long term deformation of EPS specimens

- *Dimensions of specimens used for the test*

Table B.4 Data of specimens used for long term deformation test

Shape	Cube					
sample	S033	S034	S035	S036	S037	S038
mass	2,13	2,03	28,27	29,62	105,3	103,84
hi	50,01	49,89	99,74	100,05	150,42	150,31
hf	48,52	49,8	99,22	99,29		
l	50,64	48,82	97,92	99,93	150,83	147,17
w	50,09	50,01	100,31	97,68	147,65	146,95
ρ [kg/m ³]	16,79	16,67	28,86	30,33	31,43	31,94
Temperature[°C]	20	20	20	20	20	20
Applied stress, σ [Kpa]	30	30	30	30	30	30
Test duration[hr]	120	120	120	120	120	120

Shape	Cylinder	Disc	
sample	S001	S001	S002
mass	3,66	1,59	1,6
hi	49,78	25,44	25,64
hf	49,77		
ϕ_1	49,89	50,72	52,83
ϕ_2	52,15	51,25	51,89
ϕ_3	49,73	51,46	50,26
ϕ_4	53,58	50,85	52,29
ϕ_{avg}	51,34	51,07	51,82
ρ [kg/m ³]	35,52	30,51	29,59
Temperature[°C]	20	20	20
Applied stress, σ [Kpa]	30	30	30
Test duration[hr]	120	120	120

Shape	Cube			
sample	S038	S039	S040	S041
mass	2,1		3,7	4,3
hi	49,06		49,91	49,8
hf	48,64			
l	50,35		50,31	50,58
w	50,05		50,31	50,48
ρ [kg/m ³]	16,99		29,29	33,82
Temperature[°C]	-20		-10	-5
Applied stress, σ [Kpa]	30		30	30
Test duration[hr]				

- *Total materials needed*

Table B.5 Total material used for the tests

Sample type	No of sample	size
Cubic	8	50X50X50 mm
Cubic	4	100X100X100 mm
Cubic	4	150X150X150 mm
Cylindrical	4	$\Phi = 50\text{mm}$, $h = 50\text{mm}$
Disc	4	$\Phi = 50\text{mm}$, $h = 25\text{mm}$

Appendix C Accelerated creep test results

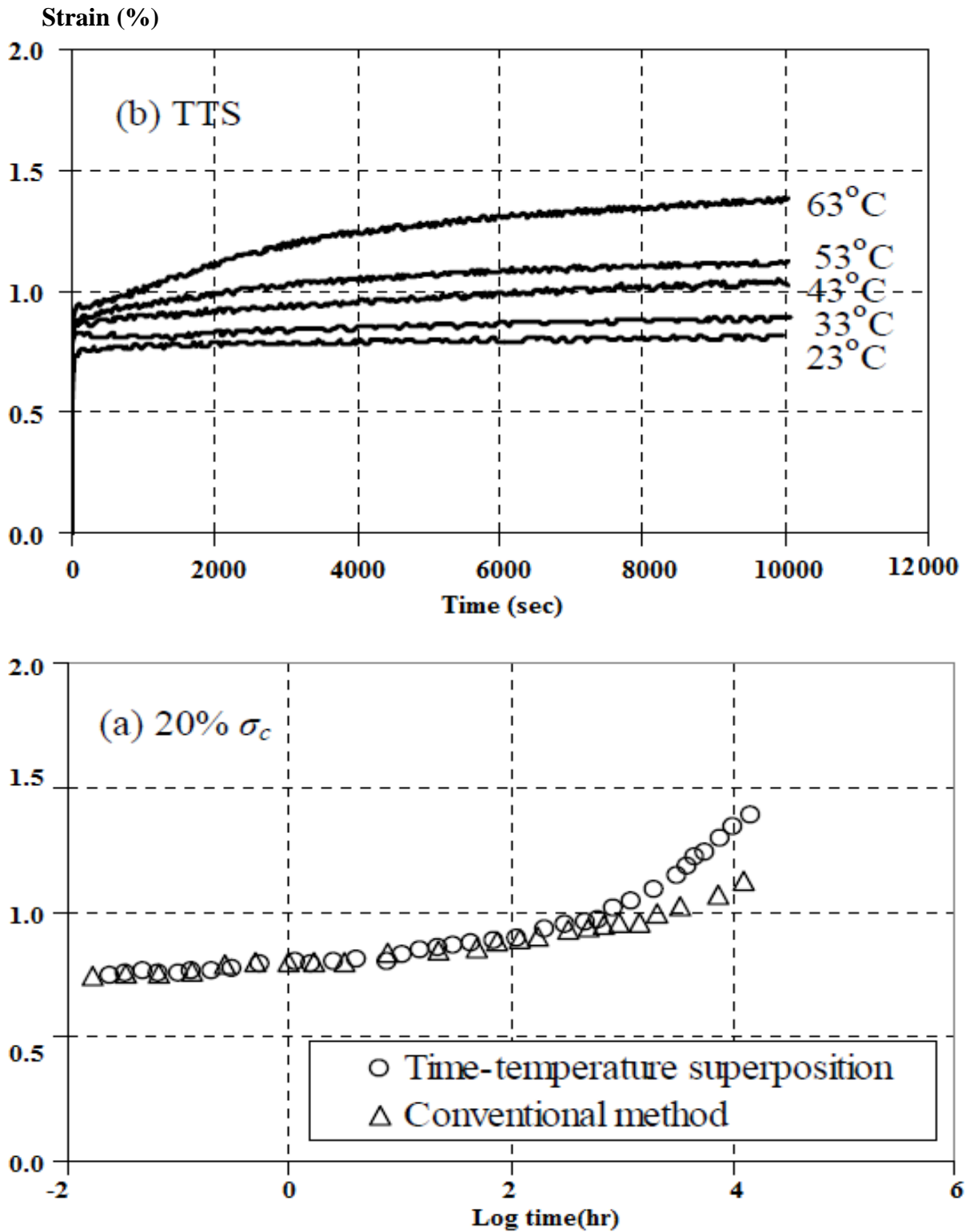


Figure C.1: TTS-accelerated creep test [12]

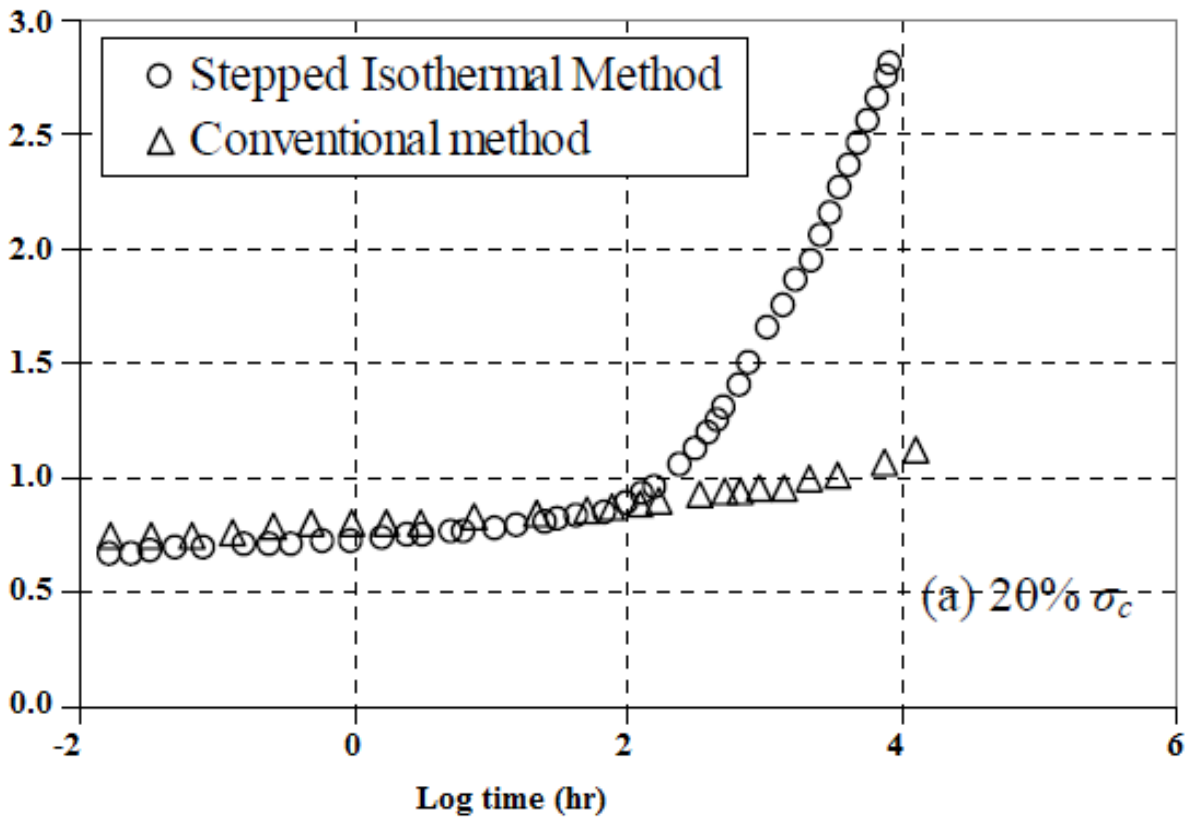
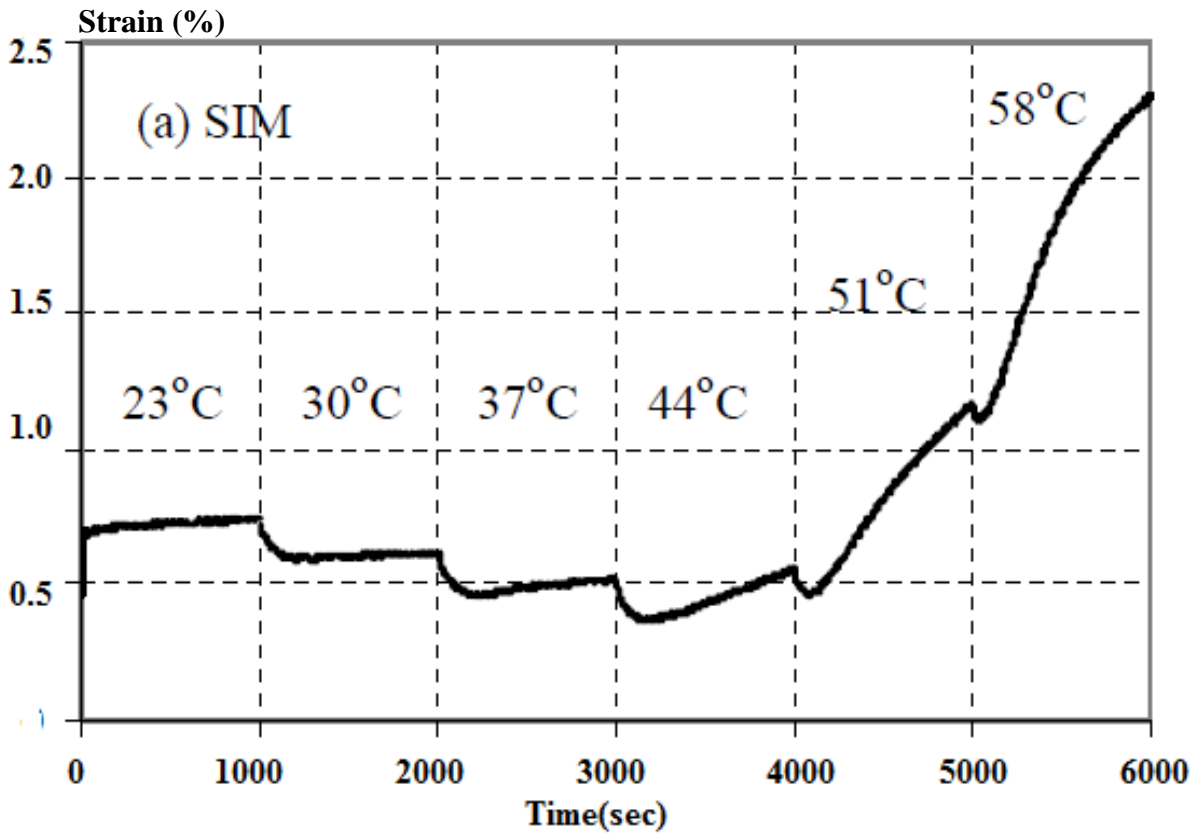


Figure C.2: SIM-accelerated creep test [12]

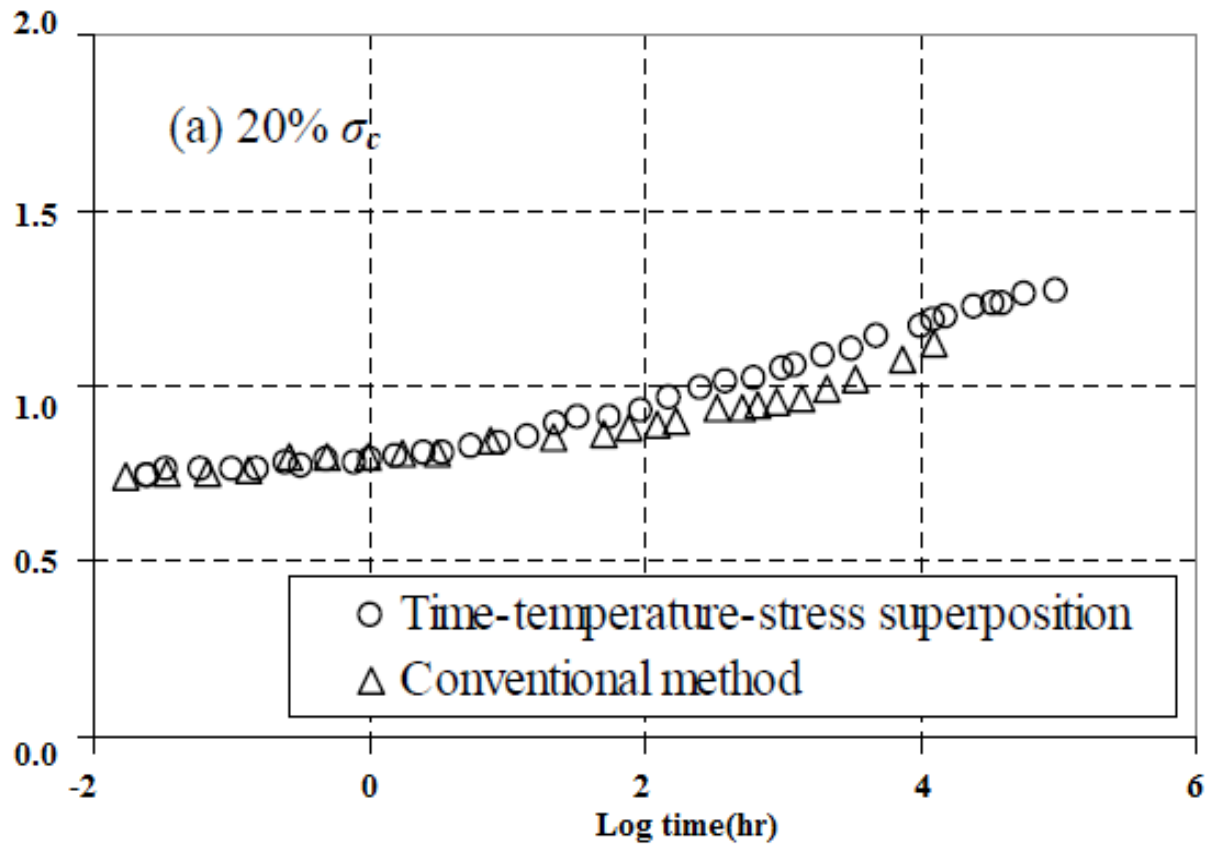
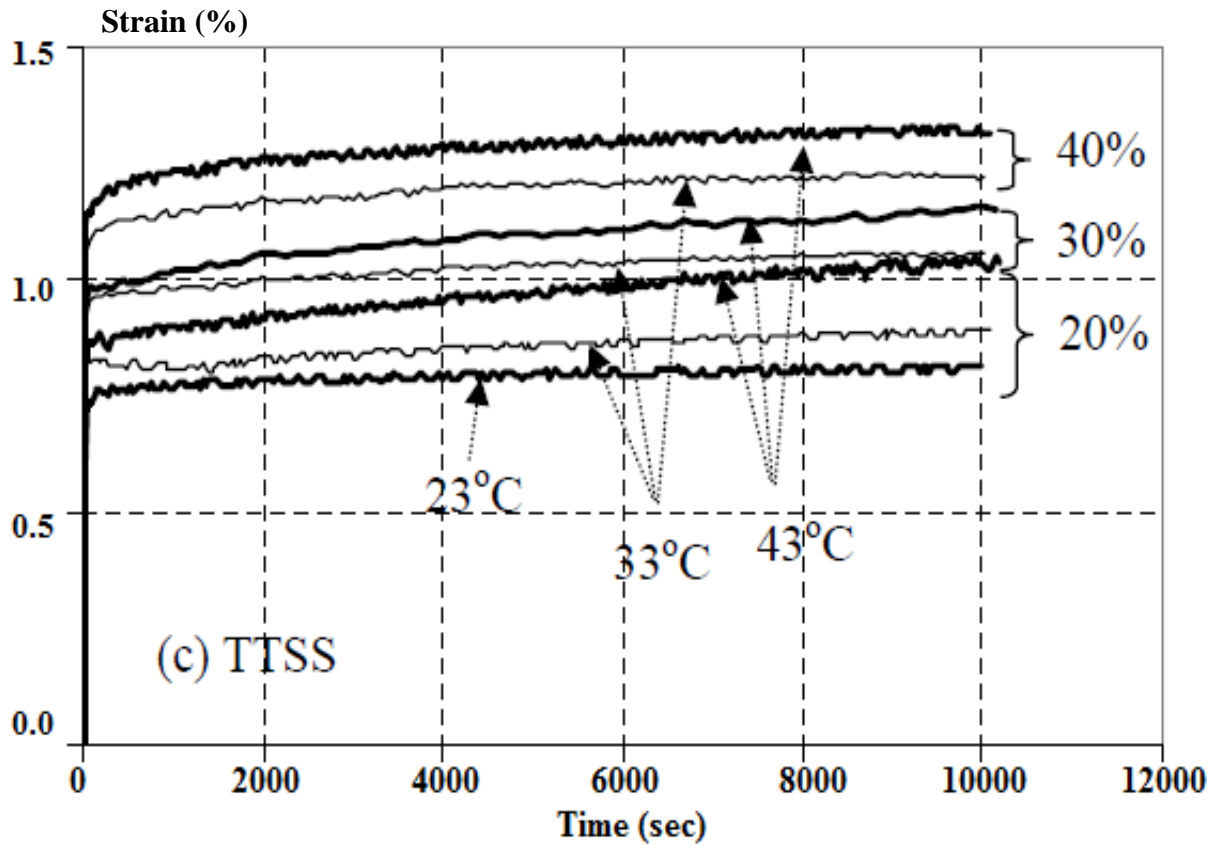


Figure C.3: TTSS-accelerated creep test [12]

Appendix D Geometry, mesh and stress points selected for full scale laboratory creep modeling

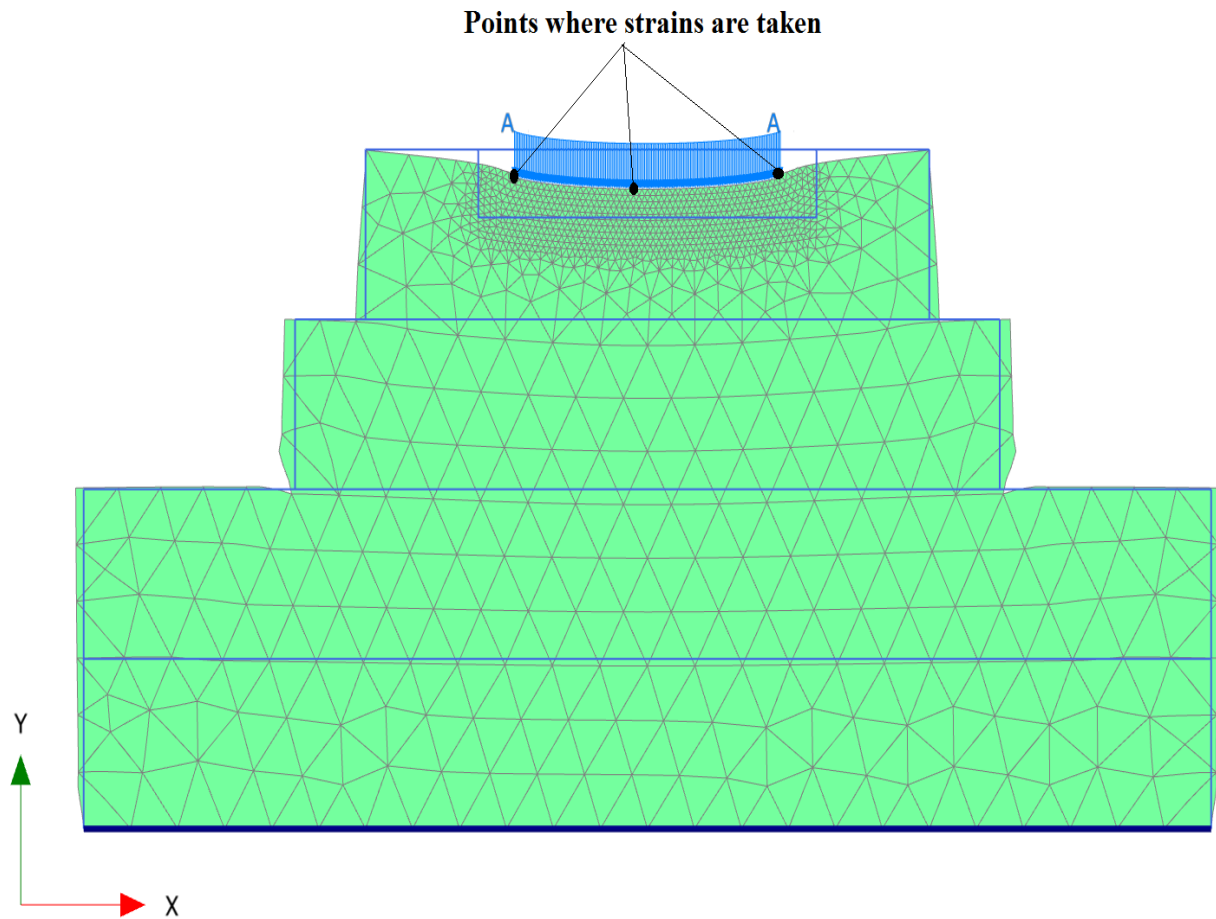


Figure D.1 Geometry, mesh and stress points selected for full scale laboratory creep modeling in PLAXIS 2D

Appendix E Data and output results for creep modeling

E.1 Long term creep test results on 50mm cubic EPS samples by BASF, Germany

The tests used were performed during 1987 to 1989 by BASF AG in Ludwigshafen, Germany as part of a broad study into compressive creep of blocked molded EPS. These creep tests extended for almost 19000 hours (2.2 years). The creep-test results for a set of three specimens of identical density (20.3 kg/m³) and size of 50mm cube are presented below.

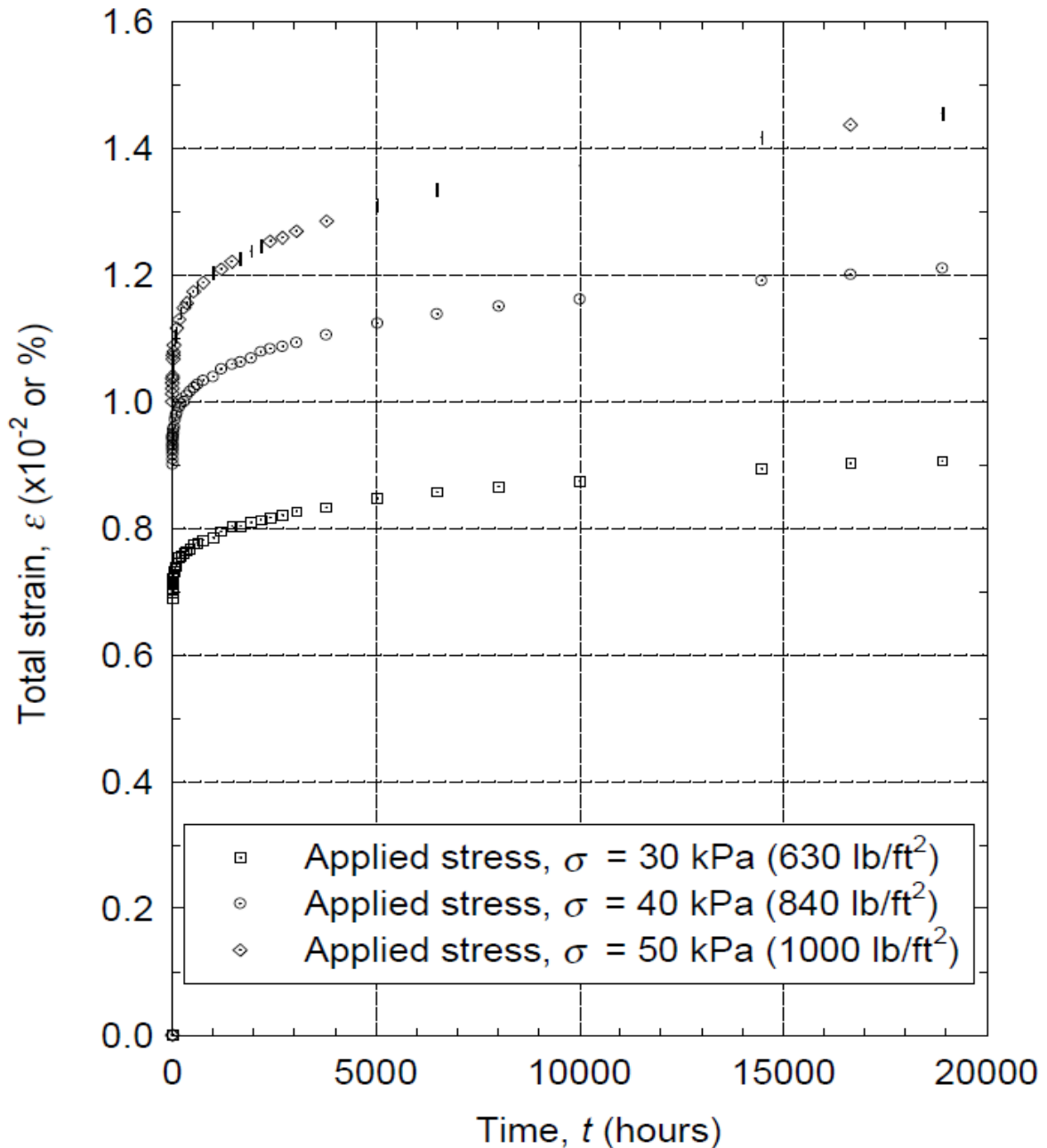


Figure E.1 Creep test results from BASF: Total strain vs time

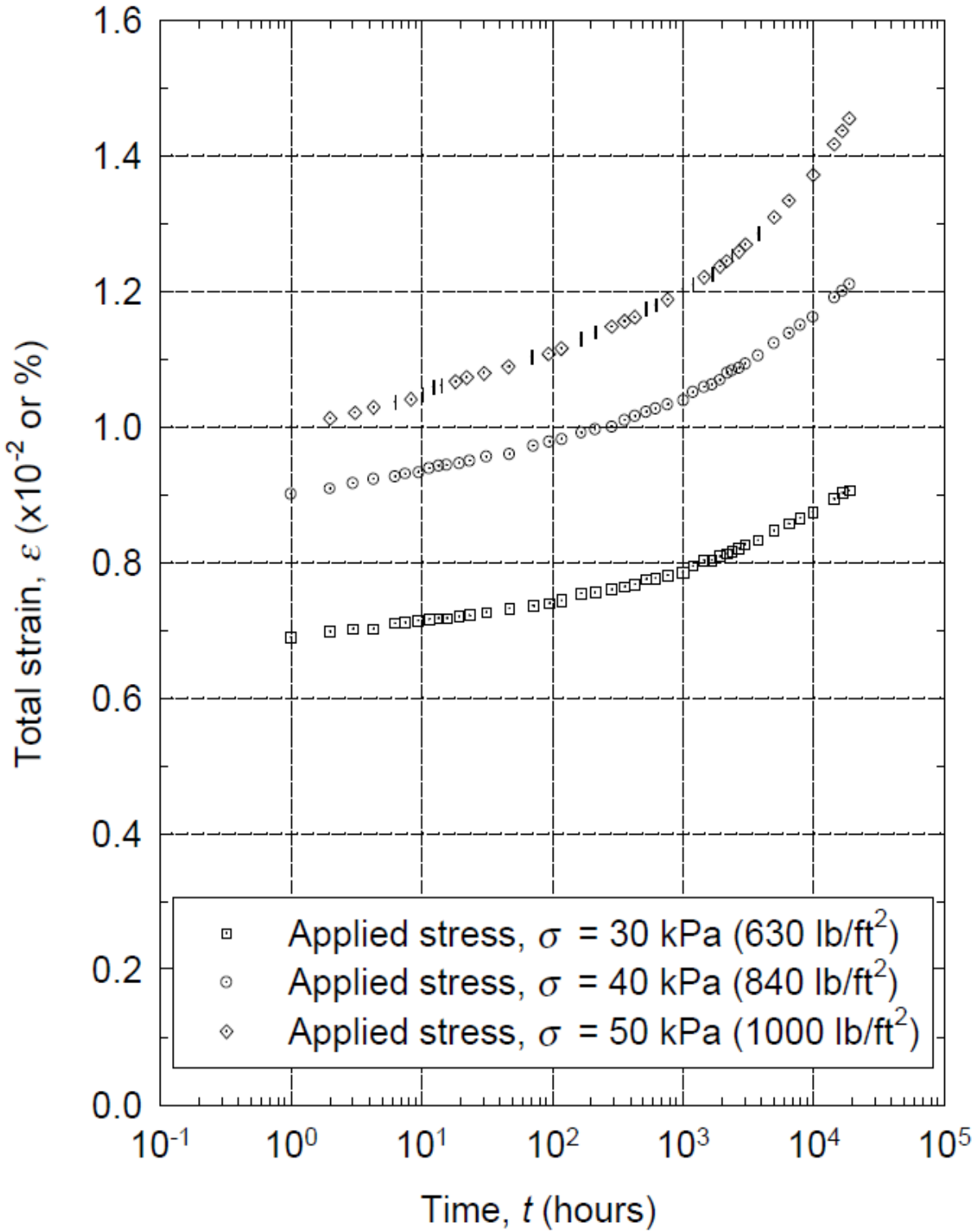


Figure E.2 Creep test results from BASF: Total strain vs log10time

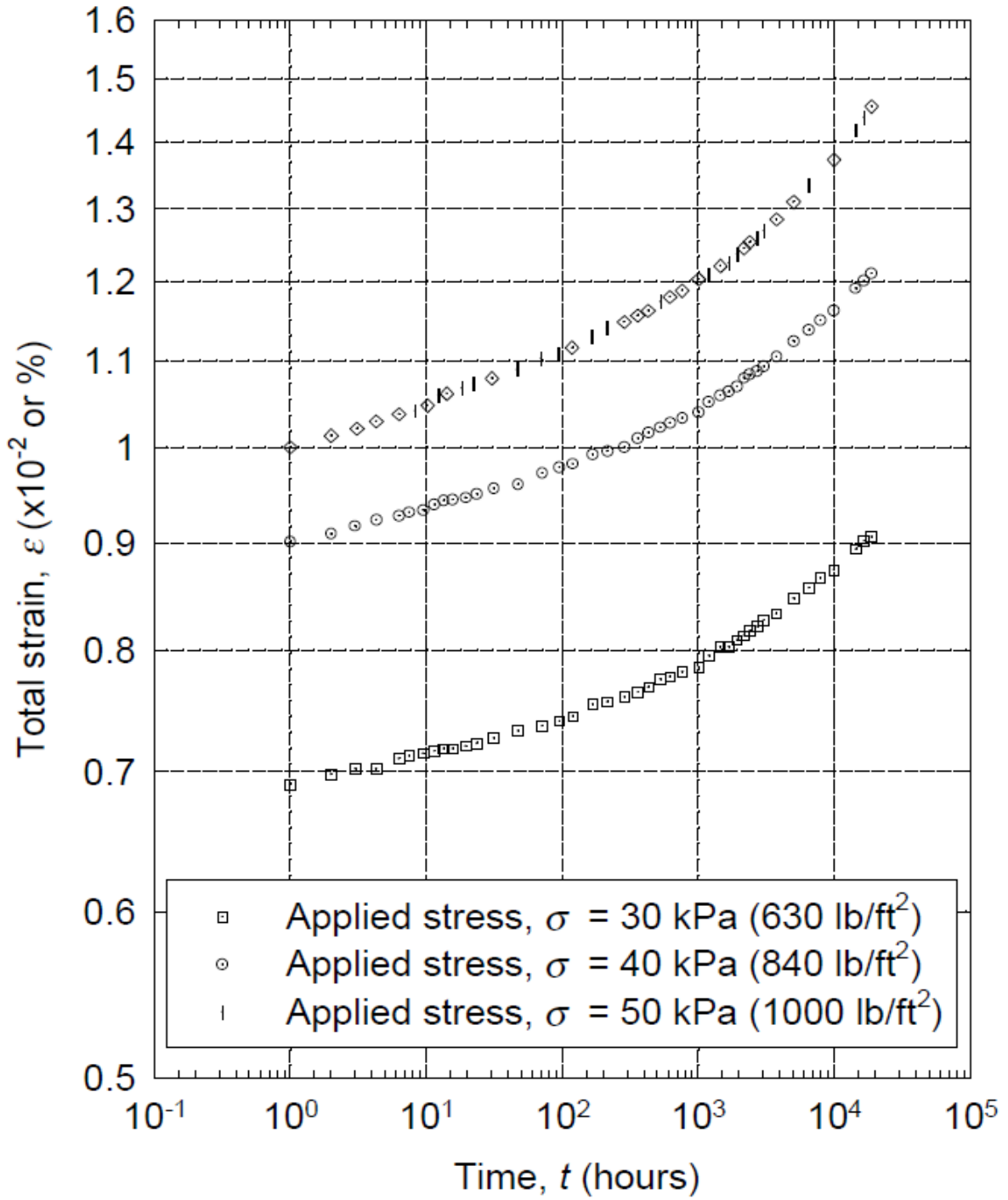


Figure E.3 Creep test results from BASF: Log10Total strain vs Log10time

E.2 Curve fitting for E(t) versus time

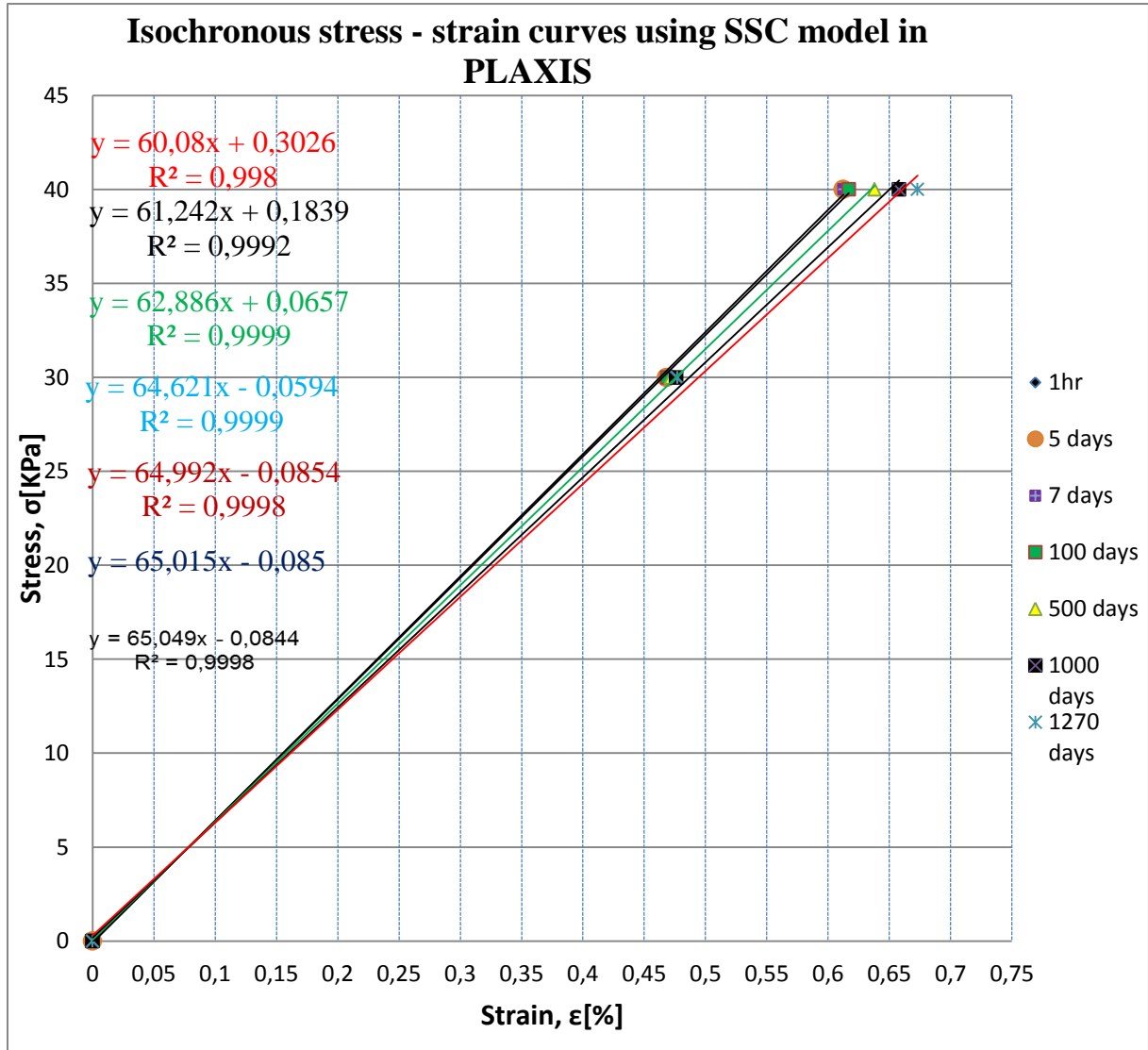


Figure E.4 Curve fitting for E(t) vs time